DISSERTATION

MODELING SEDIMENT YIELD AND DEPOSITION USING THE SWAT MODEL: A CASE STUDY OF CUBUK I AND CUBUK II RESERVOIRS, TURKEY

Submitted by

Umit Duru

Department of Geosciences

In Partial fulfillment of the requirements

for the Degree of Doctor of Philosophy

Colorado State University

Fort Collins, Colorado

Summer 2015

Doctoral Committee:

Advisor: Ellen Wohl

Sara Rathburn
Mazdak Arabi
William Sanford

ABSTRACT

MODELING SEDIMENT YIELD AND DEPOSITION USING THE SWAT MODEL: A CASE STUDY OF CUBUK I AND CUBUK II RESERVOIRS, TURKEY

Better understanding of which factors determine sediment yield rate to reservoirs can facilitate estimation of the probable lifespan of a reservoir and appropriate mitigation measures to limit reservoir sedimentation. Therefore, the research summarized here enhances understanding of correlations between potential control variables on suspended sediment yield and the resulting sediment yields to reservoirs. The Soil and Water Assessment Tool (SWAT) was applied to a portion of the Ankara River catchment, which comprises an area of 4932 km^2 in the central Anatolia region of Turkey. SWAT was calibrated and validated using monthly data from an upstream (1239 Ova Cayi – Eybek) sediment gaging site draining approximately 322 km^2.

A local sensitivity analysis was performed on 18 and 22 input parameters in terms of model outputs such as water and sediment yields, respectively. The most sensitive model parameters affecting stream flow are GW_DEL (ground water delay time) and Alpha_BF (base-flow regression coefficient). For sediment yield, the most sensitive model parameters are SOL_Z (soil thickness), and CH_N1 (Manning coefficient of the channel). Besides these parameters, all other dominant hydrological parameters were determined and a reduction of the number of model parameters was performed in order to improve the Nash-Sutcliffe coefficient of efficiency and R^2.

The SWAT model was performed to simulate water balance, stream flow, and sediment yield during recent decades. The Nash-Sutcliffe efficiency coefficient **(**NSE) and Relative Error were used to assess accuracy of the model. SWAT outputs indicate that the model performs well,

because monthly stream flow of NSE= 0.79 and monthly suspended sediment load of NSE= 0.81 are within the acceptable range of RE and R^2, which are 0.58-1.55 (RE) and 0.89-0.93 (R^2), respectively.

According to multiple regression analysis, sediment yields in the watershed are dominantly influenced by stream flow, drainage area, and channel width. No other variables can be considered as prime control factors on sediment yield in the region. Finally, remote sensing and Geographic Information System software were used to assess sedimentation through time in the Cubuk I and Cubuk II reservoirs. Results indicate that a significant amount of siltation occurred between 1978 and 1983: Cubuk I reservoir accumulated 3 m of sediment within 6 years and Cubuk II accumulated about 10 m. Siltation is the most significant problem in the catchment, so efficient siltation management practices for the reservoirs should be performed to control sediment accumulation in these human made structures.

However, there is considerable uncertainty associated with the model predictions in the Ankara Basin, due to lack of finer resolution soil data, as well as sediment stations for model parameterization, calibration, and validation. Future studies in the Cubuk catchment should focus on improving the database by obtaining higher resolution soil data and more accurate climate data, which will likely help to reduce model uncertainty. Testing the applicability of the SWAT model in the watershed and identifying the source of uncertainty has laid the groundwork for further research in the region.

ACKNOWLEDGMENTS

I am very thankful for the guidance, encouragement and helpful suggestions of my adviser Dr. Ellen Wohl. I would like to extend my appreciation to my committee members Mazdak Arabi, Sara Rathburn, and William Sanford for their great comments and suggestions. I would also thank to Sven Egenhoff, Mehdi Ahmadi and Rosemary Record for their guidance.

The writer wishes to thank the Colorado Water Institute for sponsoring his research and the Geosciences Department at Colorado State University for making possible his graduate study in an atmosphere of creativity and excellence. The writer also would like to thank the Turkish Ministry of Education for providing the financial support for this study.

Thanks to my family, for their love, wisdom and support. Lastly but not least, I would like to thank Sevcan, my darling, for her love, support and patience. To my beloved one year old daughter, Ada, I would like to express my thanks for being such a good girl always cheering me up. Thanks for helping me to keep focus on my research.

TABLE OF CONTENTS

LIST OF TABLES

LIST OF FIGURES

ACRONYMS

AIM Area – Increment Method

ANSWERS Areal Nonpoint Source Watershed Environmental Resources Simulation

APEX Agricultural Policy/Environmental Extender Model

BMP Best Management Practices

CFSR Climate Forecast System Reanalysis

CIR Color Infrared Image

CREAMS Chemical, Runoff, and Erosion from Agricultural Management Systems

DEM Digital Elevation Map

DSI State Hydraulic Works

DWSM Dynamic Watershed Simulation Model

EARM Empirical Area – Reduction Method

EIE Electrical Resources Survey Administration of Turkey

ENVI Image Analysis Software

EPIC Erosion-Predictability Impact Calculator

ESRI Environmental System Research Institute

FAO Food and Agriculture Organization

GLEAMS Ground Water Loading Effects on Agricultural Management Systems

HRU Hydrologic Response Units

HSPF Hydrological Simulation Program – FORTRAN

HWSD Harmonized World Soil Database

GDR General Directorate of Rural Service

GIS Geographical Information Systems

GLC 2000 Global Land Cover 2000

LH-OAT Latin Hypercube One Factor-At-a Time

LULC Land Use and Land Cover Classification Scheme

MUSLE Modified Universal Soil Loss Equation

NCEP National Centers for Environmental Prediction

NDSS Normalized Difference Suspended Sediment Index

ROTO Routing Outputs to Outlets

SWAT Soil and Water Assessment Tool

SWRRB Simulator for Water Research Basins

TAGEM Turkish General Directorate of Agriculture Research

TUIK Turkish Statistical Institute

USLE Universal Soil Loss Equation

USDA US Department of Agriculture

USDA-ARS US Department of Agriculture – Agriculture Research Service

USGS United States Geological Survey

WEPP Water Erosion Prediction Project

CHAPTER ONE

INTRODUCTION

1.1. Overview

Materials derived from bedrock through physical and chemical weathering processes are the main source of sediments. Soil erosion of these sediments reduces not only soil productivity but also reservoir capacity. Erosion accelerates on-site and off-site problems. On-site effects mainly refer to agricultural and economic losses. The most significant off-site effect of soil erosion is loss of water storage capacity because of sediment deposition in a reservoir (McCully, 1996). Reservoirs around the world have been filled with sediment at a rate of approximately 1% per year (WCD, 2000). This means that in 50 years most of the world's reservoirs will lose half of the current storage. Without appropriate precautions, sediment accumulation in reservoirs will cause environmental and economic consequences, especially in semiarid regions where reservoirs were mostly built for irrigation and water supply, as well as generating electricity or flood control. The capacity loss of reservoirs in arid regions is as high as 6000 – 8000 m^3/ km^2 /year (White, 2000).

Sediment yield is the net result of soil erosion and processes of sediment accumulation, so it depends on variables that control water and sediment discharge to reservoirs. Typically, sediment yield reflects the influences of climate (precipitation), catchment properties (soil type, topography), land use/cover, and drainage properties (stream network form and density) (Williams, 1975; Walling, 1994). Erosion is a natural process causing soil loss and generating sediment yield from catchment areas even in the absence of human alterations of land cover. Sediment yields vary from low values in humid, low-relief catchments to very high values in arid, mountainous areas (Lavigne and Suwa, 2004). Due to human modifications, erosion rates have

been raised above natural levels, a phenomenon known as accelerated erosion. Accelerated erosion is a serious matter that reflects increased population and finite arable lands.

The effects of soil erosion go beyond the loss of fertile land. Soil erosion has led to increased pollution and sedimentation in streams and rivers, clogging these waterways and causing declines in fish and other species. Moreover, degraded lands are also commonly less able to hold onto water, which can worsen flooding. Sustainable land use can help to reduce the impacts of agriculture and livestock, preventing soil degradation, erosion and the loss of valuable land to desertification as well as the loss of reservoir volume by sediment deposition.

Sedimentation in a reservoir can be defined by trap efficiency, which is the ratio of the deposited sediment quantity to the total sediment inflow. Trap efficiency is a function of the volume and grain-size distribution of sediment, outlet works, and method of reservoir operation (Eizel-Din et al., 2010). The smallest sediment particles may be transferred through the reservoir without settling. Larger particles may be retained, depending on how completely suspended sediment settles into the reservoir. During peak flow, inflowing water with large volumes of sediment can enter a large reservoir and cannot be subsequently redistributed. Trap efficiency of a reservoir decreases with age as the reservoir capacity is depleted by sediment accumulation (Halcrow Water, 2001).

1.2. Problem Description

This research focuses on enhanced understanding of correlations between potential control variables and the resulting sediment yield to reservoirs. Better understanding of which factors determine sediment yield to reservoirs can facilitate estimation of the probable lifespan of a reservoir and appropriate mitigation measures to limit reservoir sedimentation. Physically-based distributed watershed modelling approaches can be used to analyze the quantity and quality of

water resources, as well as existing and potential sources of sediment in the watershed. One such model was developed by the USDA in the Soil and Water Assessment Tool (SWAT) model.

Water quality in the Cubuk watershed of Turkey has been impacted by sediments from the crop lands that cover 68% of the watershed area. The increased transport of sediment from the catchment contributes to aggradation, which reduces the lifespan of the Cubuk I and Cubuk II reservoirs. Even though Cubuk I lost its functionality within 50 years because of sediment deposition, Cubuk II, a later version of the Cubuk I reservoir, is still serving as a water supply for domestic and irrigation purposes. Much of the sediment load from upstream results from the richest part of the soil, so it has become critical to consider sedimentation in the design of proposed dams, reservoirs and water management practices.

This dissertation consists of three distinct sections. The first section evaluates the applicability of smaller and larger scale SWAT models to the study area. I tested whether SWAT satisfactorily simulated observed hydrology and sediment yields under different management conditions within various agricultural catchments. The second section evaluates which physical factors dominate sediment yield in order to evaluate how sediment yield may fluctuate due to natural or human induced events. Output data from the SWAT model simulation during the calibration period (1/1/1989 – 12/31/1996) were used to evaluate relationships between potential control variables, such as topography, drainage, land use characteristics, and suspended sediment yield. In the third section, bathymetric surveys in 1978 and 1983 conducted by State Hydraulic Works (DSI) were used to compare historical areal and bathymetric data in order to determine the spatial distribution of suspended sediment yield and deposition in the pool/shore of the reservoirs. Digitized bathymetric maps were finally used to compare cross sectional change at the deepest portion of the reservoirs.

1.3. Objectives

The primary objectives of this study are to

- calibrate the mathematical model SWAT to estimate suspended sediment yield in a semiarid watershed located in central Turkey,
- determine the relative importance of 19 potential control variables on sediment yield, and
- evaluate regional and temporal variation in suspended sediment yield input and sediment accumulation in the reservoir pool based on bathymetric surveys in 1978 and 1983, and areal images.

These objectives were addressed by testing the following hypotheses:

H1. SWAT can satisfactorily estimate suspended sediment yield for the gaged watershed that is nearest to the Cubuk I and Cubuk II reservoirs.

SWAT is a continuous time model and operates on a daily time step with up to monthly and annual output frequency at a catchment scale. Predicted suspended sediment using the SWAT model was validated using the data from the 1239 (Ova Cayi – Eybek) sediment gaging station, which collected runoff and suspended sediment yield over 30 years. The criteria for evaluating satisfactory performance are explained in the Methods section.

H2. Sediment yield correlates most strongly with topography, and to a lesser extent with stream discharge, channel geometry, land cover, and drainage characteristics.

The null hypothesis is that reservoir sedimentation rate correlates most strongly with topography (e.g., elevation, relief ratio, and hypsometric integral) because this variable influences stream velocity, stream power, and sediment transport. The alternate hypothesis is that reservoir sedimentation rate correlates most strongly with one of the following factors: drainage area, land cover, channel slope, or disturbance history.

H3: It is possible to identify which tributaries dominantly contribute suspended sediment input and sediment that accumulates in the Cubuk I and Cubuk II reservoirs.

I used data from bathymetric surveys in 1978 and 1983 conducted by DSI and areal images. I determined suspended input from tributaries and sediment accumulation rate in the pool/shore of the reservoirs through historical areal and bathymetric data comparison. Areal images such as Google Earth were used to delineate the shoreline and identify change in the reservoir geometry.

1.4. Methodology

The basic methodology involved applying an existing mathematical model to a catchment within Central Anatolia of Turkey that was chosen based upon availability of observed suspended sediment data. The SWAT model was set up, calibrated, validated, and then compared to actual sediment yield data. The model performance was mainly evaluated using the Nash-Sutcliffe coefficient of efficiency (NSE) and relative error routines in Mat-Lab. The Nash-Sutcliffe coefficient provides an estimation of the relationship between the observed and predicted values. The model results are considered highly applicable if NSE values are greater than 0.75; applicable if the NSE is between 0.75 and 0.36; and failing if NSE values are between 0.36 and 0 (Motovilov et. al., 1999). Relative Error (RE) is estimated as the ratio of absolute error to the true value and is considered acceptable if RE values are less than 20% in this study.

The Nash-Sutcliffe model efficiency coefficient was used to assess the predictive power of the hydrological model based on regression based parameters were compared with corresponding values obtained through model calibration and validation. Model performance is also evaluated using global averaged parameter values. I evaluate whether regionalized parameters of the SWAT model can be used to make satisfactory predictions of hydraulic response in gaged watersheds based upon the comparison among NSE for monthly discharge using regression based on

parameters and corresponding values obtained from model calibrations. If the value of NSE is between 0.53 and 0.83, and model calibration values of stream flow and sediment yields are between 0.45 and 0.90 (Gitau and Chaubey 2010), then I infer that the model satisfactorily estimates sediment yield in the watershed.

I used multiple regression analysis to evaluate the relationship between independent variables controlling sediment yield and dependent sediment yield variables. I (i) examined sediment input and temporal control variables, either at annual intervals or averaged over time intervals dictated by the availability of information on topography, (ii) analyzed average sediment input and all control variables for all subbasins, and (iii) undertook these analyses for each subbasin individually and then for progressively larger subsets of all of these reservoirs in the same region in Turkey. Once a regression relation was developed, I constructed a graph of the expected sediment yield and measured sediment yield versus each independent variable. In addition, I used the presence of erosional and depositional features (e.g., incised channels, depositional fans), where these can be detected on aerial photos, as an indirect reflection of sediment movement. I also evaluated which factor dominantly contributes sediment yield in the form of Hydrologic Response Units (HRUs) based on the combination of soil and vegetation within the sub-catchments.

There are two common methods for illustrating sediment distribution in a reservoir: sediment distributed by depth and by longitudinal profile. Typically, reservoir sediment accumulation is distributed below the top of the dead pool or normal water surface, but in a reservoir with a flood control pool, some part of sediment accumulation may be deposited in this pool. Sediment distribution depends on: (1) the manner of reservoir operation, (2) the grain size of

deposited sediments, (3) the shape of the reservoir, and (4) the volume of sediment deposited in the reservoir (Borland and Miller, 1958).

In addition, 1967, 1991, and 2012 aerial photos showing the area surrounding Cubuk I and Cubuk II reservoirs were used to investigate how deltas expand within the reservoirs. Comparison of color infrared images taken in 2013 allows erosion to be visualized, but generally with less precision than local measurements in the field.

CHAPTER TWO

LITERATURE REVIEW

2.1. Erosion and Sediment Yield

Approximately 40% of the world's fertile lands are excessively degraded as a result of erosion (The Guardian, 2007*).* The United Nations states that an area of fertile soil the size of Ukraine is lost every year because of drought and deforestation (Smith and Edwards, 2008). Other factors influencing soil erosion are climate, landscape relief, soil or bedrock properties, vegetation cover, and human activities (Williams, 1975; Walling, 1994). Therefore, spatial variability in sediment dynamics may reflect spatial variability in watershed characteristics and human activities. This relationship is often summarized in a single regression model such as a relationship between catchment area and sediment yield (Walling, 1983; Nyssen et al., 2004), or in multiple regression models using more than one catchment characteristic (Neil and Mazarari, 1993). Even though erosion is a natural process, human activities might globally increase erosion rate by a factor of 10 – 40, a phenomenon known as "accelerated erosion" (Zuazo and Pleguezuelo, 2009).

2.2. Physical Factors Controlling the Amount of Suspended Sediment Yield

Numerous previous studies (e.g., Williams, 1975; Walling, 1994) indicate that river sediment fluxes are sensitive to many factors including change in runoff, basin characteristics, lithology, topography, and land use. Summerfield and Hilton (1994) studied the variables controlling mechanical denudation rates in drainage basins exceeding 5×10^5 km² in area and concluded that physical factors (basin area, mean annual runoff, temperature, precipitation) have no significant influence on physical denudation processes, although channel gradient and basin relief can be considered as dominant controlling variables.

2.2.1. Mean water discharge

The main source of runoff and stream flow is rainfall (precipitation), some of which is lost through evaporation, ground water recharge, and other processes. Therefore, the intensity of rainfall plays a key role in detaching particles from the ground surface and thus controlling the amount of sediment particles removed. Other meteorological parameters such as temperature, rainfall intensity, wind, number of storms, and areal distribution of precipitation also influence sediment movement. Langbein and Schumm (1958) analyzed the relationship between effective rainfall and annual sediment yield from 100 gaging stations in the United States (Douglas, 1967; Dendy and Bolton, 1976) (Figure 1). They concluded that effective precipitation influences annual sediment yields such that effective precipitation in the range of 200mm - 700mm is likely to have create the highest annual sediment yield.

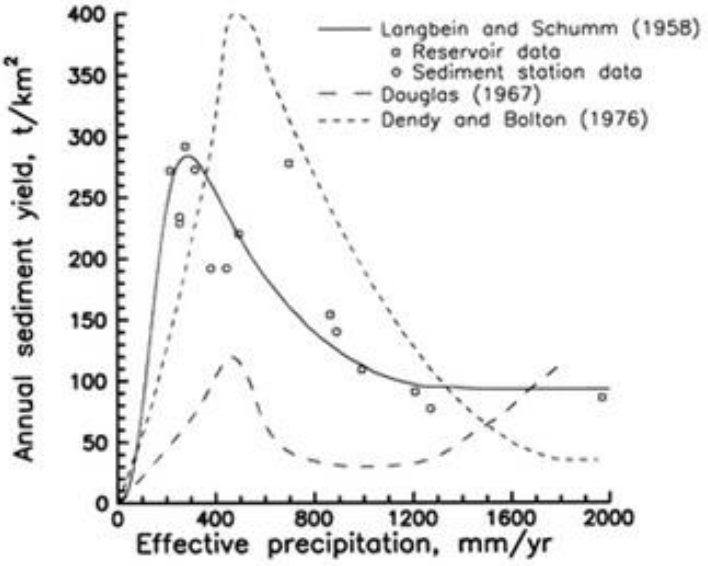

Figure 1: Schematic diagram illustrating climatic variation in sediment yield based on various models (McConvill, 2014, Figure 2).

Mean water discharge alone is not the deciding factor for sediment concentration in rivers, even though water flow is one of the most significant factors controlling stream power and the scouring capacity of rivers.

2.2.2. Basin area

Smaller watersheds typically have larger sediment yields because smaller basins are likely to have steeper slopes and stream gradients compared to larger basins. Although basin area integrates several factors such as storage capacity and gradient, basin area alone is not the determining factor of sediment yield, but likely has great influence on sediment yields in a watershed. Milliman and Syvitski (1992) studied the importance of topography and basin area as controlling factors on sediment yields for mountainous rivers in North and South America, Asia, and Oceania. They concluded that these two variables (topography and basin area) are the most dominant influences on sediment yield, with climate, land use, and geology being second-order influences.

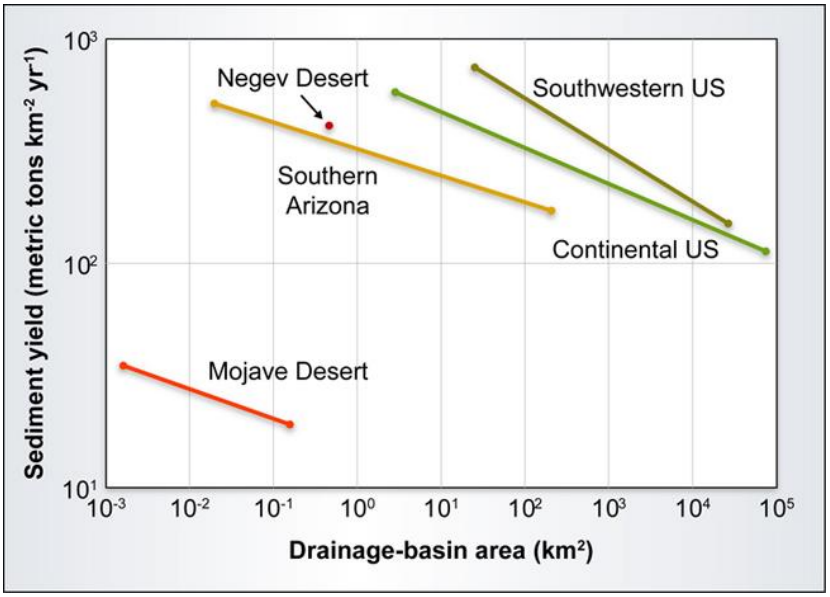

Figure 2: Graph showing the relation between sediment yield and drainage area for drainage basins in five different locations (Griffiths et al., 2006, Figure 8)

As drainage basin area increases, the catchment become more topographically complex and sediment yield often becomes transport limited, meaning that sediment cannot easily move out of the basin because of sediment deposition. In general, there is an inverse relationship between sediment yield and drainage area (Griffiths et al., 2006) (Figure 2).

2.2.3. Mean elevation and relief

Basin elevation and morphology have great influences on river sediment fluxes according to Pinet and Souriau (1988). They found that sediment fluxes are linearly correlated with mean basin elevation based on sediment yields in large world rivers, as described by the following equation:

$$Qs=\alpha R^{3/2}A^{1/2}\,E^{kT} \quad \text{(Eq. 1)}$$

Where:

Qs is the long-term sediment load (kg/s),

R is relief defined as the highest point of elevation (m) minus the elevation of discharge station (m),

A is basin area (km^2),

E is mean basin elevation (m),

T is mean surface temperature of the drainage basin (^oC),

k and α are constants (2×10^{-5} and 0.1331, respectively).

Relief is also a major controlling variable as indicating greater mechanical erosion (Montgomery and Brandon, 2002). Even though many previous studies have tried to investigate the significance of relief, only a few mathematical relationships have been published. In the early 1960s, Schumm reported a linear relationship between erosion rate and drainage basin relief for basins in the United States (Schumm, 1963; Ahnert, 1970; Pazzaglia and Brandon, 1996). Relief such as mean slope also influences micro-climate, lithology, and vegetation controlling erosion rates. Under natural conditions, sediment yields in mountainous areas are 28 times greater than in low relief areas, and mechanical erosion rate changes based on altitude and relief (Dedkov and Mozzherin, 1992).

2.2.4. Human effects

The morphology of alluvial river systems has been altered as a result of natural and human activities, which could be gradual or rapid over time. Any disturbances or modifications not only influence upstream but also downstream conditions (Simons and Senturk, 1992). Many studies have pointed to the significant influence of anthropogenic activities including construction of dams, land-use practices, soil and water conservation practices, roads, and footpaths on river sediment fluxes. Morris and Fan (1997) reported the most significant land degradation factor to be human activities. Siakeu et al. (2004) also studied suspended sediment concentration in central Japan with a special reference to human impact. They concluded that anthropogenic activities, especially in industrial countries, create a large variation in the pattern of suspended sediment along relatively small sub-watersheds.

The effects of human activities on suspended sediment load have been assessed in Turkey, as well. Reservoir construction and mining have a huge impact on riverine systems in Turkey. Isik et al. (2008) identify anthropogenic effects on stream flow hydrology and morphology. The results from this study indicate that sand mining for construction of roads and structures and over-withdrawals of sediment may increase sediment inputs to river banks. Emissions resulting from construction and mining activities may also increase greenhouse gases because of use of heavy-duty vehicles and large construction equipment.

2.3. Spatial and temporal variability in sediment yields

The spatial and temporal variability of suspended sediment load have been studied at a variety of scales from all over the globe (Webb and Walling, 1984). A wide range of studies have been done on the impact of climate, topography, land use, lithology, and drainage characteristics across varying spatial (Langbein and Schumm, 1958; Dunne, 1975; Douglas, 1967; Hwang, 1980;

Walling and Webb, 1983; Jansson, 1988; Church and Slaymaker, 1989; Lvovich et al., 1991) and temporal scales (Douglas, 1967; Meade, 1969; Abernethy, 1990; Walling, 1994). Based on the spatial distribution of global sediment yield in Walling and Webb (1996), the Central Anatolia region of Turkey has an annual suspended sediment yield rate of approximately 100 tons/km²/yr (Figure 3).

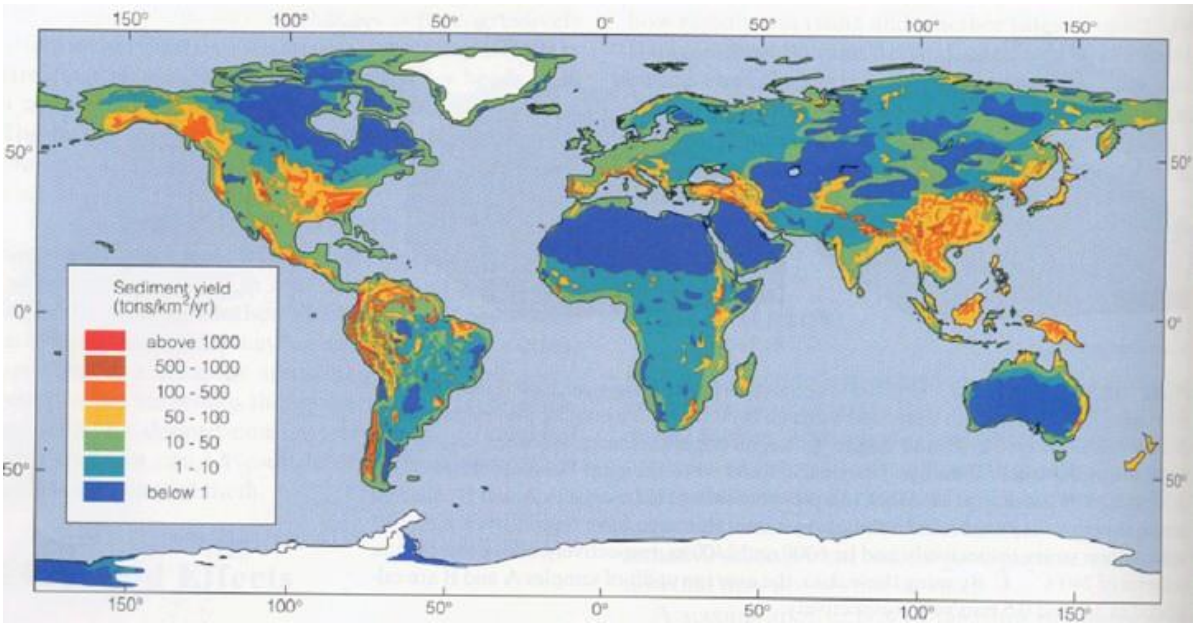

Figure 3: Global pattern of suspended sediment yield according to Walling and Webb, 1996 (Figure 1)

Studies focusing on temporal variation of suspended sediment yields mostly emphasize anthropogenic impacts and variation in macro and micro climate (Douglas, 1967; Meade, 1969; Walling, 1995). These studies suggest that soil erosion rates can be increased by the magnitude of agricultural activities, particularly given that the area of the world's surface given over to crop production and livestock grazing has increased by more than 5 fold over the past 200 years (Buringh and Dudal, 1987). For example, Milliman et al. (1987) studied Holocene rates of sedimentation in the Yellow River Basin and estimated that as a result of land clearance and agricultural development, sediment yield increased beyond values existing during the early and middle Holocene. A similar range of increase was documented by Abernethy (1990) based on

reservoir sedimentation in Southeast Asia that was influenced by land-use change during the last century. Abernethy also noted that developing countries could double the magnitude of sedimentation in reservoirs in approximately 20 years. Spatial variability in sediment yield may therefore reflect spatial variation in catchment properties and human activities, and temporal variation may also reflect climate change.

2.4. Trap Efficiency and Reservoir Sedimentation

The storage capacity of a reservoir depends upon the mean annual runoff and a reservoir traps about 97% of the input sediment yield (Basson et al., 2008). Trap efficiency is defined as the ratio of deposited sediment quantity to total sediment inflow. The two variables that predominantly influence trap efficiency are sediment particle fall velocity and flow rate along a reservoir. Particle fall velocity is influenced by shape and size of materials, viscosity and chemical composition of water. Based on the large reservoirs in the United States, Brune (1953) developed a relationship between trap efficiency (β) and C/I.

The average value of trap efficiency can be determined using:

$$\beta = \frac{C/I}{(0.012+0.102)*C/I} \qquad \text{(Eq.2)}$$

Where;

β : Trap efficiency (%),

C : The reservoir capacity (hm^3),

I : The mean annual inflow (m^3/s).

The volume and mass of sediment deposited in subsequent years of sediment trap efficiency are established on the basis of the mass of sediment transport calculated according to bathymetric surveys, USLE and MUSLE methods.

In general, trap efficiency decreases with age as the reservoir capacity is reduced by sediment accumulation. Filling half of the initial storage takes about 50 years and most reservoirs have been designed to be used 50 to 100 years (Hotckiss, 1995).

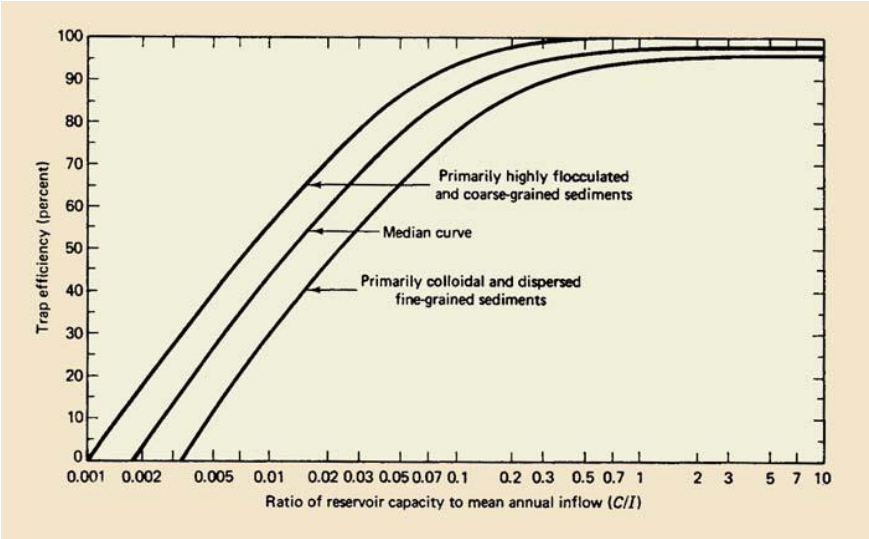

Figure 4: Brune's trap efficiency curves (Brune, 1953, Figure 12)

According to Brune (1953), the higher the retention parameters (C/I) and the higher the trap efficiency, the faster the rate of reservoir sedimentation throughout approximately three-quarters of the reservoir's range (Figure 4). In other words, smaller reservoirs will trap less sediment and last longer, while the converse is true for larger reservoirs.

2.5. Catchment erosion and sediment yield modelling

Temporal and spatial analysis of sediment yield is also useful for modelling catchment erosion and sediment yield. Such analysis is essential for water management practices, specifically identification of critical erosion areas and the source of sediment yield. Various erosion and sediment yield prediction methods have been used, none of which can be presumed to be applicable to all possible conditions because all methods have advantages and limitations. Each method infers runoff and water quality based upon catchment characteristics, ecological considerations, site conditions, engineering requirements, availability of time, and data requirements/availability.

Sediment yield in a catchment reflects the following variables (Stand and Pemberton, 1982):

- soil type
- land cover
- geologic formation
- topography
- land cover / use
- runoff
- hydrology
- drainage network
- sediment characteristics

Numerous models have been used to estimate erosion and sediment yield from a watershed and to analyze land-use/change impacts to sediment generation (Schmidt et al., 2008). In general, spatially distributed models are advantageous for modelling of sediment delivery processes at a basin scale. Applying a distributed model at the catchment scale requires variable soil loss erosion from USLE or MUSLE for catchment delivery processes. Kling (1974) suggested modeling sediment delivery ratio with a spatially distributed approach for a specified watershed.

2.6. Empirically Based Models

Empirical methods have been derived using data from specific geomorphological areas and what actually occurs versus theoretical grounding of erosion and sediment yield based on regression and statistical analysis. To compute sediment yield at the catchment scale, USLE or a modified version such as MUSLE has been widely used in most empirically based models.

The mass rate of transport is sediment discharge and the amount of eroded materials delivered to a point in a catchment within a specified period of time is known as sediment yield. Sediment yield does not necessarily equate to erosion rate because not all the eroded sediments enter the stream system. Some sediment is temporarily deposited at natural or human-created sites (e.g., reservoirs) within the catchment; other sediment might be deposited within the channels or floodplains. Sediment yield is defined as follows:

$$SY = \frac{100 * SM}{\beta * Y} \quad \text{(Eq. 3)}$$

$$SSY = \frac{SY}{A} \quad \text{(Eq. 4)}$$

Where:

SY = Absolute sediment yield (ton y^{-1})

SM = Total sediment mass deposited in the reservoirs (t)

β = Sediment trap efficiency (%)

Y = Age of the reservoir (yrs)

SSY = Specific sediment yield (ton ha^{-1} y^{-1})

A = Catchment area (ha)

Thus, sediment yield deposition depends on variables controlling erosion and sediment delivery. The Sediment Delivery Ratio (S_{DR}) expresses the ratio of sediment yield (SY) at given cross section to the gross erosion (A_T) from the watershed upstream and control point (Julien, 1998).

$$SY = A_T S_{DR} \quad \text{(Eq. 5)}$$

To compute sediment delivery ratio, gross erosion can be calculated using the Universal Soil Loss Equation (USLE). USLE is an empirical method for determining relevant parameters among the many physical variables comprising climate, soil profile, relief, vegetation, and land

use and land management practices, which are respectively indicated by R, K, LS, C, and P. Because of great variance among a large number of interrelated hydrologic and physical factors, this method may not be applicable to larger watersheds. The empirical method application might be feasible if the catchment area is subdivided into smaller sub-basins, as long as parameters are determined for each sub-basin. The USLE equation is:

$$A = R \cdot K \cdot L \cdot S \cdot C \cdot P$$ (Renard et al., 1994) (Eq. 6)

Where:

A = Expected annual soil loss (tonnes ha−1 yr−1)

R = Rainfall erosivity in (MJ mm ha−1 h−1 yr−1)

L and S = Topographic factors that describe hill slope length and hill slope steepness (dimensionless), respectively

K = Soil erodibility in (Mg ha h ha−1 MJ−1 mm−1)

C and P = Cover-management practices and support practices factors that describe land use, respectively

USLE was modified by Williams (1975) by replacing the R factor with a runoff factor to create the modified soil loss (MUSLE) equation (Equation 7). The main goal of the MUSLE is to overcome the limitations of USLE. These limitations includes less adaptation capability to new environments, site specific (not appropriate for catchment scale), and not accounting for deposition at the lower parts of the hill-slope, which is relevant in relation to sediment and pollution transport toward rivers and reservoirs.

$$As = 11.8 * (V\omega * Qp) * K * L * S * C * P$$ (Williams, 1975) (Eq. 7)

Where:

As = Calculated soil loss per area

Vφ*Qp = Vφ is the volume of runoff (m^3); Qp is the peak flow rate (m^3/s) of the storm

L and S = Topographic factors that describe hill slope length and hill slope steepness (dimensionless), respectively

K = Soil erodibility in (Mg ha h ha−1 MJ−1 mm−1)

C and P = Cover-management practices and support practices factors that describe land use, respectively

Substituting a rainfall factor with an empirical runoff energy factor allows the model to predict the sediment yield from single storms. MUSLE provides better prediction of soil loss and sediment delivery because it has improved the ability to incorporate the effects of soil roughness and the effects of local weather (Renard et al., 1997).

Gross erosion is roughly estimated by USLE and MUSLE for soil loss caused by sheet, rill, and rain splash, but erosion caused by landslides and gullies cannot be computed using these equations. The erodibility factor indices were obtained using the Modified Soil Loss Equation (MUSLE) processes in a Geographic Information System (GIS) framework. The input parameters in the GIS framework comprise erosion factors such as rainfall erosivity, soil erodibility, topography factor and a cover factor (Basson et al., 2009).

2.7. Physically Based Models

Physically based models are based on theoretical relationships between erosion and variables controlling sediment yield. Such models compute stream flow and sediment transport processes involved in erosion and sediment yield in a specific time period and space. Examples include WEPP (Water Erosion Prediction Project), ANSWERS (Areal Non-point Source Watershed Environmental Response Simulation), EUROSEM (European Soil Erosion Model),

CREAMS (Chemicals, Runoff, and Erosion from Agricultural Management Systems), and SWAT (Soil Water Assessment Tool).

2.8. Soil and Water Assessment Tool (SWAT) Model

2.8.1. SWAT Description

The Soil and Water Assessment Tool is a continuous, long term, physically distributed model designed to predict the impact of land management practices on the hydrology, sediment yield, and water quality in agricultural watersheds (Arnold et al., 1998). The SWAT model was developed by US Department of Agriculture – Agriculture Research Service (USDA-ARS) at the Grassland, Soil, and Water Research Laboratory in Temple, Texas as an integrator of simulators such as SWRRB "Simulator for Water Research Basins", ROTO "Routing Outputs to Outlets", CREAMS "Chemical, Runoff, and Erosion from Agricultural Management Systems", GLEAMS "Ground Water Loading Effects on Agricultural Management Systems", and EPIC "Erosion-Predictability Impact Calculator" (Arnold et al., 1998).

2.8.2. The structure of SWAT

The SWAT model, which operates on a daily time step with up to monthly/annual duration, can be considered as a hydrological transport model at the catchment scale consisting of weather, hydrology, erosion/sedimentation, nutrients, channel routing, plant growth, and agricultural management components. The model, based on a water mass balance, uses the stream power equation of Bagnold (1966), which also simulates hydrology as comprised of land hydrology and channel hydrology for each hydrologic response unit (HRU), which is a unique combination of soil and land-use characteristics. SWAT divides a watershed into HRUs assuming there is no interaction between HRUs; in other words, each HRU is non-spatially distributed. According to Neitsch et al. (2005), simulation computational costs can be minimized within the HRU delineating

process by lumping similar soil and land-use areas into a single unit. The main structure of the working order of the program is initially computing fluxes for each HRU, then aggregating the results to sub-basin outputs based upon the fraction of the HRUs, and finally routing sub-basin outputs through a river reach within the channel network. A physically based hydrological model, SWAT also predicts snowfall and melt, and vadose zone processes including infiltration, evaporation, lateral flow, plant uptake, percolation, and ground water flow (Neitsch et al., 2005).

2.8.3. SWAT model for sediment yield

The SWAT model can be used for sediment yield predictions for planning and management of water resources and reservoir sediment controls at the catchment scale. The modeling method is applicable to temporal and spatial analysis of sediment yields, of which the results are essential for reservoir management strategies.

SWAT can also be a potential tool in predicting sediment yield, especially at the catchment scale, because it considers spatial and temporal variation based on different potential physical variables. The model can also provide a better understanding of sediment transport and deposition processes by overland flow and allow reasonable prediction and forecasting. Sediment yield is the sum of the sediments produced by overland flow, gully, and stream channel erosion in a catchment. The main factor controlling sediment yield in general is the transport capacity of runoff (Mutchler et al., 1988). Sediment transport in the channel network is a function of degradation and aggradation (Neitsch et al., 2005). The current version of the model routes the maximum amount of sediment in a reach as a function of the peak channel velocity and estimates sediment yield for each HRU using MUSLE (Williams, 1975).

2.8.4. Sensitivity Analysis for the SWAT model

Model sensitivity analysis helps to assess the relative sensitivity of model outputs with respect to the changing of model parameters, which is generally the first step of model calibration. Sensitivity analysis can determine which parameters in the watershed are most sensitive and these parameters need to be adjusted based on the sensitivity analysis. The model calibration requires identifying the controlling parameters and parameter precision (Ma et. al., 2000). Sensitivity analyses are performed in different ways: local, which involves changing values one at a time, and global, which is the ability to change all the parameter values simultaneously. Because the sensitivity of each parameter depends on the other related parameters, the results may vary.

Numerous sensitivity analyses have been reported in the SWAT literature and the method implemented in SWAT is called the Latin Hypercube One Factor-At-a Time (LH-OAT) design (Morris, 1991). The method can be used for sensitivity analysis of stream flow and sediment load at one or multiple gages in an agricultural watershed in semiarid regions. The model performance was analyzed by using combinations of Nash-Sutcliffe efficiency coefficient (NSE), relative error (RE), and correlation coefficient (R^2) that aggregate information contents from multiple sites and multiple variables using SWAT parameters. The Spearman's rank correlation coefficient is engaged to assess the correlation between sensitivity analyses from various likelihood functions (Ahmadi et al., 2014). The parameter sensitivity with various likelihood functions might vary, mainly in relation to the objective function used for model evaluation in the sensitivity analysis.

2.8.5. Calibration - validation applications

Many previous SWAT publications describe calibration and validation approaches used for verification of model accuracy for the simulated conditions. The first step of calibration and validation in SWAT is the sensitivity analysis mentioned earlier. A second step is calibration in an

effort to better parameterize a model to a given set of local conditions, thus reducing the prediction uncertainty. Calibration is performed by selecting values for model input parameters with some uncertainties by comparing outputs (model predictions) and observed data for the same conditions. The two main calibration methods commonly applied in the literature are manual calibration and auto calibration (van Griensven and Bauwens, 2005; Van Liew et al., 2005; or SWAT-CUP, Abbaspour et al., 2007). The parameters may be manually calibrated until the model simulation results are acceptable as per the model performance measures. Next, the final parameter values can be used for the initial values for the auto-calibrations for the stream flow and sediment load in SWAT.

Model validation is the final step for the components of interest (stream flow, sediment yield, and water quality). Validation is the process of demonstrating the capability of making a sufficiently accurate simulation, which may vary based on the aim of a project (Refsgaard, 1997). Predicted and observed values are compared to determine whether the objective function satisfactory involves running a model using the parameters during the calibration, and comparing the results from the different periods of calibration to determine whether the model meets confidence limits. A good model calibration and validation should have: multiple evaluation techniques (ASCE, 1993, Boyle at al., 2000); observed data with variations including wet, average and dry seasons (Gan et al., 1997); all constituents calibrated; and verification that other important outputs are acceptable. Statistics and graphs can be used to determine when the model has been satisfactorily calibrated and validated.

2.8.6. Limitations of the SWAT model

The parameters obtained from formulas (i.e., curve number) are not directly measured, so the equation for runoff volumes has some uncertainties because the parameters are determined

empirically based on various land-use characteristics. In terms of determination of soil erosion simulation, as mentioned earlier the model uses MUSLE, but the parameters used in the equation are set from qualitative data (i.e., soil types and land cover).

The model limitations are mainly modeling snowmelt, evapotranspiration, floodplain erosion, and sediment transport routing. If the model underestimates base flow during winter and spring, the problem might relate to the snowmelt documented in previous studies. For example, Peterson and Hamlett (1998) experienced some difficulties in capturing snowmelt periods using the SWAT model. Underestimation of evapotranspiration may cause overestimation of flow in summer periods. If other systematic data beyond temperature and precipitation are unavailable, a weather generator in SWAT can be used to estimate solar radiation, wind speed, soil and canopy cover characteristics, which create more uncertainties in the SWAT output. The SWAT version of the MUSLE algorithm is the USLE, which is designed to simulate erosion based on sheet, rill, and flow runoff. The MUSLE equation employed by SWAT is developed to simulate sediment routing as a result of each storm event (William and Berndt, 1977). Consequently, the model cannot simulate detailed event-based stream flow and sediment routing even though the best results could be gathered from long term sediment and erosion simulations (Arnold et al., 1998).

Finally, the SWAT sediment routing algorithm uses Bagnold's stream power equation (1966) to predict the maximum transportable sediment yield, even though stream velocity through Bagnold's equation (Eq. 7) does not reflect other sediment transport characteristics such as bottom shear stress.

$$\Omega = \rho g Q S \qquad \text{(Eq. 8)}$$

Where

Ω is the stream power (W/m²),

ρ is the density of water (1000 kg/m3),

g is acceleration due to gravity (9.8 m/s2),

Q is discharge (m3/s),

S is the channel slope (m/m).

On the other hand, the SWAT model is capable of continuously predicting stream flow and sediment transport in a semi distributed watershed, and analyzing the impact of different sub-watersheds. It is also a viable model to use for simulating water balance and sediment transport in a larger watershed for investigation of agricultural management (Santhi et al., 2001).

2.8.7. Other mathematical models

A wide range of mathematical approaches have been used to determine sediment yield from land (natural - disturbed) surfaces (Table 1). These include "lumped" parameter models and models based on the regression analysis of USLE. Lumped and regression models may not represent all hydrologic processes and some other models do not consider the environment and dynamic changes (time – location). Stochastic modeling is another approach, but is somewhat difficult to apply and does not reflect ground water changes as a response to change in land-use activities (Shen and Li, 1976).

Table 1: Agricultural non-point source models (Compiled from: Knisel, 1980; Beasley and Huggins, 1981; Abbott et al., 1986; Young et al., 1986; Lane and Nearings, 1989; Novotny and Olem, 1994)

Process-Oriented Seidment Models	**Applications**	**Time Scale**	**Spatial Scale**
ACTMO (Agricul. Chemical Transport Model)	Hydrology, Water Quality	Event, Continious	Field
AGNPS (Agricul. Nonpoint Source Pollutoion)	Hydro., Erosion, Pesticides	Event, Daily, Continious	Grid Cell, Field
ANSWERS (Areal Non-point Source Watershed Environment Response Simulation)	Hydro., Erosion, Pesticides	Single Storm	Grid Cell
CREAMS (Chemical, Runoff and Erosion from Agriculture Management Systems)	Hydro., Erosion, Pesticides	Daily, Continious	Field
DWSM (Dynamic Watershed Simulation Model)	Hydro., Erosion, Pesticides	Event, Daily, Continious	Field
EPIC (Erosion-Productivity Impact Calculator)	Hydro., Erosion, Management	Event, Daily, Continious	Field
HPSF (Hydrologic Simulation Program-FORTRAN)	Hydro., Wtr Quality, Pollutants	Event, Daily, Continious	Watershed
SHE (Systeme Hydrologique Europeen)	Hydrology, Water Quality	Event, Daily, Continious	Watershed
SWAM (Small Wtaershed Model)	Hydro. Sed. Nutrients, Pest.	Daily, Continious	Watershed
SWAT (Soil ans Water Assesment Tool)	Hydro. Sed. Nutrients, Pest.	Event, Daily, Continious	Simultaneous simulation of subbasin
WEPP (Water Erosion Prediction Project)	Hydro. & Sediment Processes	Single storm, Daily, Continious	Hillslope watershed grid cell

Most of the models that have been developed in the last couple of decades to provide information on erosion and water quality, such as the Dynamic Watershed Simulation Model (DWSM), Chemical, Runoff and Erosion from Agricultural Management System (CREAMS), and Hydrological Simulation Program – Fortran (HSPF), are more appropriate than earlier models because of the development of computing power. However, providing catchment scale analysis and event-based predictions of sediment loads constrain model performance; therefore, these models can suffer from a range of problems including unrealistic input requirements, over-parameterization, parameter values to local conditions, unsuitability of model assumptions, and inadequate documentation of model testing and resultant performance (Simons and Senturk, 1992). The SWAT model gives more consistent results for stream flow in agricultural watersheds in various climates than HSPF and DWSM (Van Liew et al., 2003; Saleh and Du, 2004).

2.9. Depositional Processes of Reservoir Sedimentation

Soil erosion, especially from river channels and floodplains, provides a continuous supply for sediment transport in rivers. These sediments seasonally accumulate along the stream bed or in human-made reservoirs. Reservoir storage capacity can be classified into three types: (1) the dead storage volume (volume below the lowest outlet level), (2) the active storage volume (between lowest outlet and normal surface level), and (3) the flood control storage volume (between normal and maximum surface level).

2.9.1. Sediment deposition in a reservoir

All reservoirs or natural lakes are subject to some degree of sediment inflow and deposition. When stream flow enters a reservoir, transport capacity of the water is reduced; hence sediment accumulates within a reservoir based on grain size, physical shape of the reservoir, and operational practices.

The amount of sediment deposition in a reservoir is controlled by the type of sediment deposited (suspended or bed load), the detention storage time, the shape of the reservoir, and operational practices. Sedimentation falls into three basic categories in a reservoir: (1) deltaic deposition of gravel or coarse sand deposited in the entrance, (2) deposition of fine sediments (silt-mud) from homogenous flow, and (3) deposition of fine sediments (silt-mud) from stratified flow. Horizontal strata or thin bands present across the bottom of a reservoir are where incoming sediment load is trapped and deposited most of the time (van Rijn, 1993).

2.9.2. Temporal and spatial variation of sediment deposition

Temporal and spatial sediment deposition in artificial reservoirs is often controlled by the interaction of human modifications and natural factors that include floods, bed morphology, sediment supply, and hydrodynamics. However, the relative importance of and interaction between different variables thought to control temporal and spatial variations in sediment deposition rates are poorly understood because only a few studies have addressed both temporal and spatial variation and the physical processes controlling sediment variation. Such studies, which are extremely important for understanding basic mechanisms of reservoir sedimentation, have been carried out mainly in US and European dams (Williams and Matthews, 1983; Hampson, 1997; Hecht, 2000).

In terms of seasonal changes at finer scale, stream discharge has a significant influence on suspended sediment concentration, with most of the sediment load transported during the peak flow (Leopold et al., 1964; Allan, 1995). Besides spring snowmelt runoff between March and June, a catchment may have a rainfall runoff event in spring which substantially reduces deposition due to higher stream velocity and stream power. Hence, the largest peak flow corresponds to the highest suspended sediment concentration, but lower sediment accumulation.

2.9.3. Modelling the spatial distribution of sediments in a reservoir

Geographic Information System (Evans et al., 2002) and remote sensing satellite images (Solomonson, 1973; Holeyer, 1978; Khoram, 1981) can be useful tools in modeling bathymetry and the spatial distribution of sediment accumulation in a reservoir. Smith et al. (1980) also tried to determine reservoir siltation in the world's largest human made reservoir, behind the Aswan Dam, by using infrared areal images. Their results indicate that siltation during peak flow was largely confined to the deltas of main streams entering the reservoirs. The area of extensive siltation and the amount of sediment accumulation were determined by bathymetric surveys.

Previous studies have mostly focused on sediment deposited in larger reservoirs. The two most common empirical methods are the Area – Increment Method (AIM) (Cristofano, 1953) and the Empirical Area – Reduction Method (EARM) of Borland and Miller (1958), which was developed on the basis of siltation process of dead storage from 30 reservoirs. With respect to the scarce studies of sediment deposition in a small reservoir, Dendy (1982) represents the method of spatial bottom sediment distribution in reservoirs of storage capacity from 20,000 m^3 to 1.7 million m^3. Michalec et al. (2008) elaborated Dendy's method for smaller reservoirs at Zeslawice on the River Dlubnia. They found that over 58% of sediment accumulates in the reservoir delta.

CHAPTER THREE:

STUDY AREA

3.1. National Context

Seventy-nine percent of agricultural land in Turkey has slopes steeper than 10% and the average elevation is ~ 1140 m. Land use substantially affects sediment yield caused by soil erosion. Patterns of rainfall and wind also strongly affect erosion. In addition, most of the lands with agricultural potential are used for urban purposes. Studies performed by the Electrical Resources Survey Administration of Turkey indicate that 400 million tons of suspended sediment is transported by natural streams annually, which shows that Turkey has been losing 1 mm of soil every two years. Previous work in Turkey suggests that topography, land cover, and disturbances such as excessive grazing, deforestation, and improper agricultural techniques influence sediment yield. In Turkey, most attempts to manage sediment are implemented by the government on public lands. Corporations rarely practice restoration because rivers and reservoirs are owned and operated by the federal government.

The study site generally receives precipitation of less than 500 mm, and precipitation volumes fall below 400 mm on the plains and plateaus of the watershed. For example, the Ankara Plateau receives an average annual precipitation of 375 mm. However, the value of annual precipitation varies between 216 mm and 610 mm in the period from 1925 to 2000. Rainfall occurs mostly at low values and the frequency of peaks is low. Spring is the wettest season in the study area, with 34% of the annual precipitation occurring during spring based on the long term precipitation data (Figure 5).

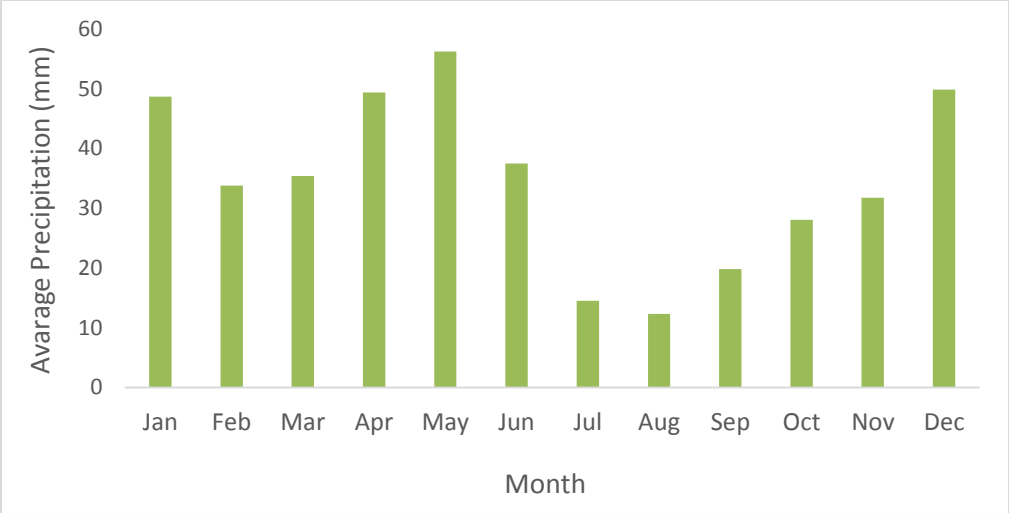

Figure 5: Variation of average precipitation (mm) in Ankara

Over long term records, temperature typically varies from -6.1^{0}C to 29.5^{0}C and is unlikely to go below -14^{0}C or above 34^{0}C. The likelihood of snow falling is highest from November 21 to March 31, occurring on 33% of days. During peak snow season, the chance of having snow on the ground is the highest at the end of January, occurring 27% of time. Snowfall occurs 14.1 days/years and temperature below 0^{0}C is around 121 days/year, so during winter the snow is typically at its deepest at the end of February, with a median depth of 3 meter. According to Langbein and Schumm (1958), a change to either a wetter or a drier climate may decrease erosion rate, owing to either increased vegetation density or a decrease in runoff without change in temperature.

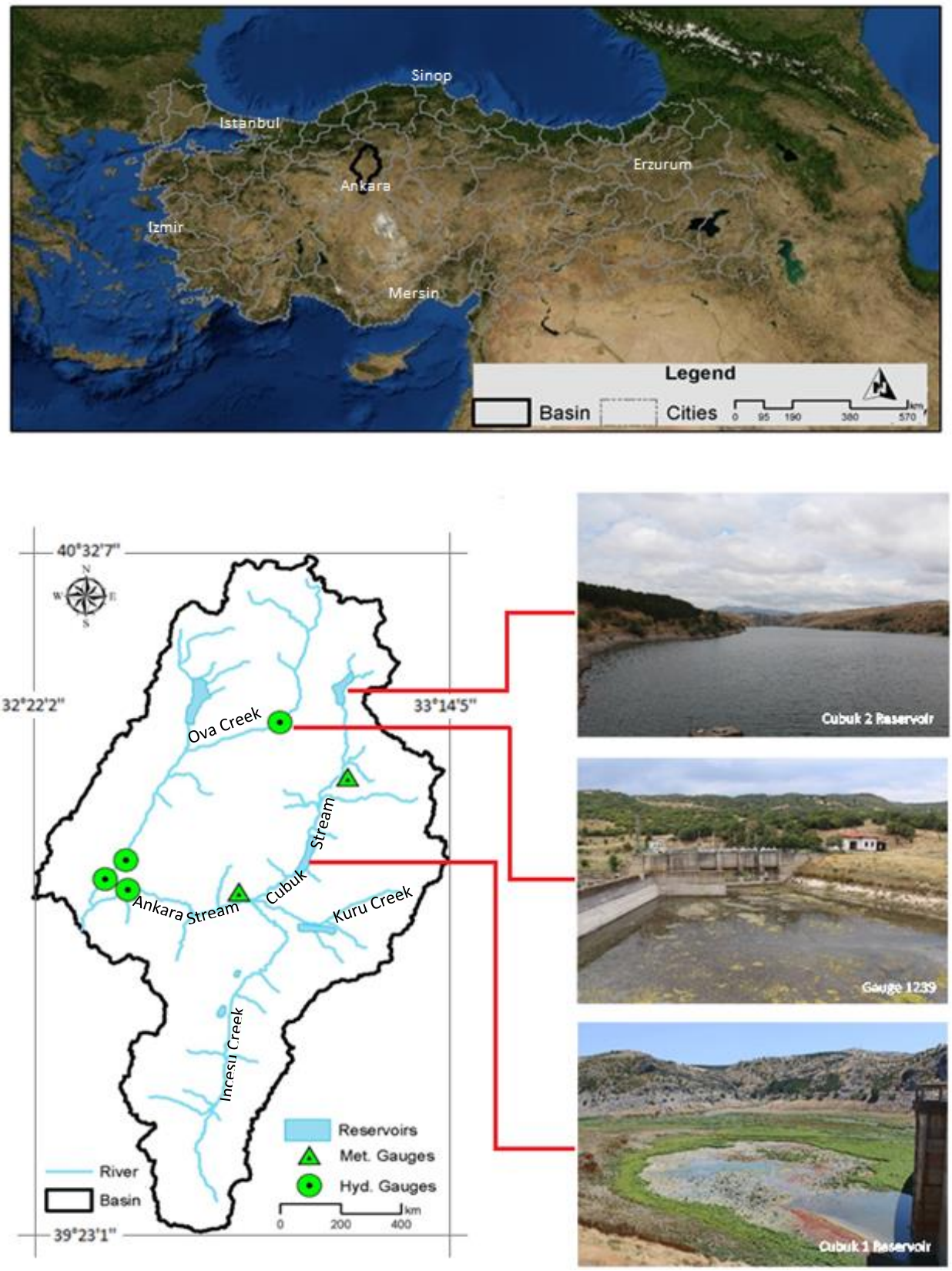

Figure 6: Location of the Ankara River Basin and its network

The city of Ankara includes 12,200 km² as agricultural lands, of which 8,100 km² was cultivated area and 3,350 km² was fallow lands in 2014 (TUIK, 2015). About 82% of the cultivated area is devoted to cereals. Wheat is the principal crop, accounting for more than half of total grain production in 2014, followed by barley. Sugar beets and grapes are the other primary crops in the study area. However, the lack of spatially distributed crop type data and agricultural practices (e.g., tillage) in the watershed can be considered another limitation on this research.

3.2. The Ankara River

The Ankara River, 140 km in length, is tributary to the Sakarya River that runs through the city of Ankara and carries waste water from the city and sediments along the river. The Ankara River network includes the tributaries Cubuk Creek, Zir Creek, Hatip Creek, Incesu Creek, and also some smaller inputs from Eymir and Mogan Lakes. The Ankara River (Figure 7) merges with the Sakarya River after passing the town of Ayas.

3.3. Cubuk Creek

Cubuk Creek is 70 km long and is the main study site of this research. The Cubuk that runs through the town of Cubuk joins the Ankara River. The stream originates from the Aydos Mountains and feeds Cubuk II and Cubuk I Reservoirs. The outputs from those reservoirs pass through the Asagi Cavundur Plain. Cubuk Creek is joined by the tributaries Koyunozu Creek, Ravlı Creek, and Akkuzulu Creek. The Cubuk merges with the Ankara River after passing the village of Omercik. According to the sediment, hydrologic, and meteorological inputs shown in Figure 6, 32 years (10,957 days) of daily data from the 1239 gage indicate that Cubuk Creek (Figure 8) is an ephemeral stream.

Figure 7: Stabilized portion of Ankara River along the town of Ayas

Figure 8: Restored portion of Cubuk Creek belongs to the lower course of Cubuk I Reservoir

Both the Ankara River and Cubuk Creek illustrate the general characteristics of flashy streams in which stream flow rises sharply after rainfall and then falls more gradually. Discharge varies seasonally, with higher flow in the winter and spring and lower flows during summer and early fall. The streams have deposited alluvial materials (gravel, sand, clay, and silt) to a depth of 25-30 m and a width of 1-1.5 km along the channels, thus many sandpits have been operated within the streams.

3.3.1. Cubuk I Reservoir

Cubuk I, a concrete gravity dam, is located 12 km north of the center of Ankara city, on Cubuk Creek (Figure 9). Cubuk Creek, with a total length of 70 km, originates from the southern side of the Aydos Mountains at an elevation of 2044 m, and has two moderately large (approximately 1 km² (Cubuk I); 1.2 km² (Cubuk II)) reservoirs. Cubuk I was the first reservoir built in the Republic of Turkey. The construction of Cubuk I began in 1930 and was completed in 1936 with no power unit (Figure 9). The main purpose of the reservoir is flood control and domestic - industrial water supply to Ankara, the capital of Turkey. Because of a huge amount of siltation, the reservoir has been recently used only for recreational purposes. The initial capacity of the reservoir is smaller than the annual discharge of the watershed: capacity loss is approximately 50% (Yilmaz, 2003). Clay and silt dominate reservoir sediments (Kilic, 1986).

3.3.2. Cubuk II Reservoir

Cubuk II Reservoir was built in 1963 on Cubuk Creek 54 km north of Ankara. After construction of Cubuk II between 1964 and 1983, sediment yield in the basin was 350 ton/year/km² (Kilic, 1986). Recently, Cubuk II Reservoir (Figure 10) has been used for recreational and water supply. Andesite, basalt, and volcanic agglomerate are abundant in the region (Table 2).

Figure 9: Cubuk I Reservoir

Figure 10: Cubuk 2 Reservoir

Table 2: Some characteristics of Cubuk I and Cubuk reservoirs in Central Turkey

Characteristics	**Cubuk I Reservoir**	**Cubuk II Reservoir**
Geographic Coordinates	40.004763, 32.933904	40.305479, 33.016605
Drainage Area	910 km²	190 km²
Mean Annual Precipitation	418 mm	448 mm
Elevation	890 m	1005 m
Basin Slope	0.013 %	0.006 %
Relief Ratio	0.0033	0.0296
Geology	Triassic aged volcanic / metamorphic rocks	Triassic aged volcanic rocks
Land Cover	Cultivated lands	Grasslands

CHAPTER FOUR

DATA COLLECTION AND ANALYSIS

4.1. SWAT Data

SWAT, a modular interactive program, provides algorithms for calculating different watershed dynamics. The ability of the SWAT model to depict processes in a particular watershed is partially dependent on the quality of input data containing hydrologic, meteorological, topographic, snow, and watershed descriptions (Table 3) (Figure 11).

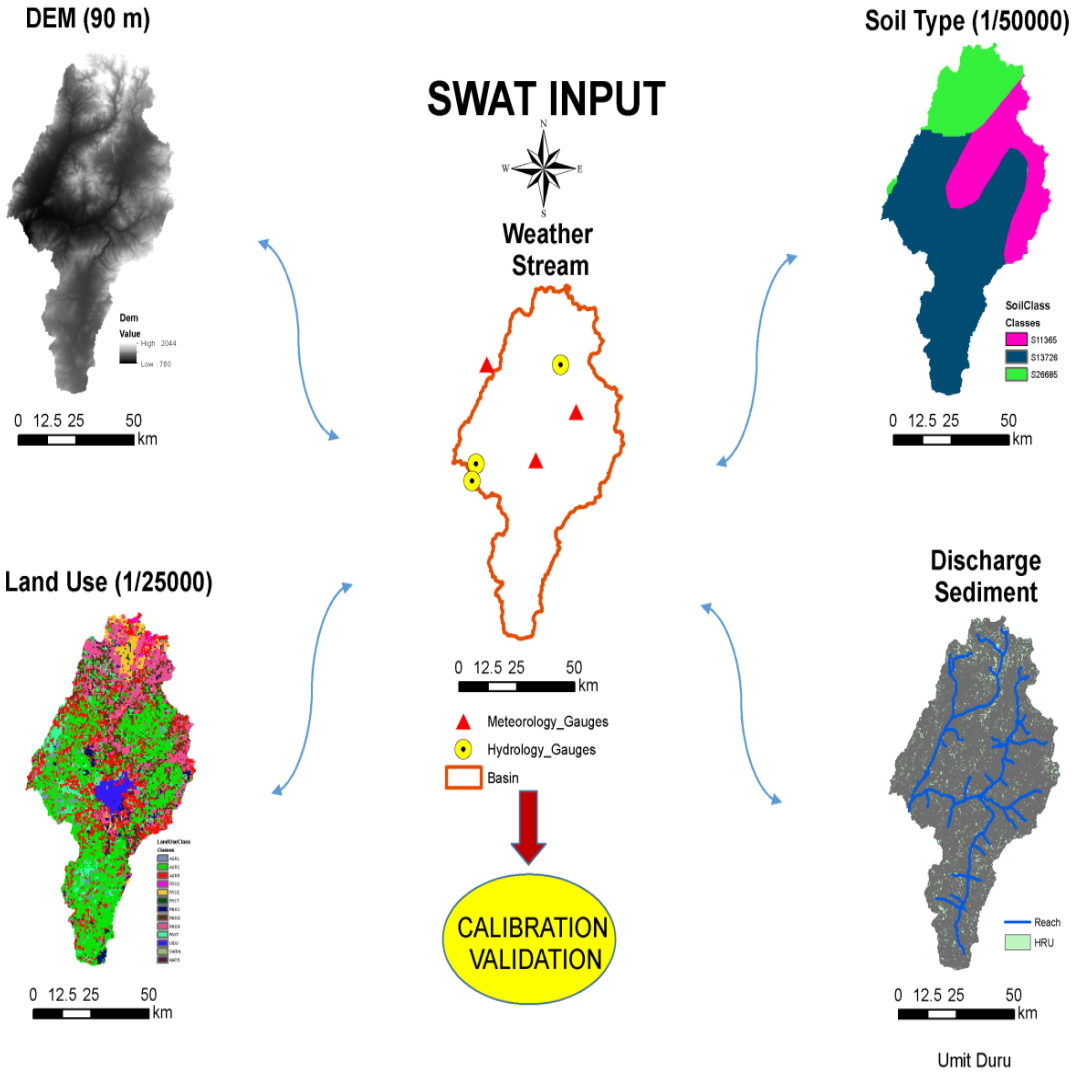

Figure 11: Demonstration of the SWAT input data

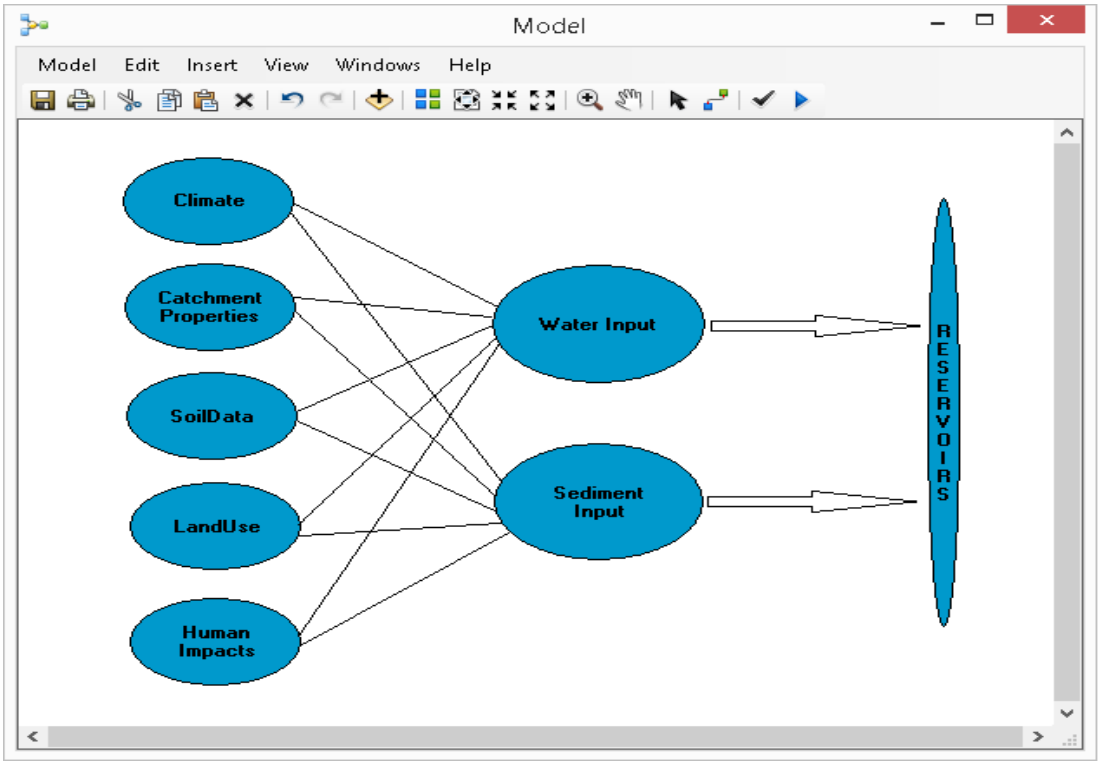

Figure 12: Screen capture of selected variables controlling input and sediment yield to the reservoirs in the study

SWAT is a river basin scale, continuous time and spatially distributed model developed to predict the impact of land management practices on water and sediment yield in large complex watersheds with varying soil, land use, and management conditions over long periods of time (Arnold et. al., 1998; Neitsch et al., 2005) (Figure 12).

Table 3: Spatial model input data for Cubuk Creek.

Data Type	Description	Source	Resolotion / Scale
Hydraulic Data	Monthly Qs (ton/month)	State Hyrdaulic Works	1239 Station
	Daily Q (m^3/sn)	State Hyrdaulic Works	1239 Station
Meteorological Data	Daily Precipitation / Temperature	Turkish State Meteorological Services	17128 - 17130 Stations
	Evaporation / Wind Speed		
Bathymetric Maps	in 1978 - in 1983	State Hyrdaulic Works	1/5.000
Areal Images	in 1967 - in 1991 - 2013	General Command of Mapping	1/50.000
Land-Use and Land Cover Map	in 1990 - in 2000 - in 2010	The Global Land Cover	1/100.000
Topography Map	Digital Elevation Map, Topography Map	USGS, Gnl Command of Mapping	90m, 1/62.500

4.1.1. Hydrologic Data

Hydrologic data consisting of stream flow and suspended sediment load were obtained from the Department of Surveys and Planning in DSI (State Hydraulic Works) as printed data. The 1239 runoff gaging station is the closest station to the study reach (Figure 6). The missing values from the Ova Cayi Eybek station (1239) were replaced with -99 in an Excel worksheet, and stream flow indicating 0 was replaced with 0.0001 for LOADEST because the program uses logarithm units, so "0" stream flow creates an error. LOADEST was used to estimate constituent loads in the stream and rivers on a monthly basis because the observed sediment load data are instantaneous.

The gage (1239) started collecting stream discharge data in 1967 and closed in 2003, so the daily discharge data between 1970 and 2002 have been obtained from this station. Water discharge is obtained from DSI (Turkish State Hydraulic Works). These are mean monthly discharges between 1973 and 2008. Using these monthly data, the mean annual discharge was calculated for the reservoirs. These two data sources have also been used for automatic calibration and validation. The model was run daily for 30 years; the period from 1987 to 1996 with 2 years warm-up period was used for automatic calibration and the period from 1980 to 1984 with 2 years warm-up period was used for validation. The modeling period considered based on data availability. Surface runoff was determined by rainfall intensity, duration, and distribution of geology and surface cover.

4.1.2. Meteorological data

SWAT requires daily data of minimum and maximum temperatures, precipitation, solar radiation, wind speed and relative humidity. The Turkish State Meteorological Organization (DMI) mainly makes rainfall and temperature observations. Both of these types of data have also been collected by the Turkish State Hydraulics Works (DSI), General Directorate of Agriculture Research (TAGEM) (former General Directorate of Rural Service (GD)), and Electrical Power

Resources Survey and Development Administration (EIE). Meteorological data such as minimum and maximum daily temperature and daily precipitation from 1970 to 2003 used in SWAT were obtained at the 17128 and 17130 stations of the Turkish State Meteorological Service (Figure 11). I have obtained monthly precipitation (total, maximum, minimum), snowy days, and evapotranspiration data from the State Hydraulic Works stations 12006 Cubuk I (1960 - 1993) and 12013 Cubuk II (between 1964 - 1989), and I have finally got monthly precipitation and temperature data from the two different stations of global weather data.

Meteorological files were prepared in an Excel sheet based on the format of SWAT using long term monthly averages of data. Statistical parameters are generated from these long term daily data. The Custom Weather Generator in the SWAT simulation was engaged in order to simulate the missing observations and input data. In addition, these data were used for deriving daily precipitation and min – max air temperature for the period of 1980 – 2003. Charts were made to understand whether long-term changes in temperature and precipitation would influence the amount of sediment in the stream.

4.1.3. Land-use data

The Global Land Cover 2000 (GLC 2000) data files consist of the water surfaces, vegetation, and cultural features on the land surface at the scale of 100,000. The European Commission provides the datasets and associated maps as part of its Land Research Management Unit in Joint Research Centre, and USGS LULC Scheme in http://edc2.usgs.gov/glcc/ tablambert_euras_eur.php was used. The land use and land cover data are available via the internet at (http://bioval.jrc.ec.europa.eu /products/glc2000/products.php) (Figure 11).

Table 4: Land cover classification of the Global Land Cover

	Code	Name	Plant Type
1	AGRL	Agricultural Land – Generic	warm season annual
2	AGRC	Agricultural Land - Close - grown	cool season annual
3	AGRR	Agricultural Land - Row – Crops	warm season annual
4	FRSD	Forest – deciduous	trees
5	FRSE	Forest – evergreen	trees
6	FRST	Forest – mixed	trees
8	RNGE	Range – grasses	perennial
9	RNGB	Range – brush	perennial
10	PAST	Pasture	perennial
11	UIDU	Mineral extraction sites	not applicable
12	WATR	Water body	not applicable

Table 5: Land use classification of the year 2010

	Code	Name
1	AGR	Agricultural Land
2	FOREST	Forest
3	GRASS	Grasses
4	BRUSH	Brushes
5	PASTURE	Pasture
6	INDS	Industry
8	ARID	Arid Land
9	WATER	Water Body

The land cover data were interpolated to the format that is applicable for SWAT by merging some of the similar land cover types and creating a look-up table (Table 4). National Land Cover Database format is commonly used in the model simulations (Table 5).

The Turkish General Command of Mapping has produced aerial images of Turkey at 1/50,000 scale. The areal images (1967 – 1991) of the areas surrounding Cubuk I and Cubuk II Reservoirs were obtained in 2012. Furthermore, infrared images taken by The Turkish General Command of Mapping in 2013 were obtained in order to identify land use characteristics and sediment deposition along the boundaries of the Cubuk I and Cubuk II reservoirs (Figure 13).

Google Earth was also used to identify sediment concentration spatially and to verify the land use/cover data obtained from the Ministry of Forestry and Water Works of Turkey. Changes in the reservoir boundaries were examined and related to bottom topography and physical variables.

These three tools have been used to classify land use and land cover types and area coverage in Cubuk Creek. In other words, the data were used to set the SWAT model and correlate land use/cover with suspended sediment yield rate in the watershed.

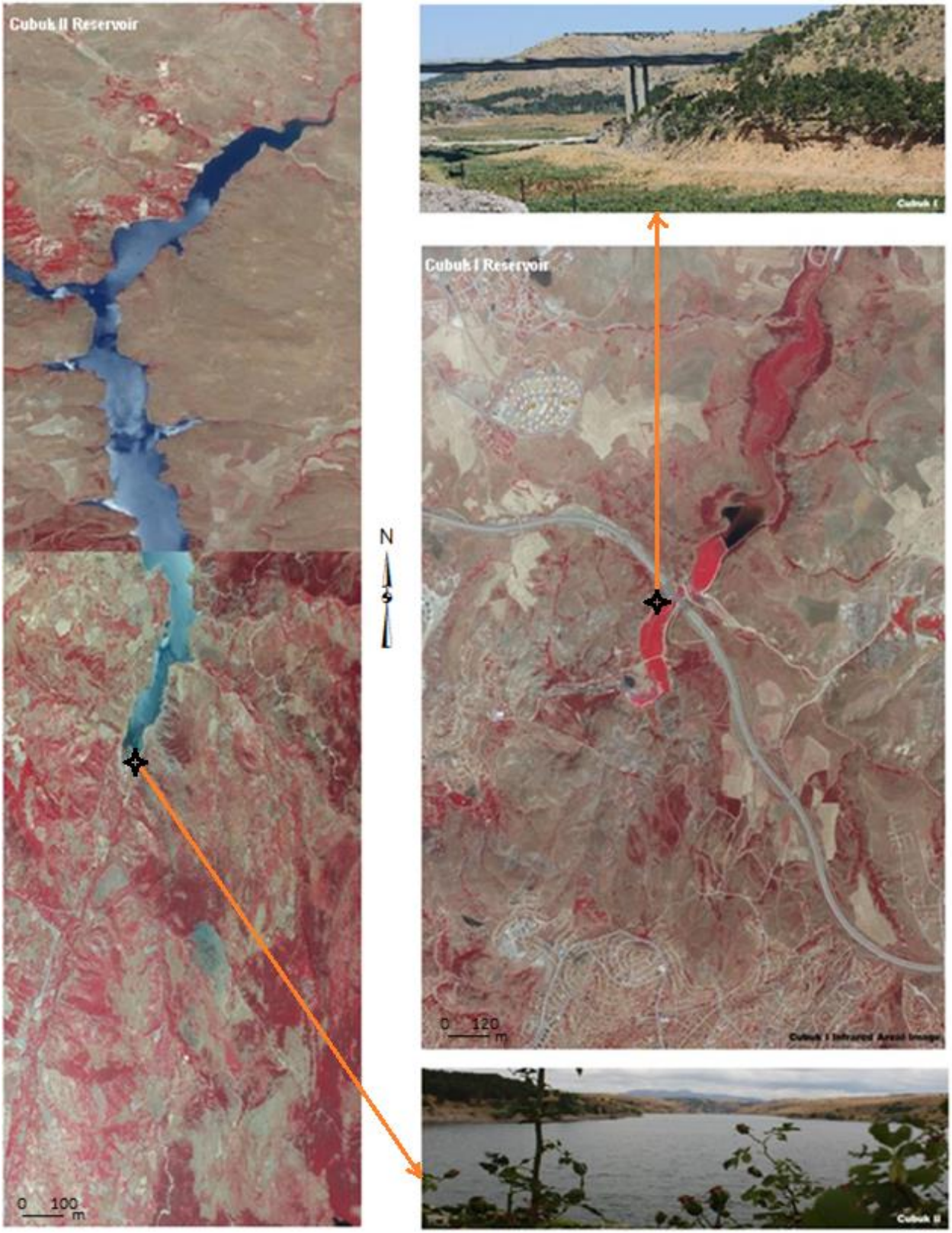

Figure 13: Infrared areal images of Cubuk I and Cubuk II Reservoirs.

4.1.4. Soil type data

The soil map of Turkey in scanned format was produced by the Turkish General Directorate of Rural Services. The service used TNT maps to convert to digital form 1/25,000 scale soil maps covering the nation. This scanned format and soil types are not appropriate for simulations using SWAT; therefore, soil classification data obtained from FAO's HWSD database (http://www.fao.org/nr/land/soils/harmonized-world-soil-database/en/) and HWSD format were converted to the APEX model within the watershed (Table 6). This could be easily used in SWAT with some minor modifications by using a lookup table for soil data.

There are three main soil types (heavy clay, silt + clay, and sand) in the study area based upon the HWSD Database. Heavy clay is widespread in the south of the watershed. The north side is mostly clay and silt, and the northeast side has sand (Figure 11). The soil map of the study site was used to set up a SWAT model and correlate soil type and suspended sediment yield rate in the watershed.

Table 6: Soil type input data

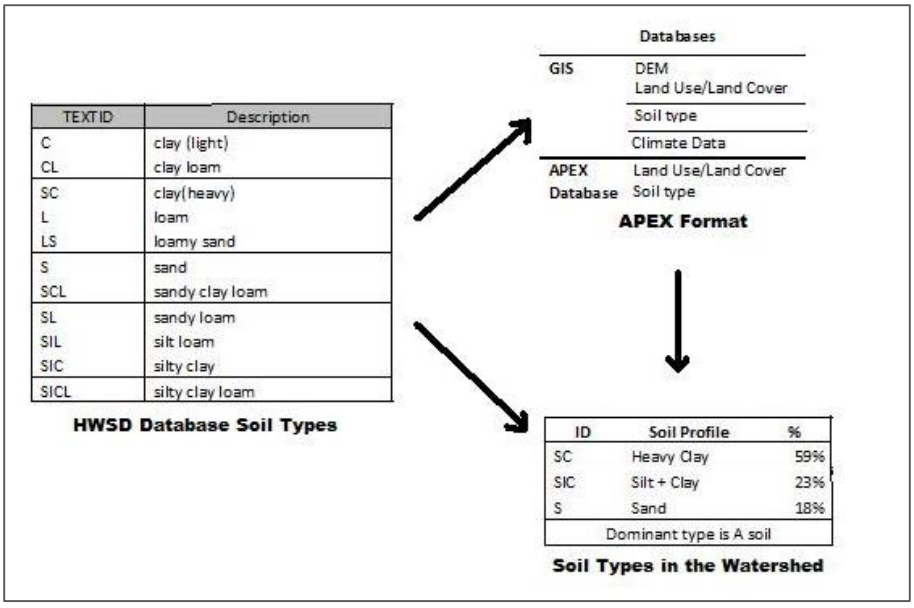

4.1.5. DEM (Digital Elevation Map)

Topographic data in the form of Digital Elevation Model (DEM) at a 90 m scale were obtained from the USGS (United States Geological Surveys web-site (http://eros.usgs.gov/#/ Find_Data/Products_and_Data Available/gtopo30_info) and DEM data were used to delineate the watershed and to analyze the drainage pattern of the land surface.

WGS_1984_UTM_Zone_36N projection is constructed in such a way that the area of Earth's surface between any pair of parallels and meridians is correctly preserved in the flat map representation. The projection parameters for the WGS_1984_UTM_Zone_36N projection are as follows:

- Units: meters
- Datum: D_WGS_1984
- Longitude of central meridian: 33
- Latitude of projection's origin: 0
- False easting: 500000
- False northing: 0

After the point coverage of the stations was created, the coverage could be used in conjunction with the DEM to determine the watershed boundaries.

4.2. Sampling Techniques

4.2.1.Stream Flow Sampling

The General Directorate of the Directorate of State Hydraulic Works (DSI) and the Electrical Survey Agency (EIE) operate the stream flow gaging stations. The gaging stations of DSI are generally installed on streams and their tributaries, whereas the gages of EIE are mainly located on the main rivers of large catchments. These data are published yearly for the corresponding water year.

4.2.2. Sediment Sampling

The State Hydraulic Works (DSI) has been gathering suspended sediment data using point sampling, point integration, and depth integration methods. Usually the most recent sampling uses the US.D-43 type of sampler, which can obtain vertical variation of suspended sediment at a river section (DSI report, 2005).

EIE has the second largest sediment collections department. The main duties of EIE are hydrologic studies, geotechnical studies, and restoration services for dams. The agency collects sediment and stream flow discharge and has published them in a book titled "Suspended Sediment Data and Sediment Transport Amount for Surface Waters in Turkey" in 1982, 1987, 1993 and 2000. Books of water quality were also published in 1989 and 1996. In the yearbook of EIE, the following sediment data were given for sediment station 1329 (Ova-Cayi Eybek);

- Rain area (km^2)
- Mean sand percentage (%)
- Net sediment weight (gr)
- Sand, silt + clay weight (gr)
- Mean sediment load (tons/year)
- Sediment yield of catchment (tons/year/km^2)

Suspended sediment concentration was also taken via the depth integration method using U.S.DH-48 and U.S.DH-49 samplers. The depth integrated sampler obtains the sample within a predefined depth range. After filtration, suspended sediment concentration is given as parts per million (ppm), which also could be converted to values of tons/day by using the following equation.

$$Q_R = 0.864 * Q_S * C_S \quad \text{(Eq.9)}$$

where

Q_R = sediment discharge (tons/day)

Q_S = water discharge (m3/s)

C_S = sediment concentration (ppm) (mg/l)

Sediment concentration (C_S) was calculated with the following equation:

$$C = \frac{\text{Sediment Weight (Total Wight of Sand + Clay+ Silt)}}{Sample\ Weight\ (Weight\ of\ Water+Sediment)} * 10^6 \quad \text{(Eq.10)}$$

The average value of trap efficiency can be determined using:

$$\beta = \frac{C/I}{(0.012+0.102)*C/I} \text{ (Brune, 1953)} \quad \text{(Eq.11)}$$

Where;

β : Trap efficiency.

I : The mean annual inflow.

C : The ratio of the reservoir capacity.

However, the agency doesn't periodically collect sediment data from any of the tributaries joining the Cubuk I and Cubuk II reservoirs, which means suspended sediment sampling has been made at a section once or twice a month, and the method for choosing the sampling date is unknown. Therefore, these data might not be sufficient for precise annual sediment inflow prediction. The agency has only been collecting suspended sediment yield and sediment concentration data from gage 1239 as instantaneous data in the catchment. I converted these data to daily and monthly sediment loads using the LOADEST simulation model (Version 2012) from the following website (https://engineering.purdue.edu/~ldc/LOADEST/).

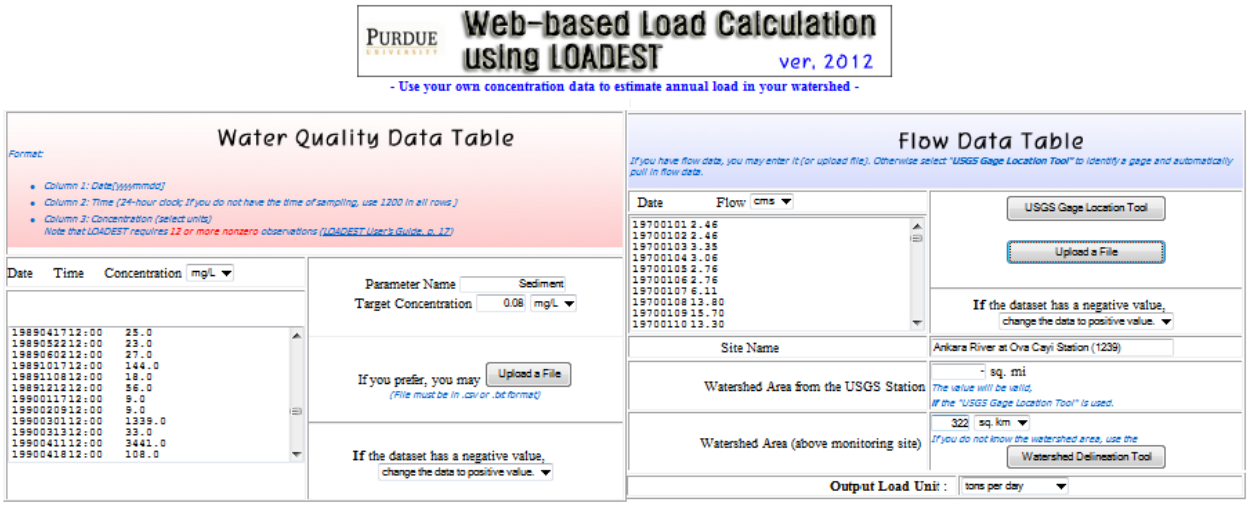

Figure 14: Purdue University LOADEST model interface

In this section, cvs files were used as a sediment input file for the web based load calculation tool (Figure 14). Not only were the missing values replaced by -99, but also negative values were replaced by positive values in the FORTRAN programing language by selecting output unit as tons per day. The outputs obtained from the LOADEST data were used as an input for SWAT, and the outputs were used to plot charts shown in the next section.

4.3. Results Obtained

The State Hydraulic Works of Turkey (DSI) has been using a network of stream gaging stations within 26 hydrological basins. The stations are mainly located on major branches of river networks. DSI measured daily stream flow from the year 1967-2003 besides two other stream gages plus monthly measurements of Cubuk I and Cubuk II inflow. EIE had been measuring monthly sediment at 1239 Ova Cayi – Eybek (Figure 15). This is the only existing sediment gaging station during the years 1970-1999. This gage also measured daily stream flow during the years 1967-2003 (Figure 16), but has recently been out of order due to drought and siltation. The systematic stream flow and sediment collection of these agencies are based on international standards for measuring stream flow and sediment characteristics.

Figure 15: 1239 Ova Cayi – Eybek sediment station

SWAT performance relies on the daily rainfall and stream flow data that were identified over the entire simulation period for the 1239 Ova Cayi -Eybek stream flow gage, and gage 398328 of global weather data for SWAT, which was completed by The National Centers for Environmental Prediction (NCEP), Climate Forecast System Reanalysis (CFSR). NCEP collected climate data including daily runoff and max-min temperature from 1979 through 2014.

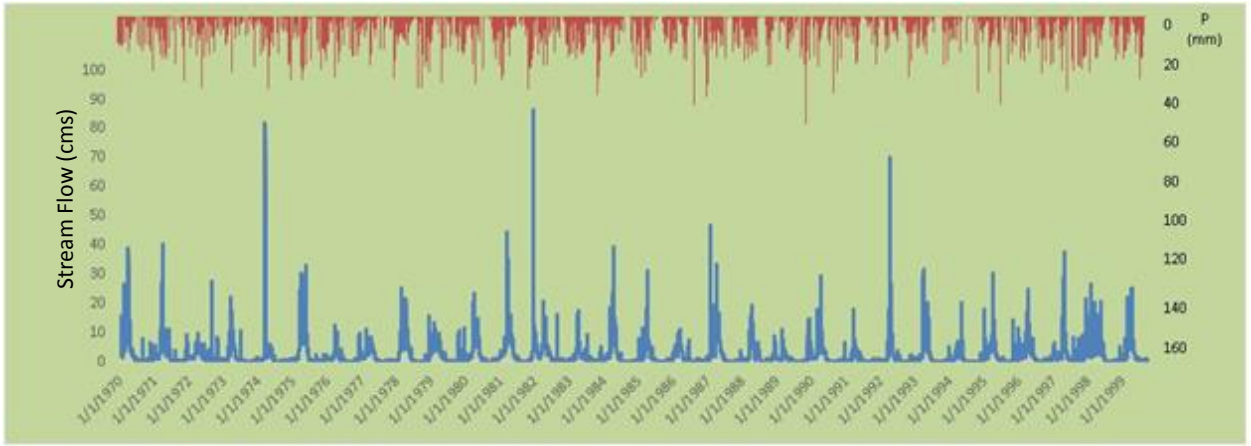

Figure 16: Mean daily stream flow and precipitation of gage 1239 based on 30 years of records

The LOADEST model interface was engaged to determine monthly sediment load and the daily stream flow data were converted to monthly data in order to identify correlations between stream flow and suspended sediment. The regression of sediment yield on mean annual runoff had a coefficient of determination of 0.93, which is significant at the 99% level. The relationship between sediment yield and mean monthly stream flow is noteworthy (Figure 17). Mean observed sediment load is 6697 ton/year and mean sediment yield 21 ton/y/km² from Ova Cayi - Eyrek gage station (38.9% = sand; 61.1% = clay + silt).

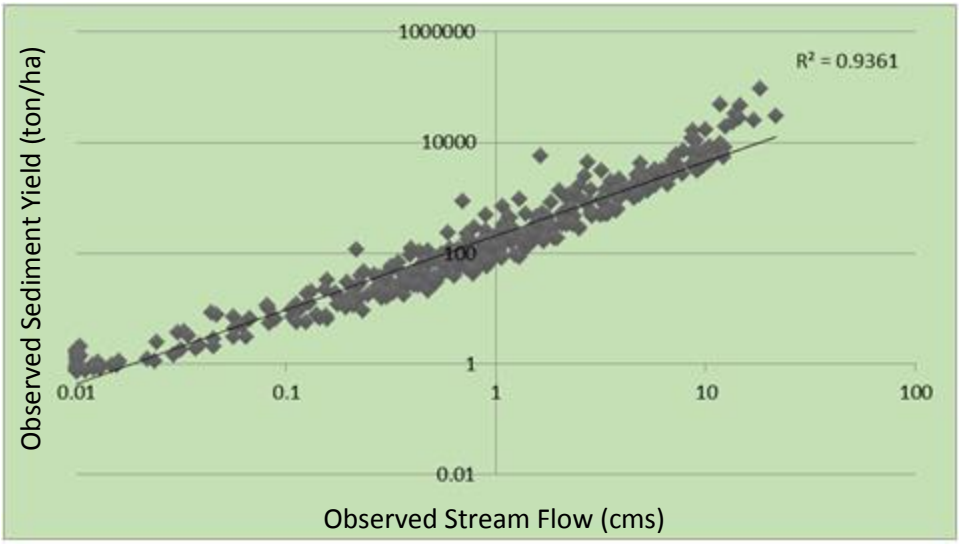

Figure 17: Relationship between monthly stream flow and monthly suspended sediment from Gage 1239 (01/1979 – 12/1999)

The global weather data from stations 398328 and 401328 have only 9 days missing for runoff and maximum - minimum temperature. Based on the data retrieved from these climate stations, the watershed has 14.1 snowy days, annual runoff of ~ 500 mm, and an annual evaporation rate of 1100 mm. These climate stations are located in a semiarid region of central Turkey, based on annual rainfall lower than 600 mm, the huge difference in daily air temperature values, and the sparse vegetation.

Climate data including max-min temperature and precipitation are important for model calibration and validation, so they should be consistent for two different periods of time. The side

by side boxplots in Figure 18 present maximum and minimum temperature for the two different stations of global weather data. There is a slight difference in location as measured by medians and difference in spread between the two distributions. The most noteworthy feature is that the second term, 1990-1999, has more variation in temperature than the first period, which is evidence that the first term should be more consistent in terms of the variation in temperature (Figure 18).

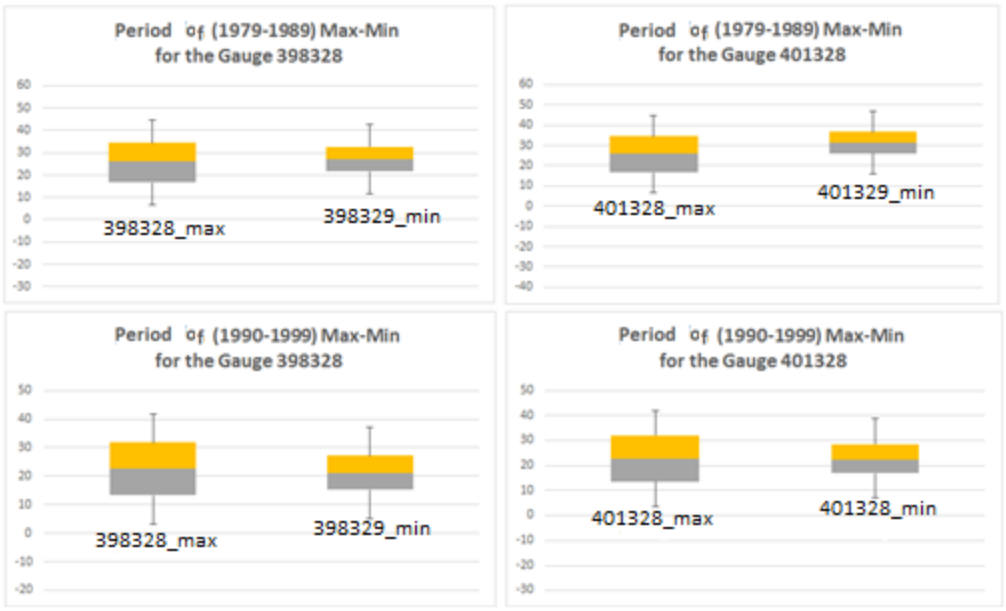

Figure 18: Box-plot charts of max-min temperature. Temperature in degrees Celsius on the y-axis.

Figure 19 presents monthly precipitation data for stations 398328 and 401328, which have only 9 days of missing data in terms of daily precipitation. The first global weather station has slightly higher monthly precipitation, which is evidence that the station likely has higher relief and altitude. However, the monthly precipitation chart indicates that the amount of total precipitation has been decreasing in the last couple of decades.

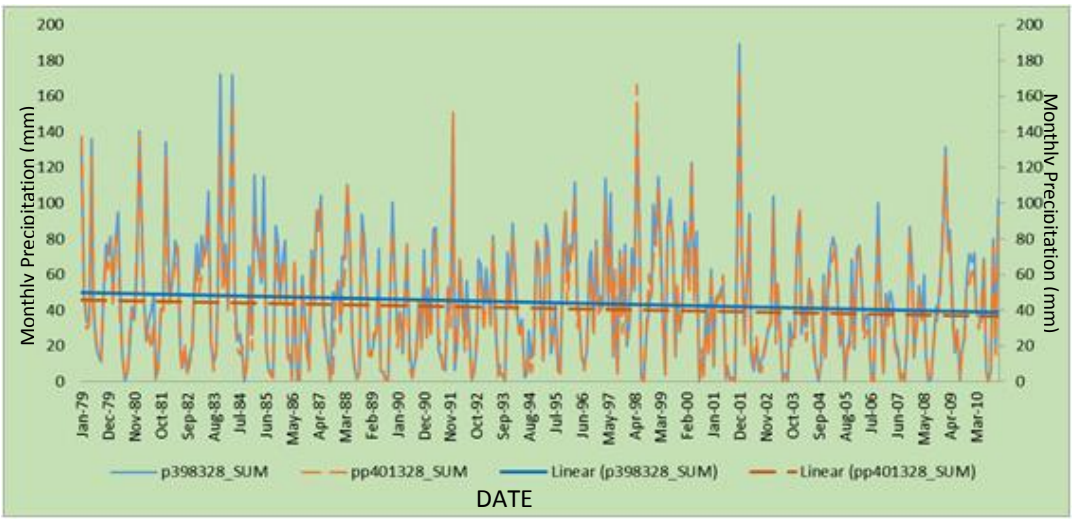

Figure 19: Variation of monthly precipitation (mm) for the two global weather stations with their long term sum and linear trend

The land use map (2000) was obtained from the Global Land Cover 2000 (GLC 2000), which is the harmonization of all the regional products into a full resolution global product with a generalized legend. GLC 2000 was created using the VEGA 2000 dataset, which comes from an instrument on board the SPOT 4 satellite. A standard classification resulted in 13 types of land use within the study area, consistent with SWAT data set requirements. These 13 land use types were generalized to 7 types for the calibration and validation periods. Land cover types present in a small percentage were summarized as generic classes such as all agricultural crops summarized as "agriculture", three types of forests represented by one mixed forest, and one class representing two types of urban classes in the detailed land use map.

The most widespread type of land use is agriculture (57%), most of which is along the Ankara River. In general, forests are dispersed in the northern portion of the watershed (4%), and the central portion of the watershed has more industrial and urbanized area (3%) (Figure 20).

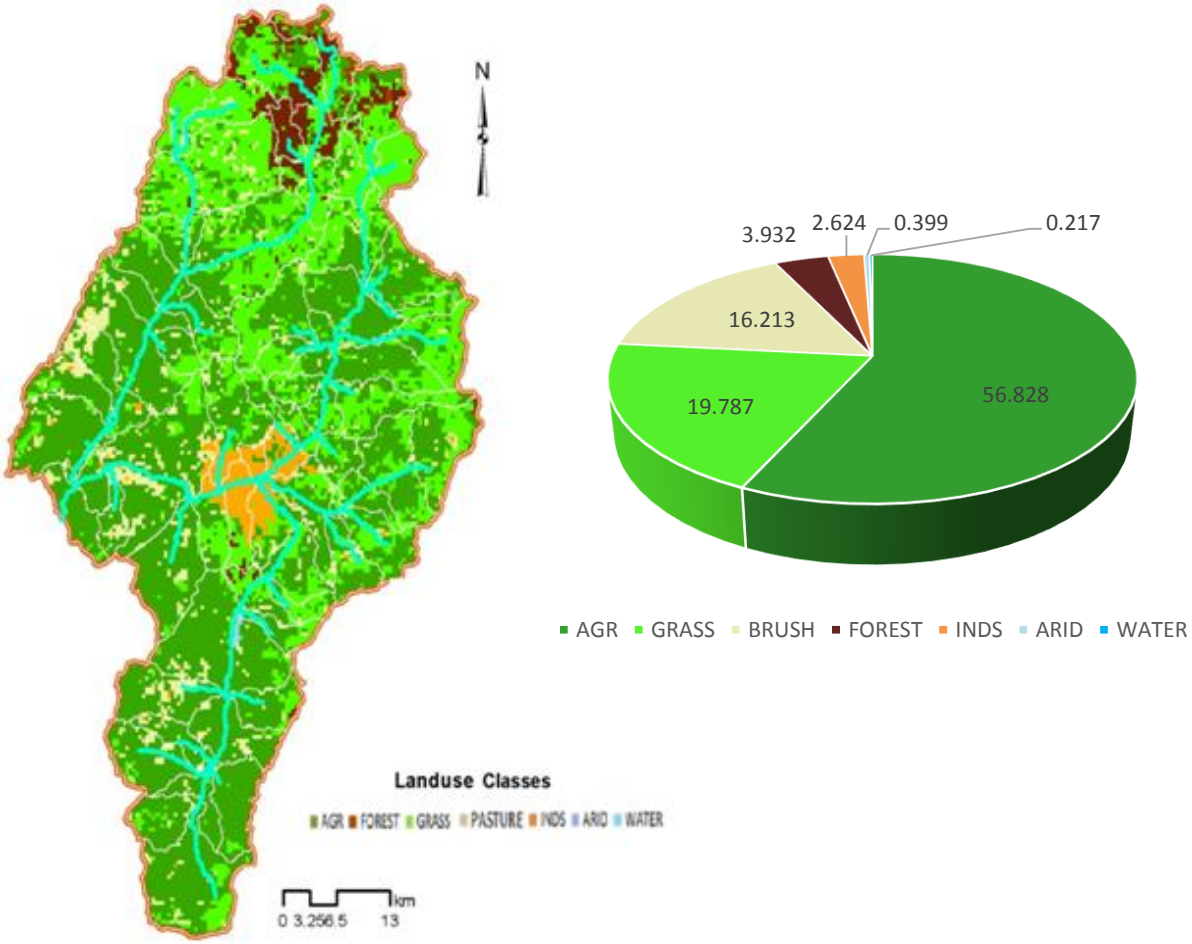

Figure 20: Land use classification of the year 2000

The soil classification data, which were obtained from FAO's Harmonized World Soil Database (HWSD), are converted to the APEX model in order to be used in SWAT with some minor modifications. A standard soil classification resulted in three types of soil type within the study area (Figure 21), which is a small number of categories relative to SWAT requirements. Unfortunately, however, no better data sets with higher resolution are available for the catchment. The main soil type in the basin is heavy clay (59%), which tends to be more resistant to erosion than sand or silt as the clay helps bind soil particles together (Mirsal, 2008). Besides the heavy clay materials, northern portions of the watershed have more sand, and the northeast side has silt

and clay. Model calibration and testing has been done for silt and clay, but more than half of the modeling area is underlain by heavy clay.

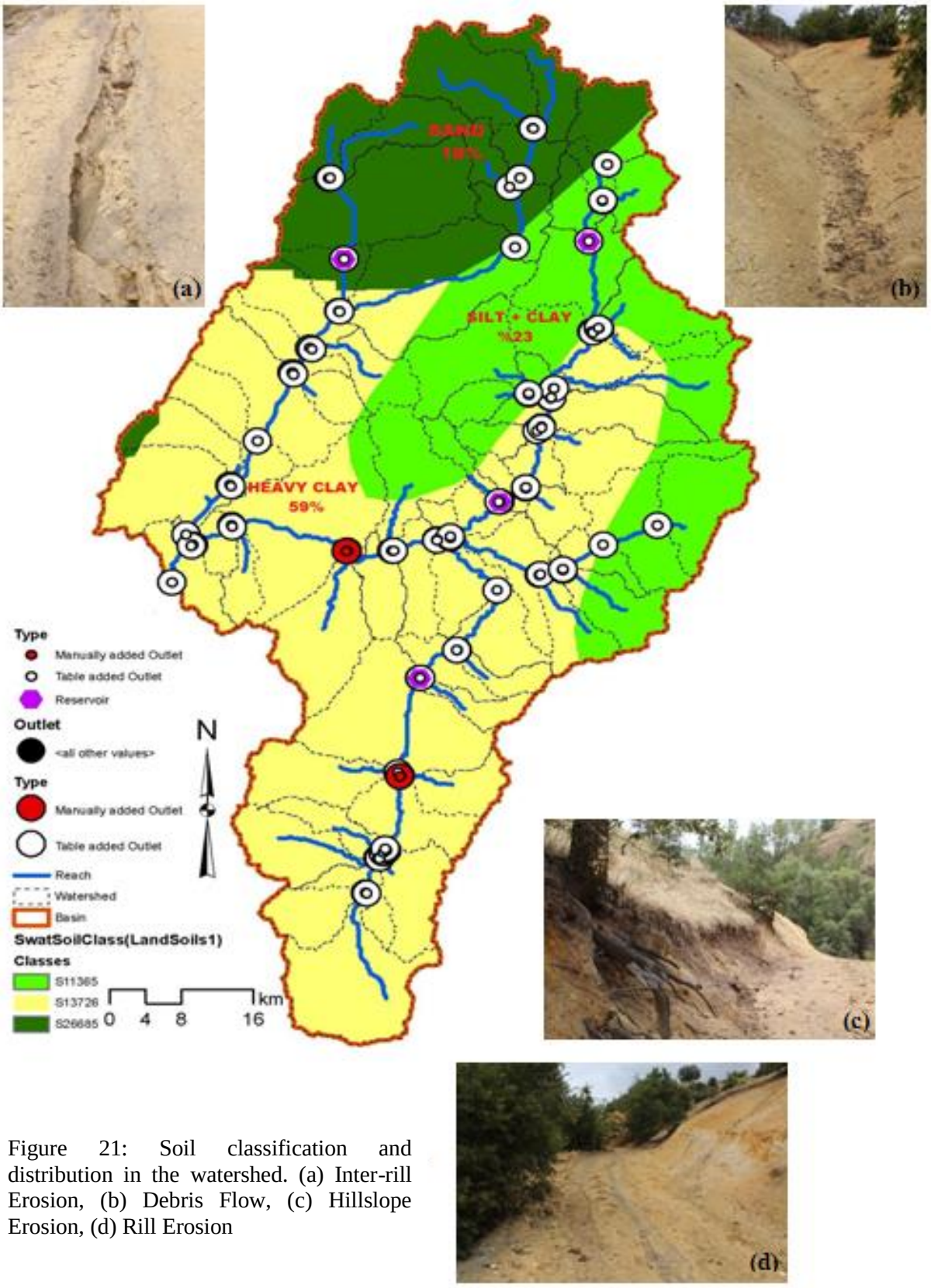

Figure 21: Soil classification and distribution in the watershed. (a) Inter-rill Erosion, (b) Debris Flow, (c) Hillslope Erosion, (d) Rill Erosion

CHAPTER FIVE

SWAT HYDROLOGIC MODELLING

5.1. Model Setup

The SWAT model has been applied to the research area and calibrated/validated using available historical and hydrological data in the catchment. The calibrated model can be used for evaluation of alternative water management practices and regional development. In this study, the SWAT model was set up following the steps outlined in the Arc-SWAT interface user's manual (Winchell et al., 2010). The SWAT model setup process can be divided into four sections: (1) watershed delineation, (2) HRU definition, (3) custom weather data definition, and (4) writing input tables.

5.1.1. Watershed Delineation

Initial stream network and sub-basin outlets are automatic and manually defined (total number of 78 outlets defined) based upon relatively higher resolution digital elevation data (90m). The DEM was clipped to a size slightly larger than the catchment before loading into the interface. A known stream location map was used to make an adjustment in order to match the known stream location to delineated streams as closely as possible. The following information was added to the map and displayed over the DEM:

1. Reach drainage network created on the basis of elevation data,
2. points with respect to stream junctions,
3. with all sub-basin outlets defined by SWAT and added by table, and
4. watershed boundary.

Selecting the boundary of the main outlet is quite important in terms of defining the border of the watershed. The outlet adjacent to Ova Creek and Cubuk Creek was chosen as the main outlet defined by the Arc-SWAT interface (Figure 22).

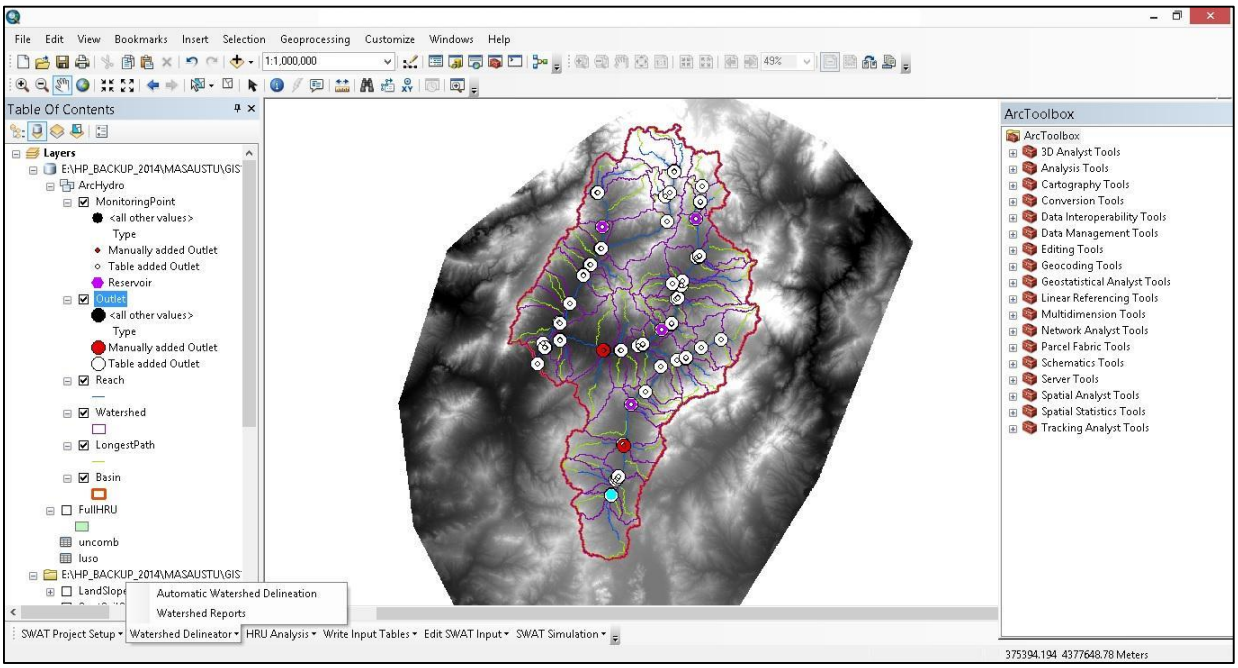

Figure 22: Automatic watershed delineation in SWAT

Once the watershed boundaries were delineated, they were used in combination with the other covers and grids to define all of the watershed characteristics. All these input data were used to predict sediment yield as a function of eight drainage basin characteristics, including surface geology, soils, climate, runoff, topography, ground cover, land use, upland erosion, and channel erosion. Each drainage basin characteristic is given a subjective numerical rating based on observation and experience. The sum of these ratings determines not only the drainage basin classification, but also the annual sediment yield per unit area by using GIS.

5.1.2. HRU Definition

The SWAT model requires defining unique sub-basins called hydrologic response units which consist of three components: land use, soil types, and slope delineation. The land use and

soil data were loaded with slope characteristics identified based on the DEM. In general, HRUs were defined depending upon the combination of land use, soil and slopes with various thresholds.

The land use dataset (2000) obtained from the Global Land Cover 2000 (GLC 2000) was used for land cover layer input. SWAT data set requirements were considered in order to analyze scenarios with SWAT. For that reason, the land use dataset was generalized from 13 land use types to 7 types, and I created a lookup table to fit the land use input table to SWAT. For the land use layer, the attribute table contains an ID for each land use type (Figure 24).

The global soil dataset from FAO was used for soil layers by incorporating soil datasets into the SWAT database file. The model reclassifies the soil data and clips them to fit the existing delineated catchment in a manner similar to that used for the land use datasets.

For the slope definition, three slope classes were defined for each catchment selected with the threshold in 0% with default parameters. These reclassified slope layers have been overlaid to define HRUs (Figure 23).

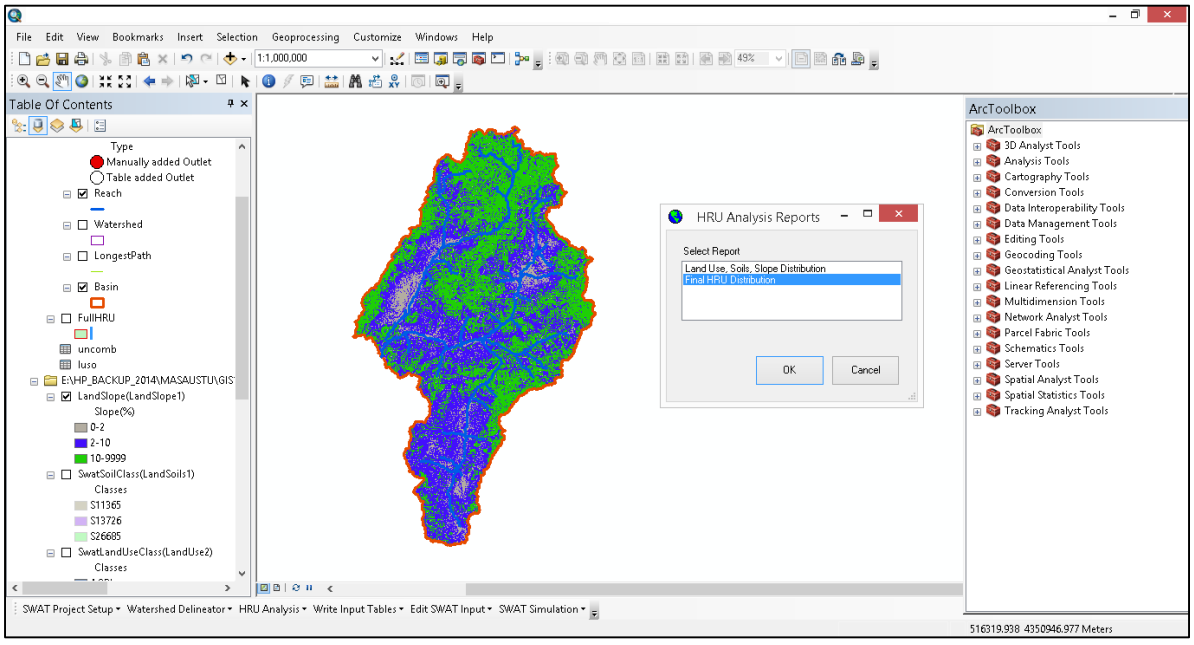

Figure 23: Definition of the three slope classes were defined in HRU

While the watershed is subdivided into separate HRUs, the model gives the option to have one or multiple HRUs in each sub-basin. For one HRU, SWAT uses the dominant land uses and soil types to designate a single HRU for each sub-basin. To have multiple HRUs in a sub-basin, the user needs to identify a threshold percentage value of land cover and soil type for each HRU. Winchell et al. (2010) recommend the thresholds for multiple HRUs on land use, soil type, and slope, respectively. In the simulation, multiple HRUs were used with the following parameter values (Figure 24):

- land use percentage (%) over sub-basin area = 8%
- soil class percentage (%) over land use area = 8%
- slope class percentage (%) over soil area = 0%

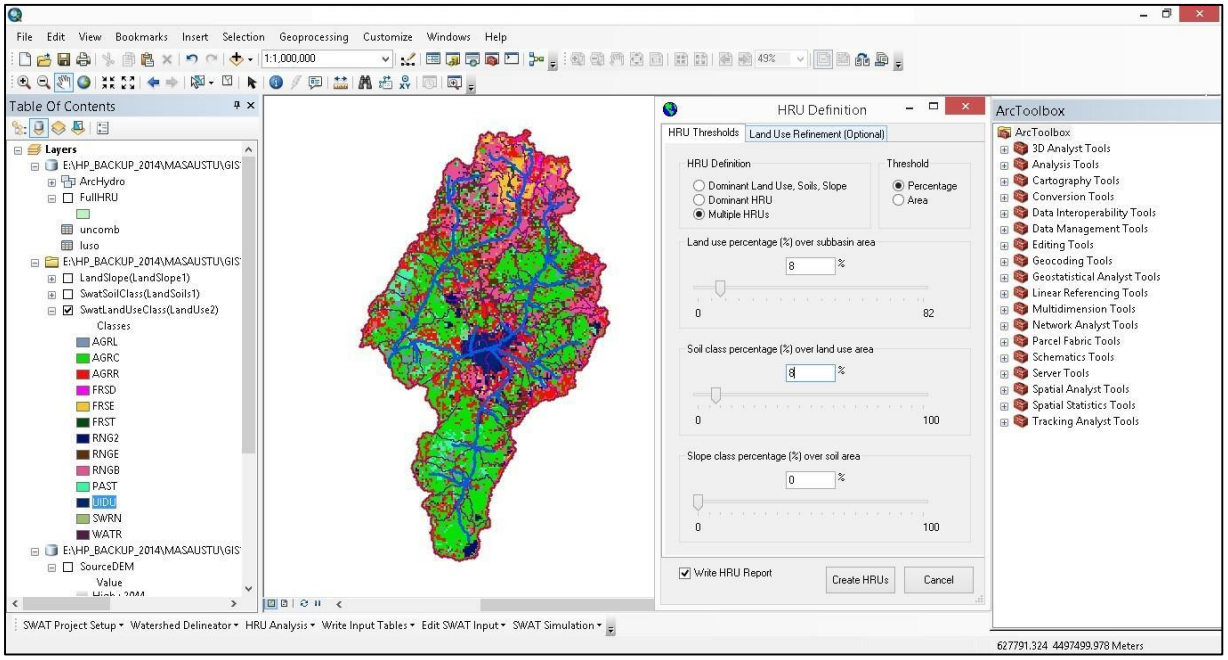

Figure 24: Definition of the Hydraulic Response Units (HRU)

Finally, the report was created with land use, soil classification, and slope characteristics for the whole Ankara river watershed, including 942 HRU's and 74 sub-watersheds.

5.1.3. Weather Data Definition

The model requires weather data including precipitation, temperature, wind speed, evaporation, solar radiation, and relative humidity. A built-in weather dataset consists of simulated weather data input in the United States. I used the custom weather generator because the study site is outside the United States. In this study, daily temperature and precipitation (30 years) data were obtained from the Turkish State Meteorological Organization (DMI) for two climate stations within the catchment area called Ankara (Station ID: 17130) and Esenboga (Station ID: 17128). The missing records were filled by using a statistical weather generator file based on the other climate stations. Wind speed, humidity, and solar radiation data were created by WXGEN parameters (Table 7).

Table 7: Variables required by the custom weather generator database

Variable name	Description
STATION	Weather station name
WLATITUDE	Latitude of weather station
WLONGITUDE	Longitude of weather station
WELEV	Elevation of weather station
RAIN_YRS	Number of years of rain data
TMPMX(mon)	Mean daily maximum air temperature
TMPMN(mon)	Mean daily minimum air temperature
TMPSTDMX(mon)	Standard deviation of daily maximum air temperature
TMPSTDMN(mon)	Standard deviation of daily minimum air temperature
PCPMM(mon)	Mean total precipitation
PCPSTD(mon)	Standard deviation of precipitation data
PCPSKW(mon)	Skew coefficient of precipitation data
PR_W1_(mon)	Probability of a wet day following a dry day
PR_W2_(mon)	Probability of a wet day following a wet day
PCPD(mon)	Average number of days of precipitation
RAINHHMX(mon)	Maximum 0.5 hour rainfall
SOLARAV(mon)	Average daily solar radiation
DEWPT(mon)	Average daily dew point temperature
WNDAV(mon)	Average daily wind speed

In order to make a comparison of which type of data gives better model performance, the meteorological data were also retrieved from the Global Weather website. This website provides only two weather stations (398328 and 401328). These data from the Global Weather stations give better results, so they have been used to improve the model efficiency. To increase model efficiency, daily rain gage data were selected during weather data delineation within the SWAT interface (Figure 25).

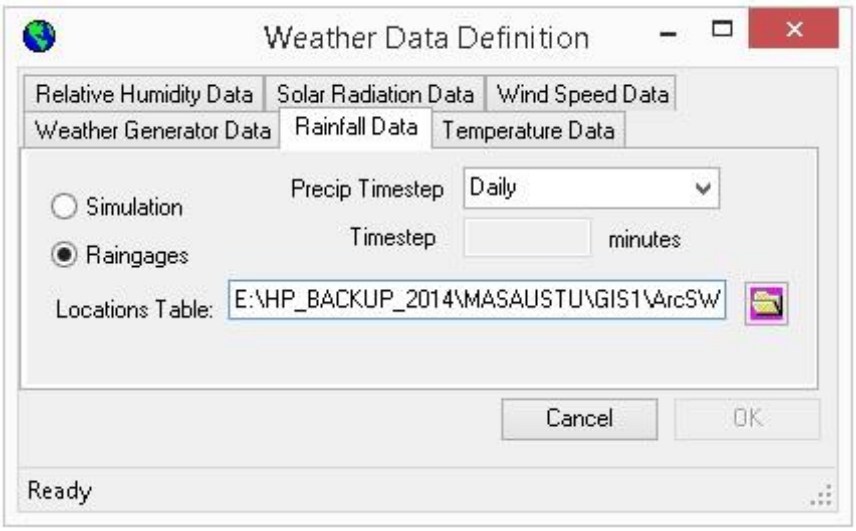

Figure 25: Weather data definition menu in Arc-SWAT interface

Finally, observed data on max/min temperature and daily precipitation were loaded into the simulation to improve efficiency because meteorological data, especially rainfall, have a huge effect on model performance because rainfall is the main source of runoff (Abbaspour et. al., 2007).

5.1.4. Writing Input Tables

The input files in FORTRAN format are derived from the watershed delineation, land use, and soil data. Once all the types of data were loaded into the model, the 'write all files' option in the software was selected to write all required input files. In order to build initial watershed input files, the default parameters were engaged in SWAT and the default value of Manning's n (0.0012)

was used, which seems appropriate for the catchment. Default values can also be altered after all of the default input dataset is generated by using the "Edit SWAT Input" menu. However, because not enough observed suspended sediment yield data are available in the catchment, the SWAT input data were not changed.

5.2. Run the SWAT Simulation

The Run SWAT icon, which is located under the SWAT simulation menu, was set to 01/01/1987 and 12/31/1996 with a monthly printout option "NYSKIP" was also set to 2 years as a warm up period for the model. The value of 2 in the NYSKIP operates the first output from the simulation as a start point of 01/01/1989. After the rest of the parameters were left as default values, the "Setup SWAT Run" icon was activated and the simulation was run.

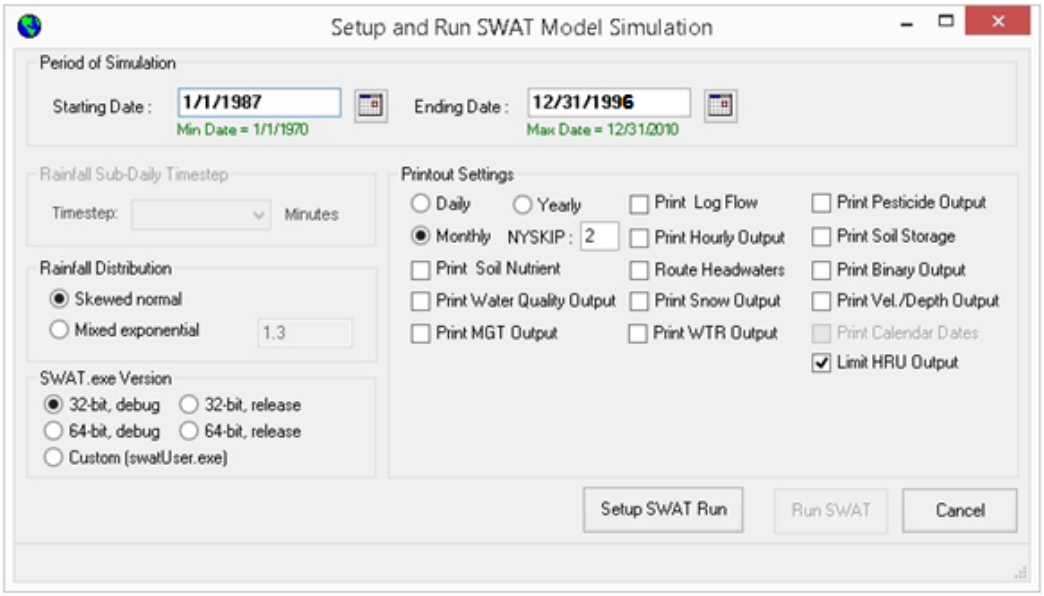

Figure 26: SWAT model setup and simulation menu

The simulation was run with two years warmup period with skewed normal distribution for rainfall data, and limited by a model boundary based on HRU output data (Figure 26). The data on watershed statistics were obtained through the "output.std" text file and the document in Microsoft Access format.

5.3. Sensitivity Analysis

Sensitivity analysis, a technique to identify the responsiveness of parameters, was conducted to determine the influence a set of parameters have on predicting total flow and sediment. In this study, parameters used in sensitivity analysis were chosen based on the previous documentation. The analysis algorithm was also built into a tool using the "Latin Hypercube One-Factor-At-A-Time (LH-OAT)". During sensitivity analysis, SWAT runs (p+1)*m times, where *p* is number of parameters being evaluated, and *m* is the number of LH loops (Van Griensven, et al., 2005). A set of parameter values was selected such as a unique area of the parameter space sampled for each loop within an identified area. Parameters were varied for a new sampling area by changing all the parameter values. The parameters producing the highest values are ranked as the most sensitive (Veith et al., 2009).

The LH-OAT method of Morris (1991) was used for sensitivity analysis, which was carried out for a period of eight years with two years of warm-up period simultaneous with the calibration period (01/01/1987 – 12/31/1996). For the flow simulation, only 14 of 35 parameters revealed meaningful effects (Figure 27). From the sediment simulation, only 10 of 35 parameters revealed meaningful effects. The sensitivity analysis results for sediment are shown in Figure 28.

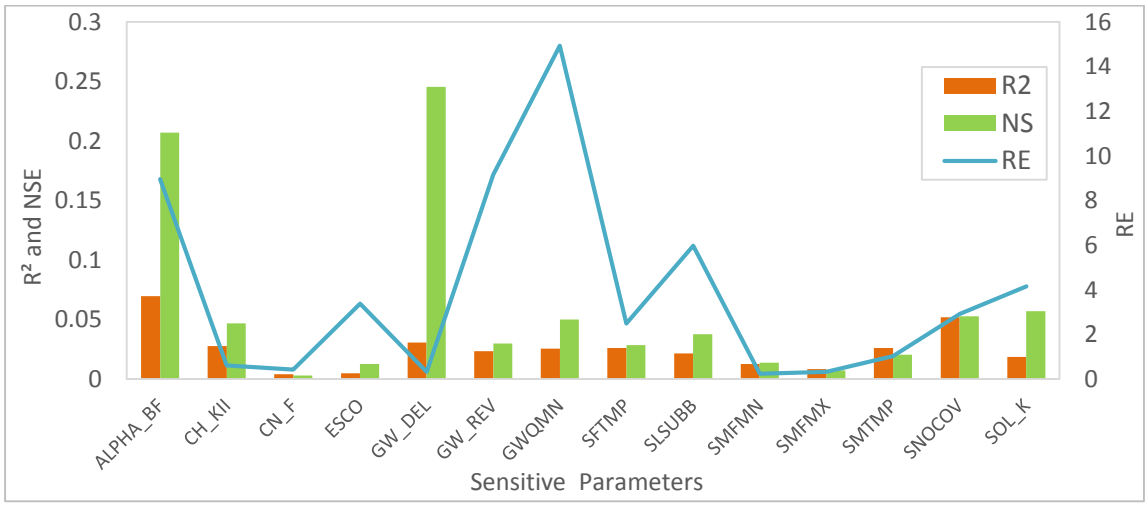

Figure 27: The most sensitive parameters revealed meaningful effect for stream flow

The results of the Morris sensitivity analysis tool indicate that Alpha_BF (Base-flow Regression Coefficient) and GW_DEL (Ground Water Delay) were the two most sensitive parameters, with sensitivity index values of R^2 of 0.07 and NSE of 0.21 (Alpha_BF) and R^2 of 0.03 and NSE of 0.25 (GW_DEL) for stream flow. Alpha_BF is the direct index of ground water flow responses to the changes in recharge. The default value of Alpha_BF led to large base flow, so adjusting this parameter value to 0.99 caused the simulated discharge recession curve to be steeper than when using the default value, which represents faster drainage behavior of the watershed. GW_DEL, the ground water delay, determines time required for water leaving the bottom of the root zone to reach the shallow aquifer.

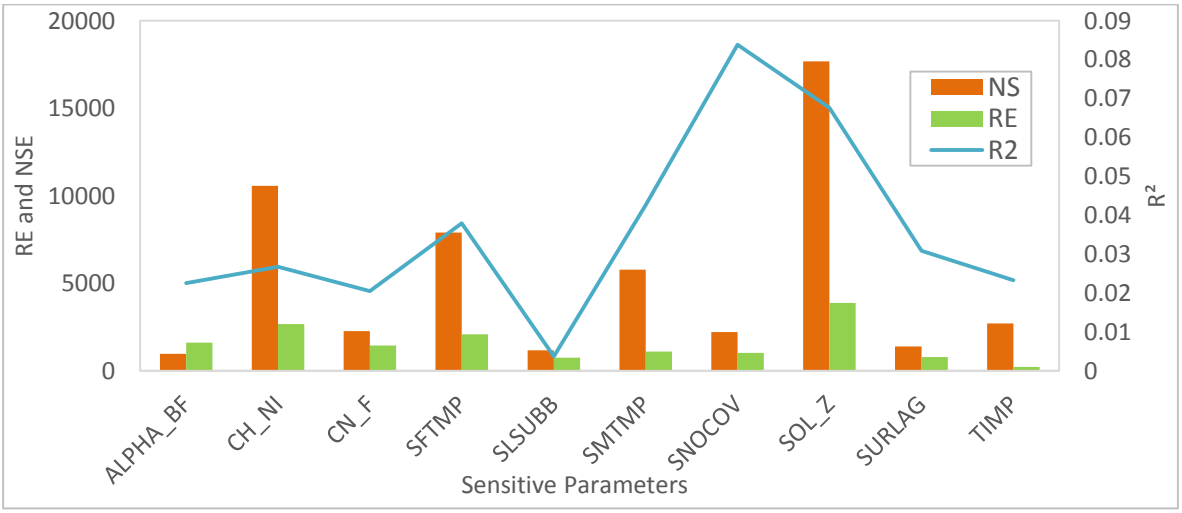

Figure 28: The most sensitive parameters revealed meaningful effect for sediment

Parameter sensitivity analysis for sediment load simulation also varies within the calibration period. SOL_Z (soil depth from surface to bottom of layer) and CH_N1 (Manning Coefficient of Channel) were the two most sensitive parameters, with sensitivity index values of RE of 3,883 and 2.668, respectively, and NSE of 17,692 and 10,577, respectively. As mentioned earlier, the basin experiences snowfall during winter, with snowfall occurring 14.1 day/year, and temperature below 0 ºC approximately 121 days/year. Therefore, SNOCOV (fraction of HRU area

covered with snow) is ranked third for stream flow. Besides the Morris sensitivity analysis, I performed a global sensitivity analysis using SWAT-CUP. I found the two most sensitive parameters to be GW_DEL and Alpha_BF for stream flow. These dominant hydrological parameters were determined and a reduction of the number of model parameters was performed in order to improve the Nash-Sutcliffe coefficient of efficiency by identifying the most dominant parameters for stream flow and sediment load.

5.4. Calibration

The model calibration was done by manually changing the most sensitive parameters and comparing the stream flow and sediment outputs to observed data that were obtained from the sediment gage of Ova Cayi Eybek. Previous studies have been done as a reference for the calibration process. In the literature, the following parameters were chosen to improve model performance with respect to calibration. Fifteen model parameters can be summarized in three categories (Neitsch et al., 2001):

(1) controlling runoff: curve number (CN), soil evaporation compensation factor (ESCO), surface lag coefficient (SURLAG), Manning's "n" value for overland flow (OV_N), available water capacity of the soil layer (SOL_AWC), and maximum canopy storage (CANMX)

(2) governing ground water: capillary coefficient from groundwater (GW_REVAP), ground water delay (GW_DELAY), base flow Alpha factor (ALPHA_BF), plant uptake compensation factor (EPCO), threshold depth of water in the shallow aquifer (GWQMN), threshold depth of water in the shallow aquifer for return flow (REVAPMN), Initial groundwater height (GWHT), and deep aquifer percolation fraction (RCHRG_DP).

(3) influencing routing process: Manning's roughness coefficient (CH_N2)

Both manual and auto-calibration approaches were used to train the sensitive model parameters and all the channel sediment routing parameters were calibrated and validated as explained in the following paragraphs.

5.4.1. Stream Flow Calibration

Initially, each parameter value affecting stream flow was changed one at a time to identify its individual effect on the simulated stream flow. The model was run with the altered combination of different parameter values in order to identify how the parameters influence regression statistics and an efficiency of simulation. Once an applicable statistical result came through, the parameters influencing sediment started to be altered to improve calibration. During the calibration process, I learned that the rainfall data from the Turkish State Meteorological Organization (DMI) are not representative because some localized storms do not have any response in the simulation. Also, the model consistently over-predicts the stream flow with the initial variables. Therefore, the meteorological data were replaced with Global Weather data, which had a better response to every storm in the catchment. In terms of the over prediction of stream flow, curve number (CN), available water capacity (SOL_AWC), and soil evaporation compensation coefficient_(ESCO) parameters were changed, but changing the parameter values did not give better results during calibration.

In this section, three model evaluation methods were used as a guideline (Moriasi et. al., 2007). These methods are: (1) Nash-Sutcliffe Efficiency (NSE), (2) Relative Error (RE), and (3) the Coefficient of Determination (R^2). Fifteen parameters were included in calibration, 1000 simulations were run, and satisfactory calibration results were achieved for daily and monthly stream flow simulations (Table 8).

The SWAT stream flow predictions were calibrated against daily stream flow from 1987 to 1996 with two years (the period from January 1, 1987 to December 31, 1988) as a model warm-up period at the gaging station of Ova Cayi Eybek. Some years, such as 1979, 1998, and 1999, did not represent the calibration period because of too many missing observations. Also, land cover data used in this research were obtained circa the year 2000, so weather data and discharge data closer to the year 2000 were chosen for the model calibration process. As a result, the simulated monthly stream flows represent the observed values for the calibration period with values of NSE, RE, and R^2 of 0.79, -0.58, and 0.89, respectively (Table 8). As a result of the stream flow calibration process, the simulated monthly discharge is within an acceptable range of the observed data.

Table 8: The statistical results of SWAT model applicability for stream flow

Calibration (1/1/1989-12/31/1996)	STREAM FLOW		
	NSE	RE	R^2
Daily	0.61	-0.55	0.78
Monthly	0.79	-0.58	0.89

After running the model regression statistics, a scatter plot of calibrated and simulated stream flow and time series of observed and simulated discharge were plotted in order to evaluate the model performance on stream flow (Figure 29).

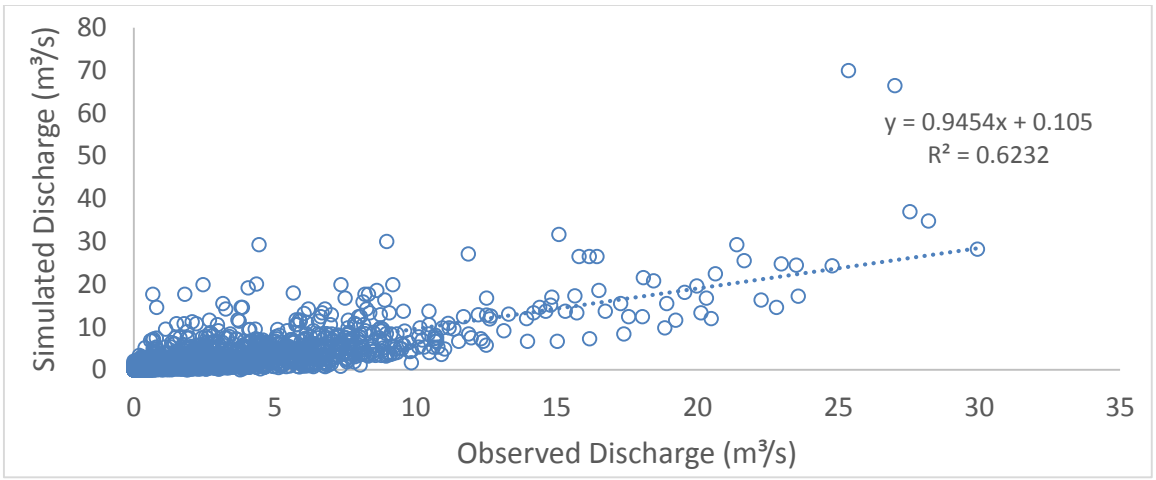

Figure 29: Scatter plots of simulated vs observed discharge during the calibration period (1/1/1989-12/31/1996)

Figure 29 illustrates a 62% correlation between observed and simulated discharge. Most of the moderate to high flows are reasonably described by the SWAT model. There are some mismatches in the simulated flow, particularly during the annual dry season, although most simulated flow is graphically and statistically close to observed flow. Although the scatter plot indicates that daily stream flow data have some errors relative to measured stream flow, simulated daily flow data generally capture the signal of observed stream flow well.

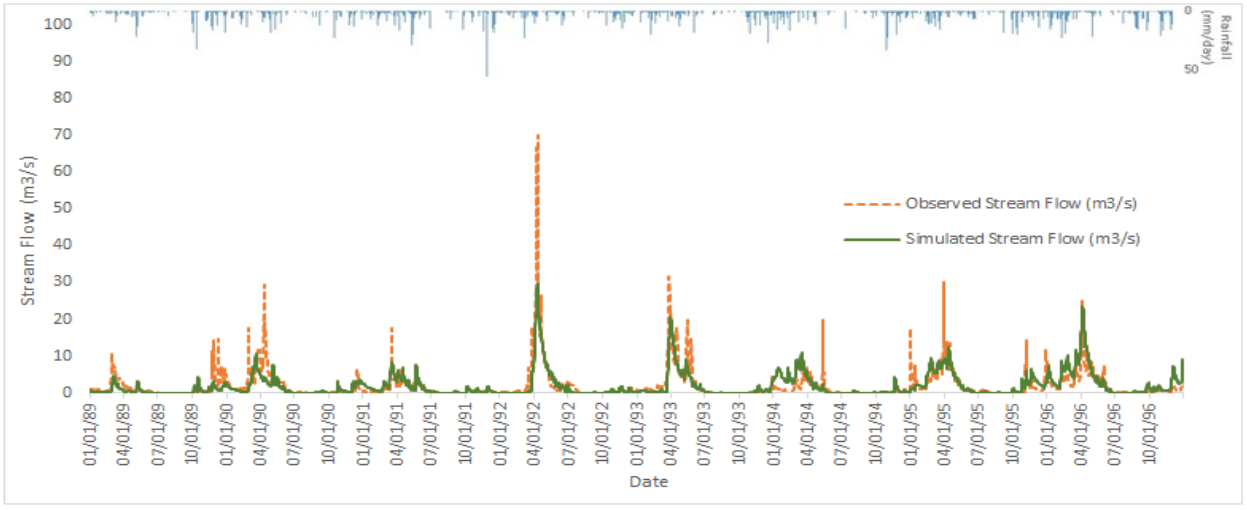

Figure 30: Time series of observed vs. simulated discharge (daily). Comparison between "observed" and simulated daily stream flow for calibration period from 1989 and 1996 at the gage of Ova Cayi – Eybek

The time series chart of daily observed versus simulated discharge (Figure 30) indicates that the calibrated SWAT model is poor at simulating small scale events such as individual storms, but is able to simulate long term trends such as seasonal variation or annual averages relatively successfully. The mismatches in small scale storm event prediction might be related to spatial variability of precipitation, which was not adequately collected by the existing rain gage. Daily flow simulation also produces a good agreement between observations and simulations.

5.4.2. Suspended Sediment Yield Calibration

Monthly overland erosion rates were determined by the model, but SWAT did not simulate bed load transport. The same inputs were used for the sediment calibration except that the final parameter value of the USLE cover factor was reduced to 0.068 in the calibration period. The statistics obtained from sediment simulation are shown in Table 9.

Table 9: The statistical results of SWAT model applicability for sediment

Calibration (1/1/1989-12/31/1996)	SEDIMENT		
	NSE	RE	R^2
Monthly	0.81	1.55	0.93

The monthly calibration statistics of sediment can be considered as highly applicable since NSE is higher than 75%, RE values are lower than 20%, and R^2 is close to one (Motovilov et. al., 1999).

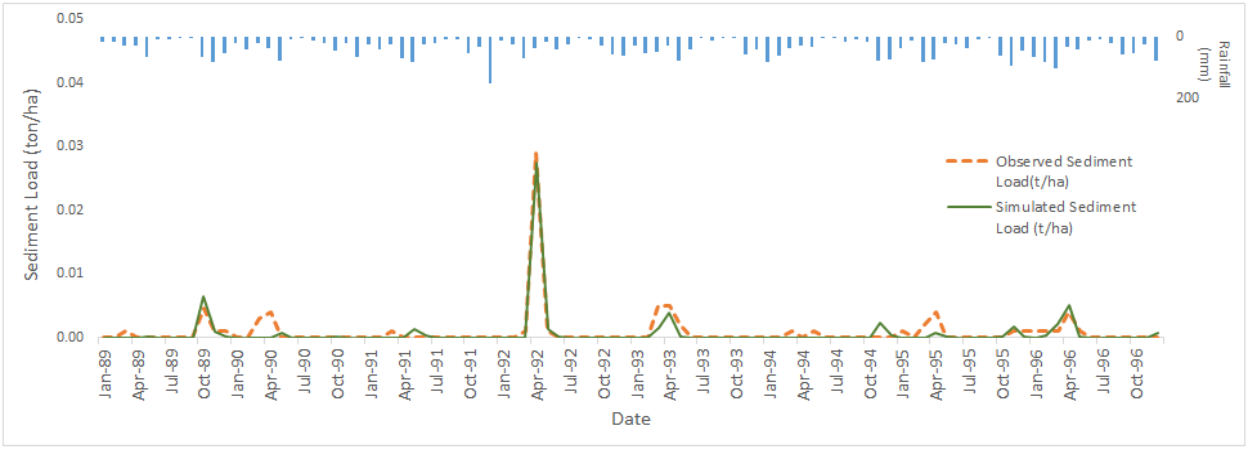

Figure 31: Time series of observed vs. simulated sediment load (monthly). Comparison between "observed" and simulated sediment load for calibration (1989–1996) at the gage of Ova Cayi–Eybek

Monthly sediment simulation produces a good agreement between simulated and observed data. However, the model is somewhat poor at simulating small scale events such as individual sediment peaks from small storm events. The model captures long term trends such as seasonal variation or annual averages successfully.

5.5. Validation

Validation is undertaken to assess the model adequacy and to determine whether the simulation period of stream flow and sediment confirmed that the model performs satisfactorily. A variety of models has been developed for this purpose, but the manual calibration method was used for validation in this research. The SWAT model stream flow and sediment load outputs were validated against monthly stream flow and sediment load from 1982 until 1984 (3 years) at the gaging station of 1239 (Ova Cayi Eybek).

Table 10: The statistical results of validation period for flow and sediment load

Validation (1/1/1982-12/31/1984)	STREAM FLOW and SEDIMENT		
	NSE	RE	R^2
Stream Flow (Daily)	0.65	-1.88	0.82
Stream Flow (Monthly)	0.83	-1.70	0.92
Sediment (Monthly)	0.77	-2.61	0.87

The model validation statistics illustrate a similar relationship between predicted and observed data to calibration results. The validation results are also within an acceptable range for the observed 3 years of discharge and sediment data. As a result, the simulated daily stream flows represent observed values for the validation period with a NSE of 0.65, RE of -1.88, and R^2 of 0.82, respectively (Table 10). After running the validation, a box plot of validated daily stream flow and sediment data were created and time series of observed and simulated discharge were plotted in order to evaluate the model performance for the validation period (Figure 32).

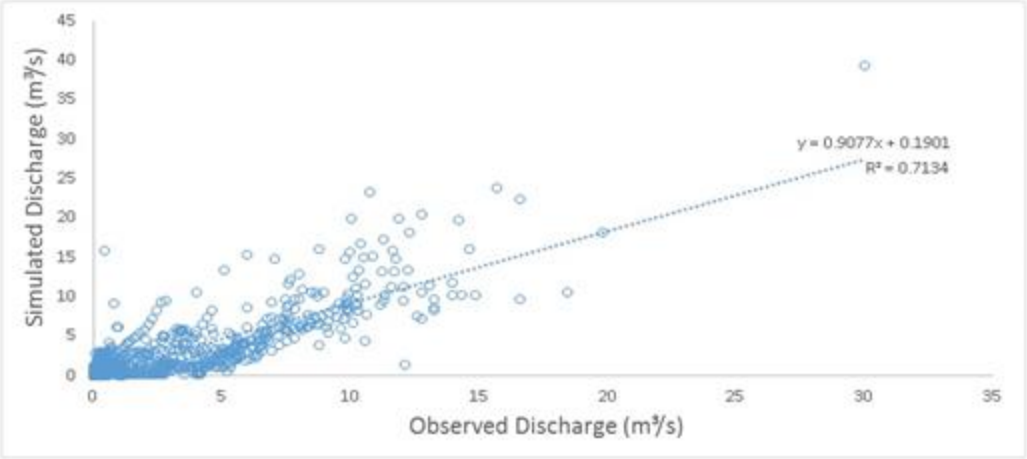

Figure 32: Scatter plots of simulated vs observed discharge for calibration period (1/1/1982-12/31/1984)

The scatter plot of simulated against observed discharge indicates a correlation value of 71%. The scatter plot also indicates that the daily stream flow data have fewer mismatches and less error than the scatter plot for the calibration period because the data have fewer "0" values in precipitation, which means that the validation period had fewer droughts. The measured annual dry season for the calibration period is 215 days, and for the validation period 117 days. In general, these values indicate that the simulated daily stream flow during validation captures observed stream flow satisfactorily.

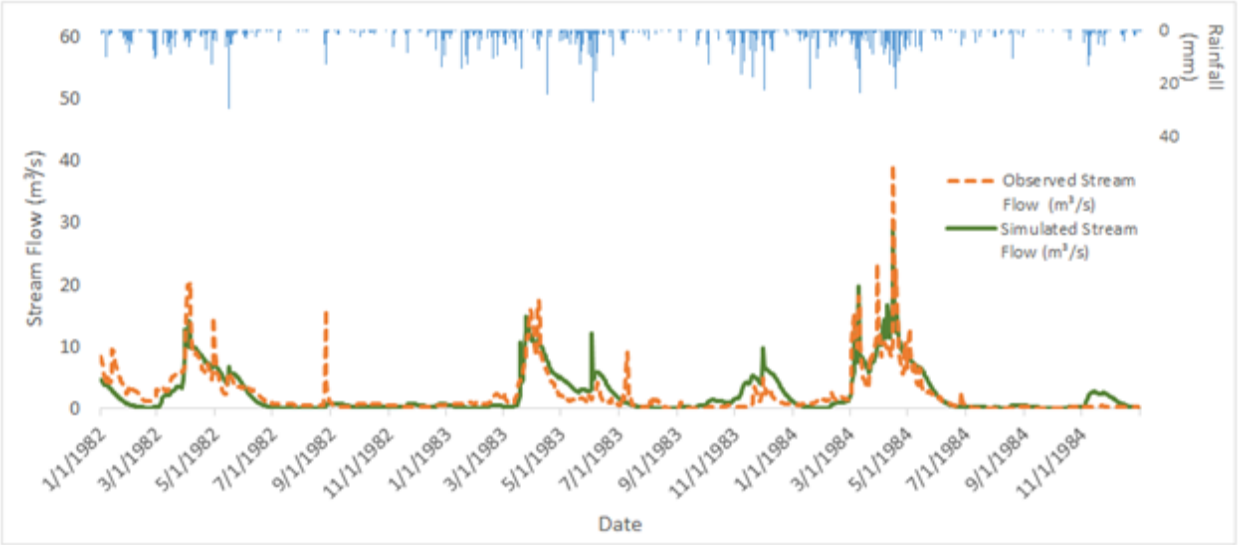

Figure 33: Time series of observed vs. simulated discharge (daily). Comparison between "observed" and simulated daily stream flow for validation period from 1982 and 1994 at the gage of Ova Cayi – Eybek

Stream flow validation indicates that the model over predicted daily flow during certain periods (especially the year of 1983) and under predicted in some periods, such as in the beginning of 1982. The model simulates the daily flows based on the daily average, although observed stream flows are based on instantaneous readings, for example at 10 am. The results in peak flow are likely to reflect observed values if the storm occurs close to the time when the measured precipitation values are collected, such as 9 am.

However, it is possible that the resulting runoff might leave the catchment earlier if the precipitation occurs well before the measurement -- for example, in the previous day. In that case, the peak flow simulation may not be reflected in the daily flow observation. During a large storm, daily surface flow is reasonably high, so the simulation has an ability to compute more accurate stream flow. If the storm event occurs closer to the time of observation, the model captures peak flows better.

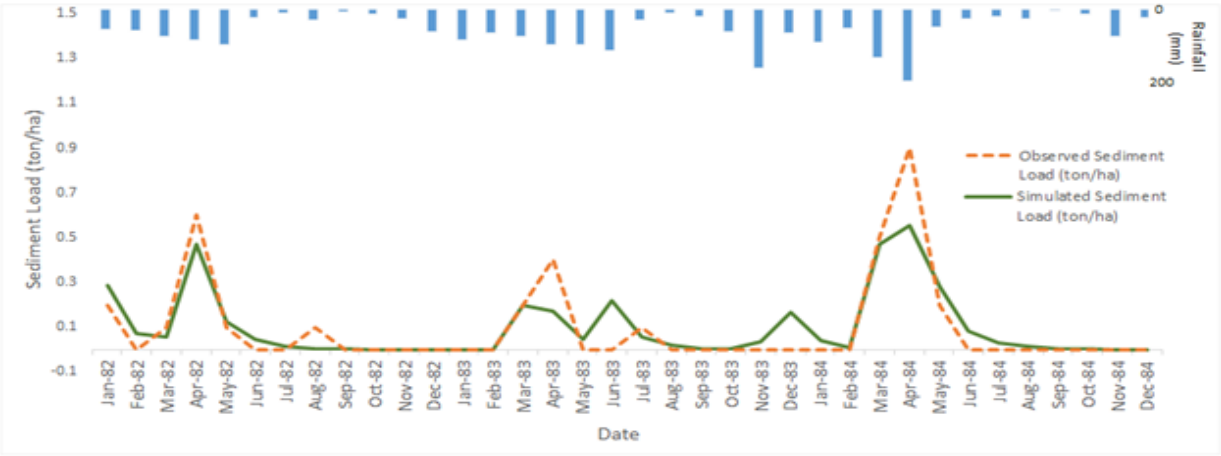

Figure 34: Time series of observed vs. simulated sediment load (monthly). Comparison between "observed" and simulated sediment load for validation (1982–1984) at the gage of Ova Cayi–Eybek

The sediment validation analyses suggest that the model tends to under-estimate sediment load during peak flow. During drought the model performs better because sediment simulation reflects the peak seasons, seasonal variation or annual averages. However, SWAT does not produce a good agreement between observed and simulated sediment load because it fails to capture smaller individual sediment peaks even though it successfully captures seasonal variation or annual averages (Figure 34). In conclusion, validation indicates that the model performance on sediment load is satisfactory with a NSE of 0.77, RE of -2.61, and R^2 of 0.87. It also verifies that SWAT is a useful tool for investigating watershed management strategies to achieve management goals.

5.6. Results and Discussions

An evaluation of the performance of the SWAT 2010 version of ARC-SWAT was conducted in order to better understand the model strengths and weaknesses in simulation of stream flow and sediment from sheet erosion and channel aggradation and degradation in the upstream portion of the Ankara River watershed. Model performance was tested using the long term measured discharge and suspended sediment data from the sediment gage of 1239.

Fifteen model parameters that govern surface and subsurface response in the simulations were calibrated in the watershed. Based on these parameters, sensitivity analysis was completed using the Morris sensitivity analysis tool. The output from sensitivity analysis illustrates that hydrological parameters have a dominant effect on modeled sediment yield. These hydrologic parameters also influence water quality in the simulation. The most sensitive parameters are GW_DELAY and Alpha_BF for stream flow; SQL_Z and CH_N1 for sediment load.

Simulation results are considered well for values of NSE > 0.75, whereas values between 0.75 and 0.36 are considered to be satisfactory (Motovilov et al. 1999). In other words, the model calibration for stream flow and sediment yield is considered highly acceptable. The simulation results demonstrate the uniqueness of the corresponding response, and reflect the model performance based on the sediment statistics in the calibration period, such as NSE, RE, and R^2 of 0.81, 1.55, and 0.93, respectively, and for the validation period NSE, RE, and R^2 of 0.77, -2.61, and 0.87, respectively. Moreover, SWAT can be used as a tool in decision making in water resources planning and management practices in the watershed.

A general recommendation is that more attention be given to the spatial parameters and input data. First, the model requires higher resolution data such as DEM, land use and soil type. The soil type dataset used in this study is particularly broad because only three types of soil were distinguished in the watershed. Having higher resolution data for soil type and DEM would likely improve the model performance (Bosch et al., 2004). Second, more recent and accurate daily flow and sediment input data are critical for model performance, so government agencies need to establish more sediment gaging stations and observe water quality data on a regular basis. Third, important geomorphic features need to be studied more in order to improve the representation of

natural processes such as sediment and water fluxes. Finally, prospective researchers need to consult previous studies.

CHAPTER SIX

THE IMPACT OF CONTROLLING VARIABLES ON SEDIMENT YIELD CHANGES IN THE ANKARA RIVER CATCHMENT

6.1. Introduction

Study of variables controlling sediment yield, particularly at the catchment scale, provides important insight into the linkage between soil erosion and suspended sediment deposition in riverine environments. Numerous studies have focused on the various sub-processes of soil erosion on hillslopes, whereby their controlling variables and rates have been established for small catchments. I present controlling variables that have most strongly influenced sediment yield in small catchment areas of central Anatolia. Better knowledge of the factors controlling sediment yield may help to determine sediment control strategies and to determine the best prospective reservoir location for more efficient management practices.

Nineteen factors including variables of hydrology, drainage area, morphology, and land cover, were analyzed. Hydrologic and morphologic parameters including slope, elevation, discharge, and channel width are the main controlling variables, as well as catchment characteristics including precipitation, drainage area (Pinet and Souriau, 1988; Summerfield and Hulton, 1994), and land use (Dunne, 1979). The main objective of this section is to determine the relative importance of these nineteen potential control variables in terms of influence on sediment yield.

6.2. Site Characteristics

The study was performed in the Ankara River basin, which contains different land use and land cover types (Figure 35), such as irrigated land, rangeland, and forest land, and diverse

landforms, for example, plateaus, alluvial plains, and low-relief areas ranging from 856 m to 1164 m in altitude with soils dominated by clay and silt. Annual mean air temperature over the past 30 years is 10°C and annual mean precipitation is 448 mm. The maximum precipitation occurs during winter and spring. Areas north of Cubuk II Reservoir potentially receive higher precipitation than the rest of catchment. However, these sites are in the semiarid portions of the Central Anatolian Plateau of Turkey. Therefore, the main tributary carries less water to the reservoir and the catchment area has also sparse vegetation due to drought in summer. In terms of disturbance history, the lack of forest land did not reduce the quantity of wildfires in the city limits of Ankara. A total of 152 wildfires have been recorded since 1970, with 78.44 ha burnt during this period.

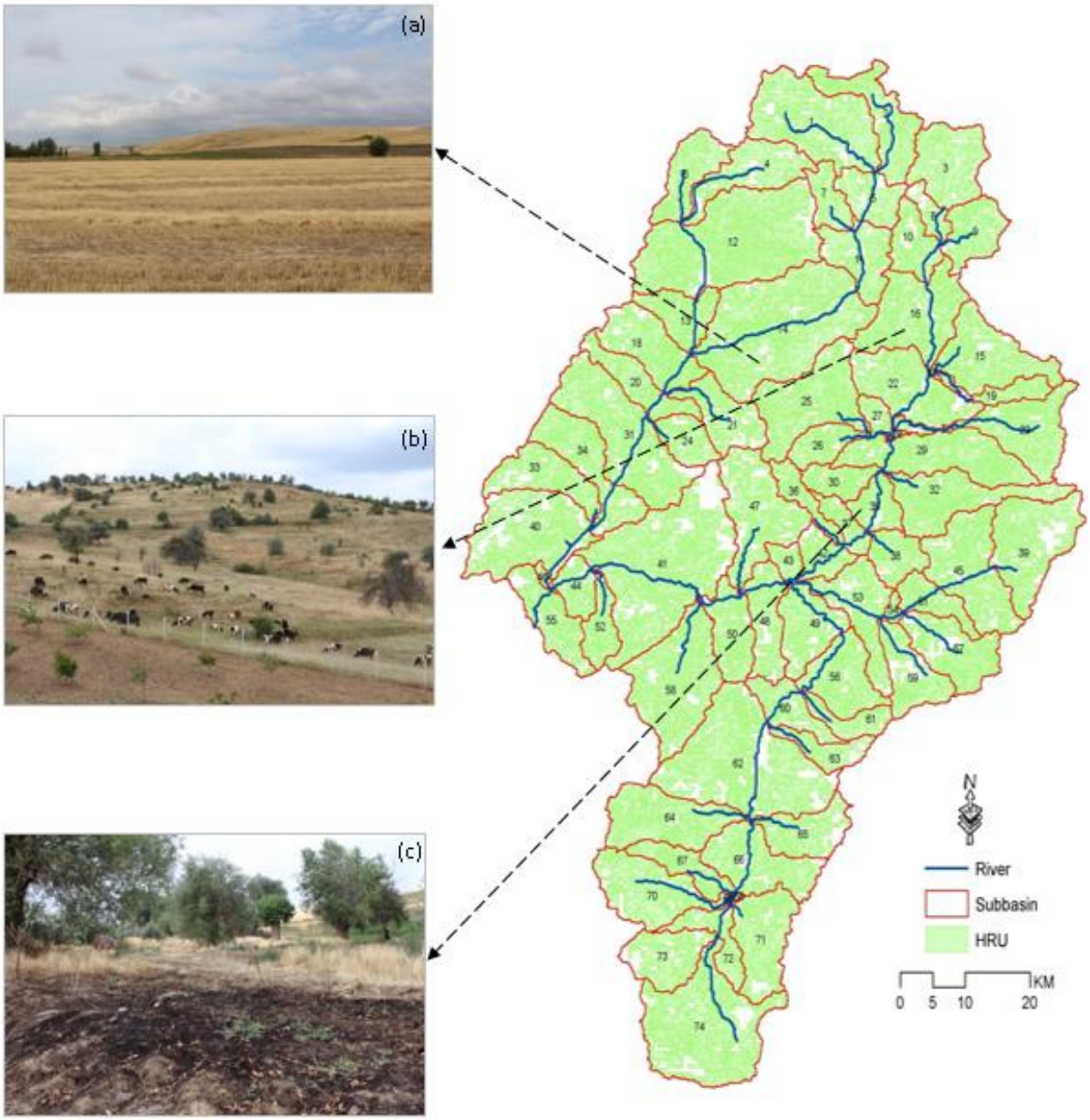

Figure 35: The map of subbasins and HRUs in Ankara River Basin. (a) Scene of cropland in the upstream of Ankara River catchment, (b) Cattle drive in upstream of Ankara River catchment, (c) Wheat residue being burned just ahead of wheat planting in the central Ankara River catchment

The results of the SWAT model indicate that subbasins 46, 50, and 55 have the highest sediment yield, with sediment yield values of 17489 ton /year^{-1}, 13552 ton/year^{-1}, and 17616 ton/year^{-1}, respectively. These high values reflect the fact that subbasin 46 submerged two

tributaries and subbasin 55 includes the outlet of the Ankara River basin, which collects sediment load from upstream. These two also have one of the highest values of channel width and stream flow within the basin, which reflects downstream cultivated lands with higher flow and channel width that likely have higher sediment load than much of the catchment (Figure 36).

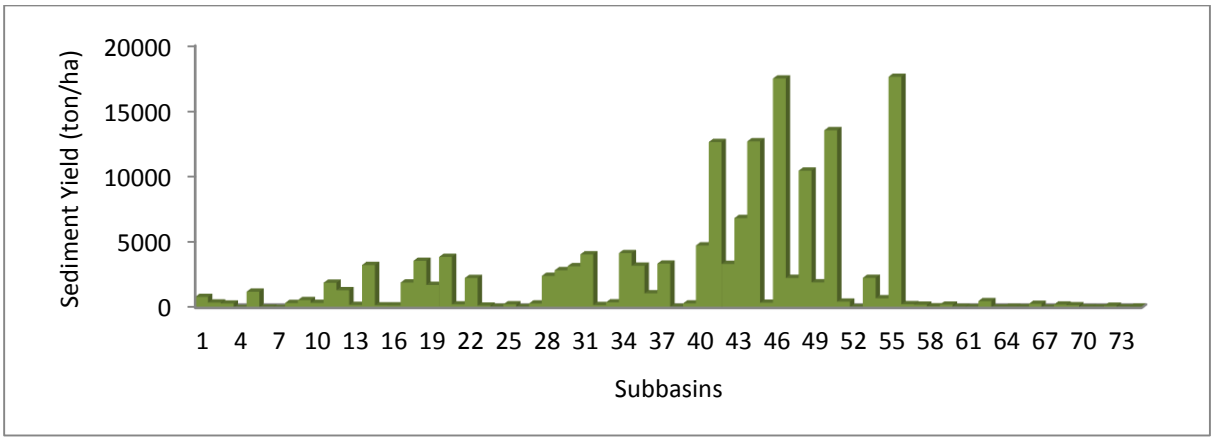

Figure 36: Suspended sediment yield from each subbasin (t year^{-1})

Subbasins 44 and 7 have the lowest value of sediment yield out of 74 sub catchments (Figure 36), even though subbasins 4 and 7 have dominantly sand and steep slopes. Measurement points at the upstream end of these two subbasins cause lower total sediment load.

Table 11-Total volume of sediment load from 74 catchments in the Ankara River basin

Sediment Yield Data for 74 small catchments in Ankara Stream Basin (t year $^{-1}$)															
1	829.27	**11**	1910.28	**21**	254.91	**31**	4080.21	**41**	12656.07	**51**	470.45	**61**	52.87	**71**	43.74
2	400.19	**12**	1342.01	**22**	2276.12	**32**	207.41	**42**	3351.58	**52**	54.91	**62**	507.92	**72**	149.27
3	323.27	**13**	217.35	**23**	162.70	**33**	415.60	**43**	6858.03	**53**	2286.26	**63**	39.43	**73**	45.64
4	0.00	**14**	3267.08	**24**	82.26	**34**	4174.95	**44**	12711.66	**54**	720.55	**64**	76.94	**74**	86.57
5	1229.46	**15**	183.60	**25**	262.03	**35**	3213.97	**45**	386.64	**55**	17615.50	**65**	59.40		
6	26.27	**16**	179.25	**26**	54.38	**36**	1106.89	**46**	17488.85	**56**	270.23	**66**	302.66		
7	0.00	**17**	1932.36	**27**	326.95	**37**	3374.00	**47**	2279.38	**57**	231.79	**67**	21.00		
8	363.27	**18**	3588.09	**28**	2439.10	**38**	78.66	**48**	10478.76	**58**	110.70	**68**	244.25		
9	588.36	**19**	1748.22	**29**	2871.07	**39**	330.31	**49**	1941.43	**59**	238.47	**69**	193.02		
10	371.74	**20**	3889.37	**30**	3174.38	**40**	4764.47	**50**	13551.77	**60**	81.52	**70**	48.79		

In the Ankara River catchment, the most common land use types and land cover are irrigated land (%57), rangeland (13%), and forest land (3%) (Figure 20). More than half of the Ankara catchment, especially the southern portion of the watershed, is covered by cultivated plants such as wheat, barley, beet, potato, and sunflower. Three types of land uses (arable land, grassland,

forest) are particularly widespread. Each land use type has various responses to soil erosion because these plant covers protect the ground surface from the impacts of raindrops and reduce the runoff and velocity by controlling infiltration capacity (Thornes, 2001; Descheemaeker et al., 2006).

6.3. Data Collection

Variables such as sediment yield are influenced by topographic factors and human activities. Consequently, sediment yield is an adjustable or dependent variable while topographic factors including drainage area and channel width are controlling or independent variables. Moreover, sediment in the channel system is supplied by soil erosion, which can also be controlled by hill slope vegetation cover and many other factors. Because the relationships among controlling variables are quite complicated, it can be very difficult to isolate the influence of one parameter from another.

Table 12: Investigated catchment properties, data sources, methods of data collection in the catchment

Investigated catchment properties, data sources and methods of data collection in Ankara		
Data Type	**Controlling variables**	**Data collection, sources and data derivation**
Topographic	Catchment area (A, ha)	Digital elevation model (DEM, 90m).
	Minimum elevation (H_{min}, m)	Digital elevation model (DEM, 90m).
	Maximum elevation (Hmax, m)	Digital elevation model (DEM, 90m).
	Mean Channel Width (m)	Field mapping using GIS.
	Mean catchment slope (m/m)	Field mapping using GIS.
	Elevation (m)	Field mapping using GIS.
	Depth (m)	Field mapping using GIS.
	Relief Ratio	RLR = (HD/HL), (USDA, 1972).
	Drainage density (DD)	DD=(TDL/A) (Morris and Fan, 1998).
	Hypsometric integral (HI)	HI=((Hmean-Hmin)/(Hmax-Hmin)) (Strahler, 1964)
Human Activities	Land use mainly cultivated land (Cult., % of A)	Field mapping and practices using GPS.
	Land use mainly indistrial land (Ind., % of A)	Field mapping and practices using GPS.
	Land cover mainly forests (Frst., % of A)	Field mapping using GIS.
	Land cover mainly grass land (Grass, % of A)	Field mapping and practices using GPS.

The topographic parameters were either directly derived from a DEM or from field maps or computed using established equations. The 90 m DEM for the whole catchment was obtained

from the USGS (United States Geological Survey) web-site http://eros.usgs.gov/#/ Find_Data/Products_and_Data Available/gtopo30_info. Relief ratio and drainage density were computed for each sub-basin using topographic maps (Figure 37) and the equations mentioned above. Furthermore, human activities were identified by land use/land cover maps and aerial photo interpretation, geology, and soil maps from the Republic of Turkey Ministry of Food, Agriculture and Livestock.

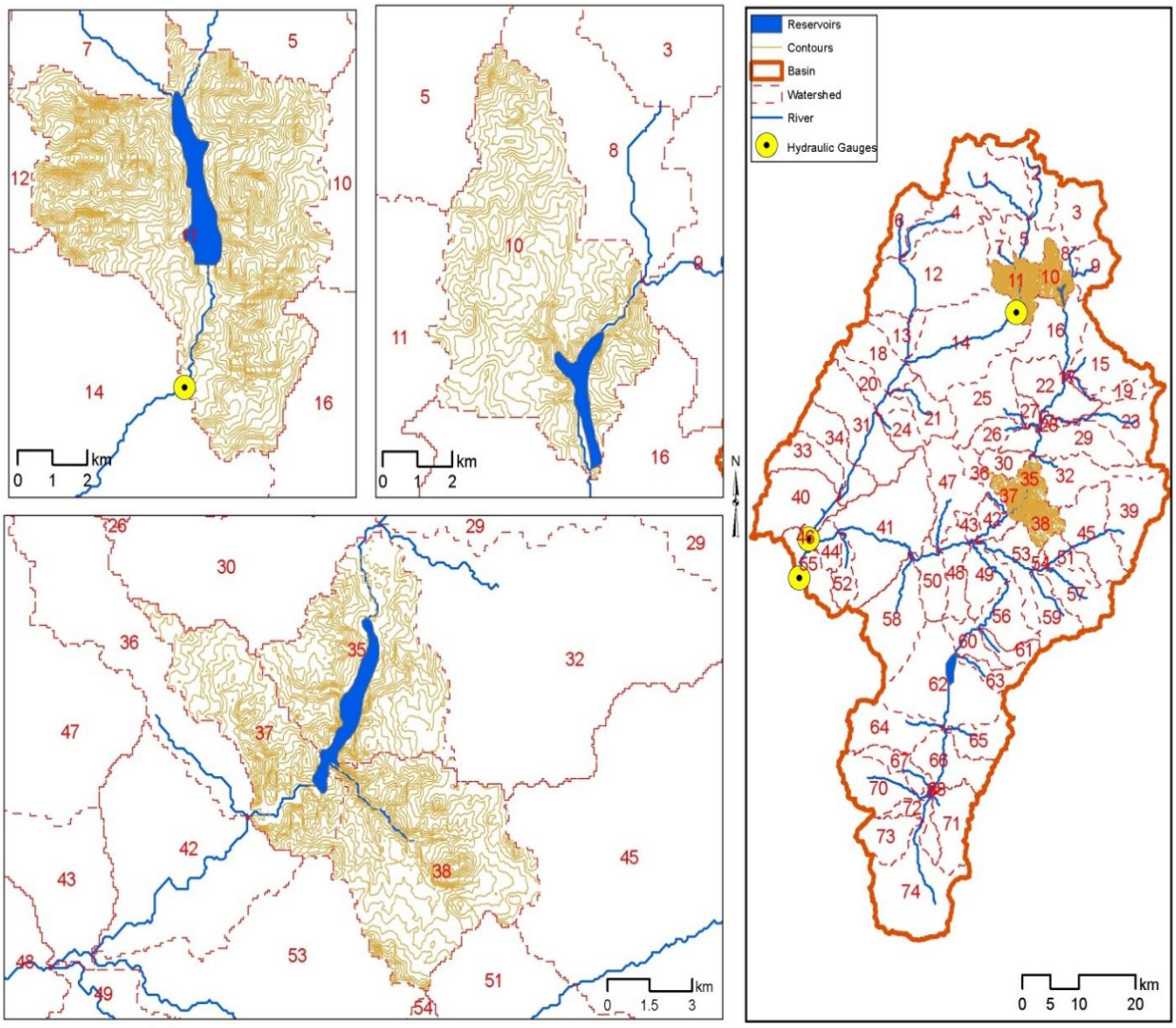

Figure 37: Contour maps of the surrounding area of reservoirs in the watershed

In order to obtain precipitation data, the Kriging interpolation technique was used to identify distribution of mean annual rainfall. Five meteorology stations within the watershed and one outside of the watershed were used as reference points for mean annual precipitation (Figure 38). The 74 subbasins were categorized with the rank 1 to 9 based on the dominant type of mean annual precipitation to examine correlations between rainfall and sediment load (Figure 39). According to the Kriging interpolation, the northern and northwestern boundaries of the watershed likely have more precipitation. This likely also explains why vegetation cover is denser in the northern part of the catchment.

Other physical factors of relief ratio (RR), drainage density (DD), and hypsometric integral (HI) were computed using the following equations:

$$\text{Relief Ratio} = RR = \frac{\text{Elevation Difference}}{\text{Horizontal Distance}}, \quad \text{(USDA, 1972)} \quad \text{(Eq.12)}$$

$$\text{Drainage Density} = DD = \frac{\text{Total Lenght of Stream}}{\text{Drainage Area}}, \quad \text{(Morris and Fan, 1998)} \quad \text{(Eq.13)}$$

$$\text{Hypsometric Integral} = HI = \frac{\text{Mean Elevation} - \text{Min Elevation}}{\text{Mean Elevation} - \text{Max Elevation}}, \quad \text{(Strahler, 1964)} \quad \text{(Eq.14)}$$

The absence of spatially distributed data on anthropogenic disturbance history (e.g., grazing and cropping) is one of the limitations of this study. However, I reclassified land use and land cover type in five main categories including percentage of cultivated areas, percentage of forest areas, percentage of range lands, percentage of industrial areas, and percentage of surface water for each subbasin. The categorization of land use type may significantly correlate with sediment yield because widespread cultivated areas correspond to more lands with seasonal farming or other farming methods that result in soil erosion, especially in semiarid regions.

6.4. Methodology

The overall objective of this research is to develop a statistical model to determine the factors that are most important for sedimentation and sediment yields in reservoirs of Central Turkey. For both reservoirs chosen for inclusion in this study, I conducted multiple regression analyses in SPSS and MS Excel in order to evaluate the relationship between independent (variables controlling sediment yield) and dependent (sediment yield) variables. I (i) examined sediment input and temporal control variables at monthly time intervals dictated by the availability of information on land cover and disturbance, (ii) analyzed average sediment input and all control variables for each subbasin, and (iii) undertook these analyses individually, and then for progressively larger subsets of all of these subbasins in the same watershed. I plotted a graph of the expected sediment yield and measured sediment yield versus each independent variable in order to determine which factor dominantly influences sediment yield in the watershed.

Sediment yield, as indicated by total sediment outflow from a sub-basin measured at a point at each sub-basin's outlet, can be obtained either by monitoring or by using a conceptual model. Use of a conceptual model can also be based on sediment rating curves in order to simultaneously monitor suspended sediment yield versus discharge. Spatial variability in sediment yield might reflect spatial variability in controlling factors such as drainage area, elevation, mean channel slope, runoff, channel width, depth, and land-use types. As a dependent variable, simulated sediment data from the SWAT model outputs were used due to lack of spatially distributed sediment data in the watershed. I conclude that the simulated sediment data from the SWAT model are within the acceptable range through time and space. For that reason, the simulated data were used in multiple regression analysis even though the data have many uncertainties and lower ability to reflect correlations between dependent and independent variables. Before applying multiple

regression analysis, I tried to limit the number of explanatory variables to 12 to avoid any problem of inflated R^2, and I tried to minimize the influence of auto correlation of physical controlling variables in multiple regression analysis (Phippen and Wohl, 2003). In addition, I drew scatter plots among sediment yield and other potential parameters.

6.5. Multiple Regression Analyses

Multiple regression analysis is a statistical tool for estimating the relationship between dependent and independent variables (Table 13). The model computes the conditional expectations of controlling variables against sediment yield in this study, contributes to better understanding of which controlling factors dominantly affect sedimentation processes, and allows me to explore the form of this relationship in a watershed. Although numerous techniques can be used to carry out regression analysis, I used Pearson's pair wise correlation, which is sensitive only to a linear relationship among variables. Other correlation coefficients have been developed to be more robust than Pearson's (Dietrich, 1991). In general, multiple regression equation of Y on X_1, $X_{2,\ldots,}$ X_k is given by:

$$Y = b_0 + b_1 X_1 + b_2 X_2 + \ldots\ldots\ldots\ldots\ldots\ldots + b_k X_k \qquad \text{(Eq. 15)}$$

Where

Y=Dependent variable

X= Independent variable

b_0 = Intercept

b_1, b_2, b_3, …, b_k = regression coefficients

The analysis was performed by using the following data for multiple regression in SPSS. The question I am trying to answer in this multiple linear regression analysis is whether I can predict sediment yield associated with other dependent variables with an acceptable level of accuracy. I used the stepwise method of including or excluding independent variables in the model with respect to their statistical significance with a confidence interval of 90%.

Table 13: Catchment properties for the 74 studied catchments in central Turkey.

S_Bsn: Subbasin number, Area: Subbasin area, E_Min: Minimum elevation, E_Max: Maximum elevation, E_Diff: Elevation difference, Width: Channel width, Slope: Mean slope, E_mean: Mean elevation, Depth: Average depth, RR: Relief ratio, DD: Drainage density, HI: Hypsometric integral, Lgnpth: Long path, CULT: The ratio of cultivated areas, FRST: The ratio of forested lands, RGN: The ratio of rangelands, INDUST: The ratio of industrial lands, WATR: The ratio of surface water, FLOW_OUT: Stream flow, SED_OUT: Sediment load.

Sbn	Precip	Area	ElevMin	ElevMax	Elv Difference	Width	Slope	M_Elevation	Depth	RR	DD	HI	Longpath	CULT	LUofFOREST	LUofGRASSLAND	LUofINDSUTRY	WATR	FLOWOUTcms	SEDOUTtons
1	3	129.3	1226.00	2044.00	818.00	0.91	0.02	1602.38	8.116	0.46	0.5	0.85	17115.00	16	37	46	0	0	2222.9	829.3
2	3	70.91	1226.00	1998.00	772.00	0.71	0.03	1668.10	8.116	0.57	0.6	1.34	14379.00	32	42	26	0	0	1226.3	400.2
3	3	73.58	1203.00	1881.00	678.00	0.73	0.04	1514.64	8.116	0.46	0.5	0.85	168.00	26	30	43	0	0	1007.7	323.3
4	2	67.72	1014.00	1884.00	870.00	0.70	0.01	1386.58	8.116	0.43	0.4	0.75	15066.00	5	13	75	0	0	1172.5	0.0
5	2	241.60	1125.00	1857.00	732.00	1.17	0.01	1418.86	8.116	0.40	0.4	0.67	7124.00	8	58	34	0	0	4142.3	1229.5
6	2	51.82	1010.00	1642.00	632.00	0.63	0.01	1187.38	8.116	0.28	0.3	0.39	7621.00	10	1	80	0	0	905.9	26.3
7	2	29.77	1134.00	1882.00	748.00	0.50	0.06	1566.36	8.116	0.58	0.6	1.37	4670.00	1	88	10	0	0	500.9	0.0
8	2	92.55	1128.00	1856.00	728.00	0.80	0.01	1358.36	8.116	0.32	0.3	0.46	6298.00	8	16	76	0	0	1375.9	363.3
9	2	47.68	1130.00	1594.00	464.00	0.61	0.02	1313.32	8.116	0.40	0.4	0.65	10712.00	1	1	97	0	0	666.1	588.4
10	2	181.10	1065.00	1807.00	742.00	1.04	0.01	1300.44	8.116	0.32	0.3	0.46	12288.00	19	1	75	0	0	2835.8	371.7
11	2	328.90	1027.00	1721.00	694.00	1.32	0.01	1291.46	8.116	0.38	0.4	0.62	24316.00	19	16	60	0	0	5679.8	1910.3
12	1	334.70	910.00	1785.00	875.00	1.33	0.01	1211.63	8.116	0.34	0.3	0.53	13685.00	17	4	67	0	1	5835.5	1342.0
13	1	379.60	876.00	1507.00	631.00	45.52	0.00	1016.79	1.4	0.22	0.2	0.29	1098.00	57	1	32	0	1	619.7	217.3
14	2	550.50	876.00	1625.00	749.00	1.62	0.01	1111.71	8.116	0.31	0.3	0.46	6191.00	41	1	52	0	0	8754.1	3267.1
15	4	85.88	963.00	1566.00	603.00	18.66	0.00	1124.19	0.77	0.27	0.3	0.36	4266.00	69	0	28	0	0	1578.8	183.6
16	3	282.70	962.00	1401.00	439.00	38.14	0.01	1131.75	1.24	0.39	0.4	0.63	10495.00	42	0	51	0	0	2036.9	179.2
17	4	112.30	960.00	997.00	37.00	21.92	0.00	971.72	0.86	0.32	0.3	0.46	4765.00	81	0	19	0	0	1874.0	1932.4
18	1	1002.00	848.00	1445.00	597.00	81.48	0.01	1019.45	2.06	0.29	0.3	0.40	861.00	82	0	12	0	0	9512.1	3588.1
19	4	25.14	967.00	1504.00	537.00	0.47	0.01	1246.30	8.116	0.52	0.5	1.08	10900.00	51	0	46	0	0	290.7	1748.2
20	2	1106.00	843.00	1326.00	483.00	86.44	0.00	990.07	2.14	0.30	0.3	0.44	7080.00	87	0	5	1	0	10026.5	3889.4
21	3	56.18	862.00	1464.00	602.00	0.65	0.02	1122.93	8.116	0.43	0.4	0.77	3750.00	68	0	25	0	0	464.4	254.9
22	4	485.30	931.00	1317.00	386.00	52.75	0.00	1018.92	1.54	0.23	0.2	0.29	9687.00	89	0	9	0	0	4969.5	2276.1
23	5	87.25	932.00	1767.00	835.00	0.78	0.01	1279.70	8.116	0.42	0.4	0.71	16671.00	33	0	65	0	0	1441.4	162.7
24	3	34.32	850.00	1491.00	641.00	0.54	0.02	1097.53	8.116	0.39	0.4	0.63	5744.00	64	0	30	0	0	102.0	82.3
25	4	106.00	950.00	1628.00	678.00	0.84	0.01	1170.62	8.116	0.33	0.3	0.48	7451.00	56	0	39	0	0	2130.4	262.0
26	5	31.82	949.00	1429.00	480.00	0.52	0.01	1116.38	8.116	0.35	0.3	0.54	2078.00	36	0	57	0	0	641.2	54.4
27	5	152.70	925.00	1138.00	213.00	26.35	0.01	972.41	0.97	0.22	0.2	0.29	5814.00	90	0	9	0	0	3042.1	327.0
28	5	574.20	929.00	959.00	30.00	58.35	0.00	942.58	1.65	0.45	0.5	0.83	12880.00	33	0	48	11	0	6408.3	2439.1
29	6	830.70	915.00	1669.00	754.00	72.82	0.00	1073.13	1.91	0.21	0.2	0.27	6990.00	72	0	26	0	0	10079.2	2871.1
30	6	946.20	914.00	1340.00	426.00	2.02	0.01	1070.04	8.116	0.37	0.4	0.58	13700.00	49	0	47	0	0	10886.1	3174.4
31	3	1278.00	812.00	1420.00	608.00	94.31	0.00	972.95	2.27	0.26	0.3	0.36	6507.00	77	0	7	0	0	10276.7	4080.2
32	6	85.73	920.00	1895.00	975.00	0.77	0.01	1206.21	8.116	0.29	0.3	0.42	11767.00	45	0	51	0	0	459.7	207.4
33	3	61.37	795.00	1469.00	674.00	0.68	0.00	1009.77	8.116	0.32	0.3	0.47	10258.00	68	0	11	1	0	248.1	415.6
34	3	1357.00	796.00	1408.00	612.00	97.73	0.00	921.91	2.33	0.21	0.2	0.26	14033.00	70	0	7	1	0	10344.1	4174.9
35	5	977.80	904.00	1216.00	312.00	2.04	0.00	1030.36	8.116	0.40	0.4	0.68	8066.00	50	1	45	0	1	10921.9	3214.0
36	6	26.64	877.00	1458.00	581.00	0.48	0.03	1200.18	8.116	0.56	0.6	1.25	11405.00	54	0	31	12	0	460.4	1106.9
37	7	1037.00	874.00	1260.00	386.00	2.09	0.00	1038.46	8.116	0.43	0.4	0.74	16801.00	46	0	47	2	0	11081.7	3374.0
38	8	36.39	902.00	1369.00	467.00	0.55	0.02	1120.25	8.116	0.47	0.5	0.88	5423.00	62	0	32	0	0	73.5	78.7
39	7	103.50	1069.00	1909.00	840.00	0.83	0.01	1308.66	8.116	0.29	0.3	0.40	5534.00	53	1	39	0	0	2087.2	330.3
40	4	1542.00	781.00	1471.00	690.00	2.45	0.00	983.64	8.116	0.29	0.3	0.42	7251.00	82	0	10	1	0	10764.2	4764.5
41	6	3267.00	782.00	1474.00	692.00	165.62	0.00	913.52	3.31	0.19	0.2	0.23	5345.00	70	0	9	3	0	14918.0	12656.1
42	7	1094.00	842.00	1131.00	289.00	85.92	0.00	939.06	2.14	0.34	0.3	0.51	7473.00	15	0	0	82	0	4825.6	3351.6
43	7	1555.00	837.00	1159.00	322.00	106.07	0.00	949.61	2.46	0.35	0.3	0.54	11600.00	13	0	0	87	0	11089.2	6858.0
44	6	3329.00	773.00	1008.00	235.00	167.49	0.00	869.72	3.33	0.41	0.4	0.70	22239.00	87	0	7	2	0	14971.4	12711.7
45	8	208.00	1001.00	1504.00	503.00	1.10	0.01	1191.34	8.116	0.38	0.4	0.61	4004.00	65	0	34	0	0	3713.8	386.6
46	4	4876.00	768.00	1056.00	288.00	3.88	0.00	872.81	8.116	0.36	0.4	0.57	6472.00	85	0	0	0	0	25725.2	17488.9
47	6	101.60	830.00	1487.00	657.00	0.83	0.01	1093.92	8.116	0.40	0.4	0.67	4390.00	55	0	22	16	0	1822.0	2279.4
48	8	2746.00	823.00	1303.00	480.00	149.22	0.00	955.31	3.09	0.28	0.3	0.38	4289.00	6	5	27	62	0	12404.4	10478.8
49	8	1137.00	835.00	1304.00	469.00	87.90	0.01	981.74	2.17	0.31	0.3	0.46	1281.00	33	0	19	42	0	812.9	1941.4
50	7	2901.00	809.00	1269.00	460.00	154.22	0.00	944.76	3.15	0.30	0.3	0.42	6086.00	37	1	39	18	0	14381.8	13551.8
51	9	242.00	957.00	1469.00	512.00	1.17	0.01	1118.44	8.116	0.32	0.3	0.46	3176.00	69	0	28	0	0	4047.1	470.4
52	6	32.65	784.00	1241.00	457.00	10.45	0.01	973.58	0.52	0.41	0.4	0.71	8613.00	74	0	1	1	0	48.4	54.9
53	8	445.80	844.00	1546.00	702.00	1.49	0.01	1050.55	8.116	0.29	0.3	0.42	5418.00	60	0	20	12	0	6099.5	2286.3
54	9	319.40	933.00	1272.00	339.00	1.30	0.01	1042.21	8.116	0.32	0.3	0.48	4220.00	42	0	49	0	0	5379.0	720.6
55	5	4932.00	760.00	1244.00	484.00	3.90	0.00	919.94	8.116	0.33	0.3	0.49	4421.00	88	0	5	0	0	25768.8	17615.5
56	8	1076.00	909.00	1637.00	728.00	2.12	0.01	1138.98	8.116	0.32	0.3	0.46	9298.00	56	0	40	0	0	383.9	270.2
57	9	71.39	956.00	1686.00	730.00	0.72	0.03	1312.49	8.116	0.49	0.5	0.95	1896.00	60	0	36	1	0	1320.8	231.8
58	6	130.30	810.00	1299.00	489.00	23.97	0.01	1045.23	0.91	0.48	0.5	0.93	11118.00	88	0	4	0	0	182.2	110.7
59	9	55.80	937.00	1865.00	928.00	0.65	0.03	1337.05	8.116	0.43	0.4	0.76	6002.00	63	0	29	1	0	502.8	238.5
60	8	981.00	965.00	1523.00	558.00	2.05	0.00	1106.67	8.116	0.25	0.3	0.34	7644.00	40	8	43	0	2	138.2	81.5
61	8	28.57	972.00	1802.00	830.00	0.50	0.02	1344.57	8.116	0.45	0.4	0.81	2884.00	32	0	64	0	0	78.8	52.9
62	6	908.40	967.00	1512.00	545.00	76.84	0.00	1086.36	1.98	0.22	0.2	0.28	12503.00	83	0	8	0	3	898.0	507.9
63	7	31.48	973.00	1699.00	726.00	0.52	0.01	1264.52	8.116	0.40	0.4	0.67	10655.00	58	0	35	0	1	68.0	39.4
64	5	89.86	981.00	1343.00	362.00	19.17	0.01	1156.59	0.79	0.49	0.5	0.94	6388.00	79	0	1	1	0	88.2	76.9
65	6	54.74	980.00	1521.00	541.00	0.64	0.01	1162.74	8.116	0.34	0.3	0.51	5291.00	72	3	21	0	0	81.4	59.4
66	5	556.00	981.00	1380.00	399.00	57.23	0.00	1051.99	1.63	0.18	0.2	0.22	7717.00	88	0	3	0	0	522.0	302.7
67	5	37.10	998.00	1315.00	317.00	11.28	0.01	1109.43	0.55	0.35	0.4	0.54	7238.00	84	0	0	1	0	23.7	21.0
68	5	436.90	996.00	1064.00	68.00	49.53	0.00	1023.11	1.48	0.40	0.4	0.66	7540.00	70	0	30	0	0	430.5	244.3
69	5	348.30	998.00	1057.00	59.00	43.22	0.00	1009.03	1.35	0.19	0.2	0.23	475.00	72	0	28	0	0	346.0	193.0
70	5	87.79	998.00	1441.00	443.00	18.91	0.01	1160.80	0.78	0.37	0.4	0.58	965.00	81	0	8	0	0	84.0	48.8
71	5	77.34	1000.00	1297.00	297.00	17.52	0.00	1078.84	0.74	0.27	0.3	0.36	14974.00	93	0	6	0	0	75.7	43.7
72	5	270.50	1000.00	1289.00	289.00	37.14	0.00	1058.03	1.22	0.20	0.2	0.25	2707.00	94	0	3	0	0	270.9	149.3
73	4	58.21	1009.00	1431.00	422.00	14.78	0.00	1170.42	0.66	0.38	0.4	0.62	5324.00	80	0	14	0	0	64.5	45.6
74	4	175.50	1012.00	1438.00	426.00	28.65	0.00	1159.25	1.03	0.35	0.3	0.53	371.00	78	0	17	0	0	180.4	86.6

The model performance was tested using the F-test in the ANOVA table, and the result indicates that there are statistically significant linear relationships among the variables analyzed based on the coefficient of determination (R^2). The coefficient of determination, R^2, is a useful tool as it presents how well the regression line represents the data, and gives the proportion of the variance of each variable which can be predicted from independent variables. The coefficient of determination is calculated by the following equation:

$$R^2 = \frac{SSR}{SST} \quad \text{(Eq. 16)}$$

Where

R^2 = Coefficient of determination

SSR = Sum of Squares Regression

SST = Total Sum of Squares (SSR + SSE)

The value of R^2 can range between 0 and 1, with higher values reflecting more accurate regression models. A strong relationship exists between several variables and sediment yield with a value of R^2 above 0.5 by using a 90% confidence interval (CI). The SPSS tool started with the multiple R, adjusted R^2 of the variability of sediment load, and adjusted R^2, which is somewhat lower than the original R^2 as it takes into account sample size. The standard error of estimation is associated with R^2, not adjusted R^2. I also used "Durbin Watson" statistics to test the hypothesis that there might be serial correlation in the data. If the Durbin Watson value is within the acceptable range of 1.5 to 2.5, meaningful serial correlation is absent in the dataset (Khorasani and Zeyun, 2014).

Table 14: The model summary of multiple regression analysis by using SPSS

Model Summary[f]

Model	R	R Square	Adjusted R Square	Std. Error of the Estimate	Durbin-Watson
1	.966[a]	.934	.933	1011.9324	
2	.973[b]	.947	.946	911.7780	
3	.977[c]	.955	.953	847.5090	
4	.979[d]	.959	.956	818.7903	
5	.981[e]	.962	.960	784.6945	2.580

a. Predictors: (Constant), Area_m²

b. Predictors: (Constant), Area_m², FLOW_OUT_cms

c. Predictors: (Constant), Area_m², FLOW_OUT_cms, WATR

d. Predictors: (Constant), Area_m², FLOW_OUT_cms, WATR, RR

e. Predictors: (Constant), Area_m², FLOW_OUT_cms, WATR, RR, Width_(m)

f. Dependent Variable: SED_OUT tons

Table 14 shows the multiple linear regression model summary and overall fit statistics for sediment yield and other controlling variables. The stepwise method chooses the independent variable that has the largest Pearson correlation with the dependent variable, and puts that into the regression analysis. Then it sequentially does the same for the next highest independent variable until it finds a non-significant predictor. The model found two statistically significant variables with R^2 above 0.9, which indicates that more than 90% of variability of sediment yield can be accounted for by two controlling variables: drainage area and stream flow (Table 14). The Durbin Watson value is above 2.5, so I conclude that there is a negative serial correlation in the dataset.

Collinearity in the regression model illustrates inter-correlation among the independent variables. The non-collinearity assumption can be explained through the values of the tolerance and the evidences inflation factor (VIF). The tolerance values ranged from 0 to 1 and VIF values ranged from 0 to 10. The cutoff value is 0.2 for tolerance and for VIF values under 4.

Table 15: Collinearity statistics of multiple linear regression estimates

Model		Collinearity Statistics	
		Tolerance	VIF
1	(Constant)		
	Area_m²	1.000	1.000
2	(Constant)		
	Area_m²	.188	5.319
	FLOW_OUT_cms	.188	5.319
3	(Constant)		
	Area_m²	.180	5.544
	FLOW_OUT_cms	.179	5.581
	WATR	.953	1.049
4	(Constant)		
	Area_m²	.178	5.614
	FLOW_OUT_cms	.179	5.581
	WATR	.924	1.083
	RR	.908	1.101
5	(Constant)		
	Area_m²	.151	6.602
	FLOW_OUT_cms	.174	5.756
	WATR	.915	1.093
	RR	.804	1.244
	Width_(m)	.601	1.664

In terms of the tolerance values, drainage area and stream flow were within the acceptable range (below 0.2) for the statistically significant parameters. The VIF values of drainage area and stream flow were slightly over the cutoff number, with a value of 5.3 (Table 15). Therefore, the assumption of multicollinearity was not met for these two controlling variables.

Table 16 illustrates the multiple regression estimates including the intercept and the insignificance levels of the parameters. In the stepwise multiple regression analysis, I found a highly significant intercept and highly significant values of stream flow, drainage area, channel width, water surface, and relative ratio.

Table 16: ANOVA table of multiple linear regression estimates

ANOVA[a]

Model		Sum of Squares	df	Mean Square	F	Sig.
1	Regression	1042270294	1	1042270294	1017.835	.000[b]
	Residual	73728524.30	72	1024007.282		
	Total	1115998818	73			
2	Regression	1056973735	2	528486867.3	635.705	.000[c]
	Residual	59025083.63	71	831339.206		
	Total	1115998818	73			
3	Regression	1065719817	3	355239938.9	494.576	.000[d]
	Residual	50279001.46	70	718271.449		
	Total	1115998818	73			
4	Regression	1069740004	4	267435001.1	398.908	.000[e]
	Residual	46258813.83	69	670417.592		
	Total	1115998818	73			
5	Regression	1074128132	5	214825626.3	348.887	.000[f]
	Residual	41870686.61	68	615745.391		
	Total	1115998818	73			

a. Dependent Variable: SED_OUT tons

b. Predictors: (Constant), Area_m²

c. Predictors: (Constant), Area_m², FLOW_OUT_cms

d. Predictors: (Constant), Area_m², FLOW_OUT_cms, WATR

e. Predictors: (Constant), Area_m², FLOW_OUT_cms, WATR, RR

f. Predictors: (Constant), Area_m², FLOW_OUT_cms, WATR, RR, Width_(m)

A strong relationship exists between suspended sediment yield and drainage area and stream flow, as well as channel width. Higher stream flow and channel width correspond to higher soil erosion risk. Similar results are reported in Schumm (1954). In his research, channel width and stream flow were selected for the best sediment yield model as they exhibited higher partial correlations: sediment yield increases with higher channel width and stream flow. Also, in central Ankara, an increase in channel width usually corresponds to: (1) an increase in stream flow; (2) an increase in sediment yield; and (3) a decrease in mean elevation.

Table 17: Correlation matrix between catchment properties and sediment yield

S_Bsn: Subbasin number, PCP: Mean Annual Precipitation, Area: Subbasin area, E_Min: Minimum elevation, E_Max: Maximum elevation, E_Diff: Elevation difference, Width: Channel width, Slope: Mean slope, E_mean: Mean elevation, Depth: Average depth, RR: Relief ratio, DD: Drainage density, HI: Hypsometric integral, Lgnpth: Long path, CULT: The ratio of cultivated areas, FRST: The ratio of forested lands, RGN: The ratio of rangelands, INDUST: The ratio of industrial lands, WATR: The ratio of surface water, FLOW_OUT: Stream flow, SED_OUT: Sediment load. WATR: Surface Water

Pearson Correlation

	SED	PCP	Area	E_Min	E_Max	E_Diff	Width	Slope	E_Mean	Depth	RR	DD	HI	LgnPth	CULT	FRST	RGN	INDUST	WATR
FLOW	0.92	0.01	0.90	-0.54	-0.35	-0.15	0.44	-0.36	-0.50	0.03	-0.21	-0.21	-0.23	0.12	0.11	-0.12	-0.22	0.18	-0.08
SED		0.08	0.97	-0.55	-0.39	-0.19	0.55	-0.31	-0.50	-0.04	-0.16	-0.16	-0.17	0.07	0.11	-0.12	-0.28	0.27	-0.10
PCP			0.13	-0.26	-0.23	-0.14	0.11	0.07	-0.23	0.04	0.00	0.00	-0.02	-0.16	0.16	-0.33	-0.18	0.30	0.04
Area				-0.56	-0.41	-0.21	0.55	-0.37	-0.54	-0.07	-0.25	-0.25	-0.25	0.04	0.16	-0.14	-0.32	0.25	0.01
E_Min					0.58	0.19	-0.44	0.47	0.84	0.20	0.28	0.28	0.31	0.04	-0.41	0.58	0.43	-0.28	0.01
E_Max						0.91	-0.44	0.54	0.85	0.57	0.24	0.24	0.26	0.10	-0.48	0.49	0.50	-0.28	0.08
E_Diff							-0.31	0.41	0.60	0.58	0.14	0.14	0.15	0.10	-0.37	0.29	0.38	-0.19	0.09
Width								-0.46	-0.55	-0.59	-0.40	-0.40	-0.34	0.03	0.14	-0.18	-0.40	0.46	0.01
Slope									0.73	0.45	0.70	0.70	0.75	-0.08	-0.38	0.64	0.21	-0.15	-0.13
E_Mean										0.50	0.54	0.54	0.57	0.12	-0.52	0.66	0.49	-0.28	-0.01
Depth											0.39	0.39	0.35	-0.17	-0.48	0.26	0.58	-0.20	-0.02
RR												0.00	0.98	0.21	-0.32	0.36	0.20	-0.05	-0.18
DD													0.98	0.21	-0.05	0.41	0.20	-0.05	-0.18
HI														0.20	-0.30	0.48	0.15	-0.67	-0.16
LgnPth															-0.21	0.08	0.23	-0.03	0.10
CULT																-0.48	-0.70	-0.35	0.00
FRST																	0.06	-0.07	-0.03
RGN																		-0.21	0.05
INDUST																			-0.08

In contrast, my data indicate that most of the topographic (mean slope, local elevation, hypsometric integral, long path) and land cover (CULT, FRST, RGN, INDUST) factors are not highly associated with sediment yield. However, early geomorphologists usually found a strong relationship between slopes, morphology and soil erosion rate. According to Powell (1876) and Gilbert (1877), greater relief and steeper slopes lead to faster soil erosion rate and thus to higher soil erosion risk. This also reflects more potential energy available for erosion and sediment transport by runoff.

Descriptive multivariate analysis revealed the difficulty of separating the effects of land cover factors affecting sediment yield at the basin scale. Land cover factors including cultivated lands, forested areas, rangelands, and industrialized lands, are not highly correlated with sediment yield. However, water bodies show some degree of association between the variable and sediment yield (Table 17).

The table of Sig-1 tailed matrix indicates a significant p-value for controlling variables such as drainage area, stream flow, mean elevation, minimum elevation, and maximum elevation, mean slope, mean width, rangelands, and industrial lands (Table 18). All these variables are statistically significant because results with the p values are in the significance level with the 90% confidence interval**.**

Table 18: Sig -1 Tailed matrix between catchment properties and sediment yield

S_Bsn: Subbasin number, PCP: Mean Annual Precipitation, Area: Subbasin area, E_Min: Minimum elevation, E_Max: Maximum elevation, E_Diff: Elevation difference, Width: Channel width, Slope: Mean slope, E_mean: Mean elevation, Depth: Average depth, RR: Relief ratio, DD: Drainage density, HI: Hypsometric integral, Lgnpth: Long path, CULT: The ratio of cultivated areas, FRST: The ratio of forested lands, RGN: The ratio of rangelands, INDUST: The ratio of industrial lands, WATR: The ratio of surface water, FLOW_OUT: Stream flow, SED_OUT: Sediment load, WATR: Surface Water

Sig- 1 Tailed

	SED	PCP	Area	E_Min	E_Max	E_Diff	Width	Slope	E_Mean	Depth	RR	DD	HI	LgnPth	CULT	FRST	RGN	INDUST	WATR
FLOW	0.00	0.47	0.00	0.00	0.00	0.10	0.00	0.00	0.00	0.41	0.04	0.40	0.03	0.16	0.19	0.16	0.03	0.06	0.25
SED		0.24	0.00	0.00	0.00	0.06	0.00	0.00	0.00	0.38	0.08	0.08	0.07	0.29	0.18	0.16	0.01	0.01	0.20
PCP			0.15	0.01	0.03	0.12	0.12	0.29	0.00	0.36	0.49	0.02	0.02	0.08	0.09	0.12	0.00	0.00	0.36
Area				0.00	0.00	0.04	0.00	0.00	0.00	0.28	0.02	0.02	0.02	0.36	0.07	0.12	0.00	0.02	0.46
E_Min					0.00	0.06	0.00	0.00	0.00	0.05	0.01	0.08	0.00	0.37	0.00	0.00	0.00	0.01	0.46
E_Max						0.00	0.00	0.00	0.00	0.00	0.02	0.02	0.01	0.19	0.00	0.00	0.00	0.01	0.26
E_Diff							0.00	0.00	0.00	0.00	0.11	0.11	0.10	0.19	0.00	0.01	0.00	0.05	0.24
Width								0.00	0.00	0.00	0.00	0.00	0.00	0.41	0.14	0.07	0.00	0.00	0.47
Slope									0.00	0.00	0.00	0.00	0.00	0.26	0.00	0.00	0.04	0.10	0.13
E_Mean										0.00	0.00	0.00	0.00	0.16	0.00	0.00	0.00	0.01	0.46
Depth											0.00	0.00	0.00	0.11	0.00	0.01	0.00	0.47	0.43
RR												0.00	0.00	0.03	0.00	0.00	0.05	0.34	0.07
DD													0.00	0.03	0.00	0.00	0.05	0.34	0.07
HI														0.04	0.01	0.00	0.11	0.29	0.09
LgnPth															0.03	0.26	0.03	0.39	0.20
CULT																0.00	0.00	0.00	0.50
FRST																	0.29	0.27	0.39
RGN																		0.03	0.343
INDUST																			0.25

6.6. Results and Discussion

6.6.1. Physical Variables Controlling Sediment Yields

Accurate estimation of the relative importance of controlling variables makes it possible to better understand sedimentation processes and useful 'life time' of existing and planned reservoirs. It also can help to design sediment control strategies within the catchment and to identify the best locations for dam construction that facilitates longer usage. In this study, the control variables that explain most of the variation in sediment yield are drainage area, stream flow, channel width, and, to a lesser extent, topographic variables and human effects (Table 16). No other variables can be considered as prime control factors on sediment yield in the region. The principal controlling variables for sediment yield in the research area were investigated using multiple regression analysis, which provides fairly accurate and reliable predictions of suspended sediment yield at a basin scale, even when high spatial or temporal resolution basic data are lacking. Estimations of sediment yield data were based on the RUSLE equations using the SWAT model. The results suggest that sediment yield is likely to reflect some of the controlling variables discussed using regression analysis in the following sections.

6.6.1.1. Rainfall

Rainfall is known to be one of the most effective factors for relative erosion rate from drainage basins across diverse climatic regions because rainfall correlates with vegetation type and density. Langbein and Schumm (1958) demonstrated the negative correlation between precipitation and sediment concentration in the United States. According to this research, an increase in sediment concentration in a stream corresponds with reduced annual rainfall, which means that decreased rainfall may cause stream channel erosion. In this section, geo-statistical analysis was done using the Kriging interpolation method for mean annual precipitation based on 6 precipitation gages. Five of the stations are located in the watershed, but one of them called the

Kazan station is located out of the study area. I classified 9 different categories based upon the mean annual precipitation in the study area. Number 1 represents the highest rainfall value in mm with gradually lower values to class number 9 (Figure 38).

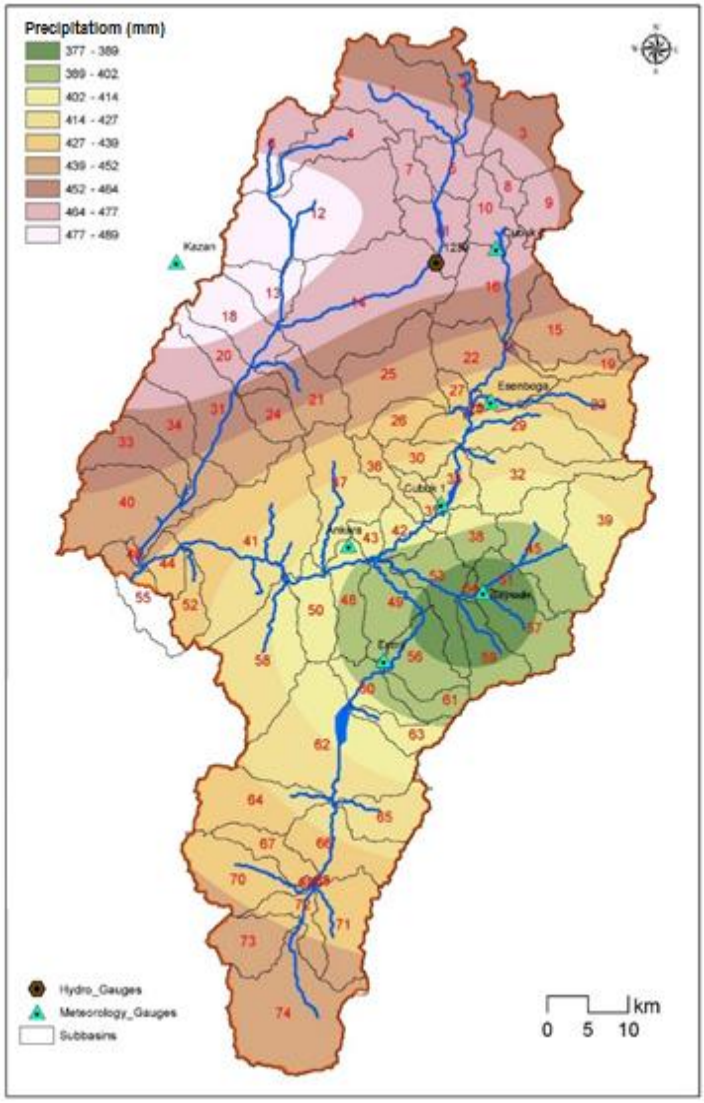

Figure 38: Kriging interpolation method for mean annual precipitation in the watershed

Results from multiple regression analyses indicate that rainfall does not have a significant influence on sediment yield (R^2 0.08) because upstream areas have less sediment yield but higher precipitation based on greater elevation. On the other hand, all tributaries have higher suspended sediment yield downstream (Figure 39).

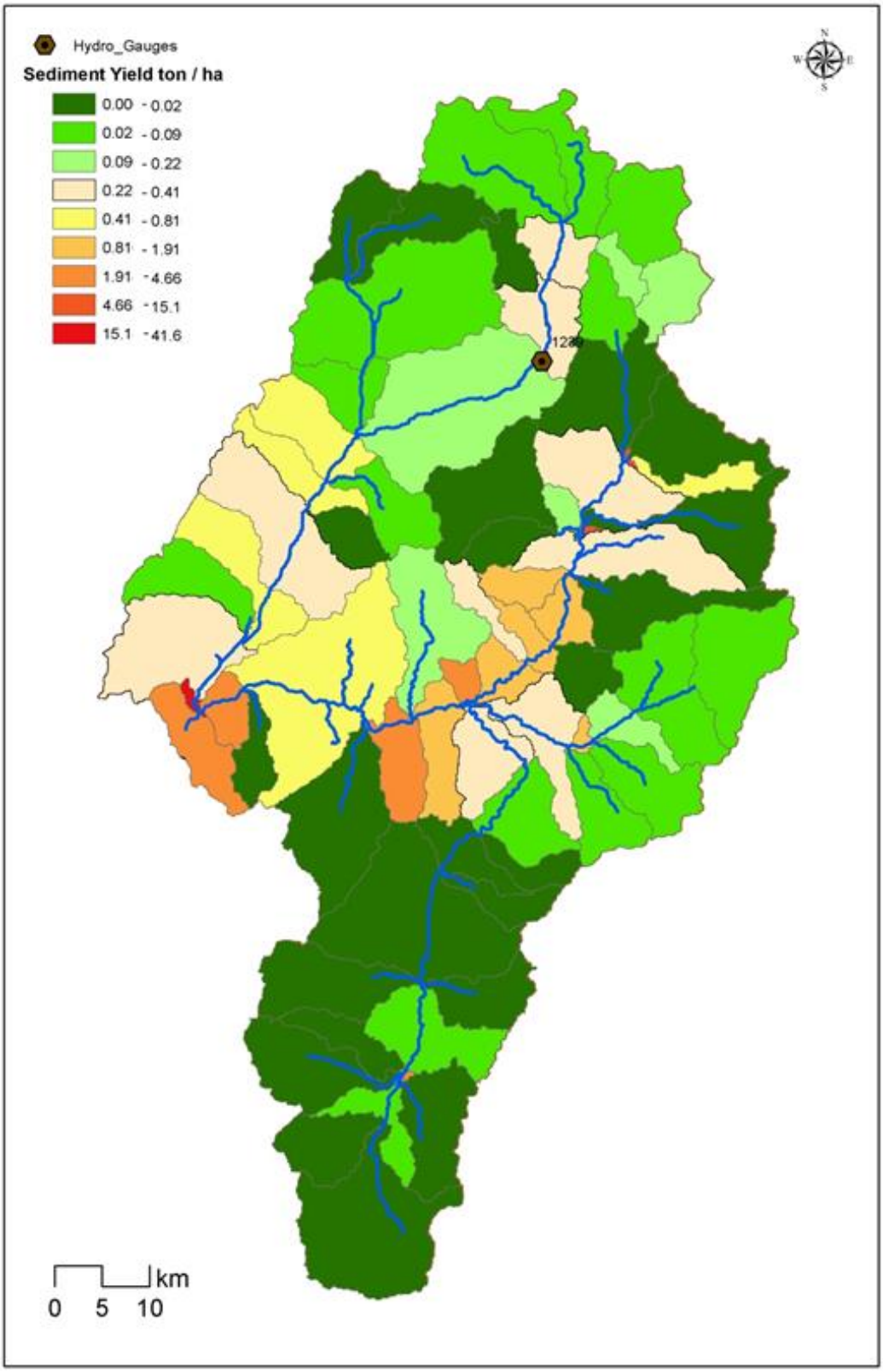

Figure 39: Distribution of sediment yield along the Ankara River (ton/ha)

6.6.1.2. Drainage Characteristics

Drainage density and drainage area are the two main variables that might affect sediment yield at a catchment scale. Catchment area is positively correlated with sediment yield (Walling, 1983; Verstraeten et al., 2003). The relationship between drainage area and sediment yield can also be positively correlated as long as the main sediment source is from channel and floodplain deposition (Walling and Webb, 1996). In other studies, drainage affects deposition processes by an inverse relationship between specific sediment yield and drainage basin area (Milliman and Meade, 1983). In general, the Ankara River data indicate that drainage area is a predominant variable which can explain sediment yield for the catchment (Figure 40).

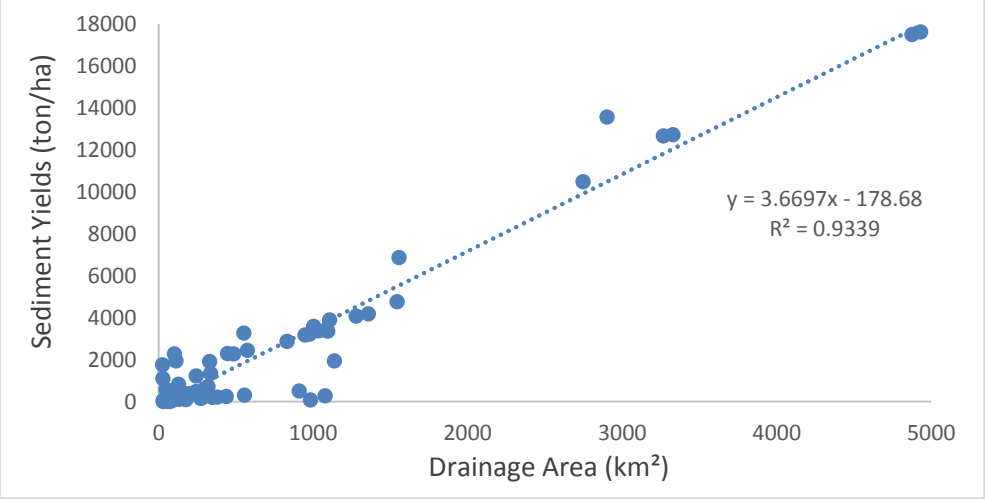

Figure 40: Sediment yield versus drainage area

According to the following plot, sediment yield and drainage area seem to be positively correlated, especially for peaks. Subbasins 40, 43, 46, 49, and 55 illustrate a reasonable fit between sediment yield and drainage area. Smaller drainage areas (subbasins 61, 64, 67, 70, 73) have a poorer correlation with sediment yield (Figure 41).

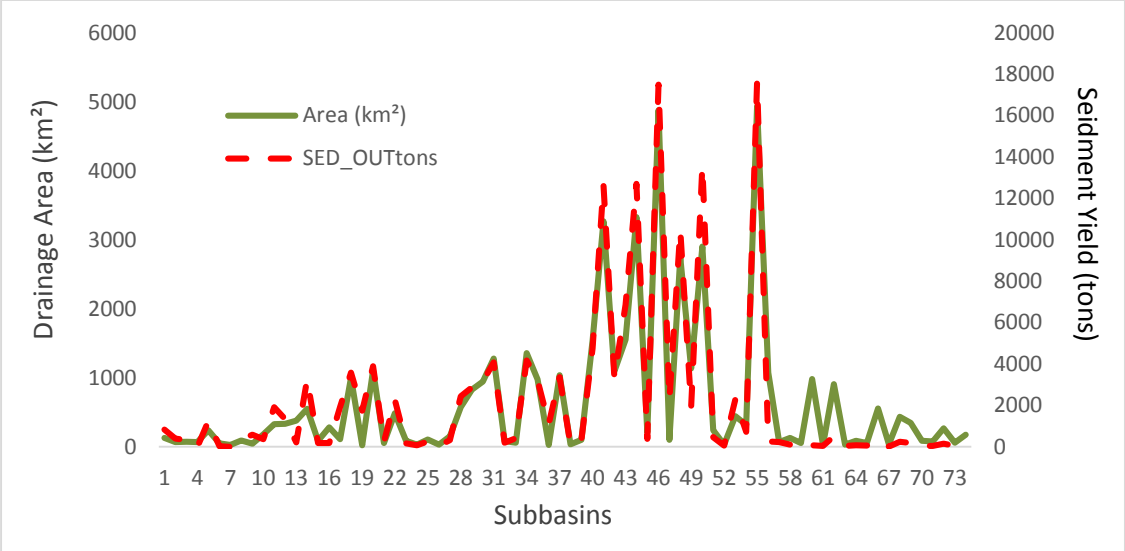

Figure 41: Sediment yield versus drainage area

Schumm (1963) concluded that a strong inverse correlation exists between sediment yield and drainage area, which is related to the increased chance of higher intensity precipitation over smaller areas and decrease in peak runoff and unit rainfall with increasing area. The correlation between sediment yield and drainage area in this research demonstrates that drainage area has a substantial impact on sediment yield at a catchment scale.

6.6.1.3. Hydrology

I plotted an average rating curve, which is also known as a sediment rating curve, in order to express the relationship between sediment discharge and stream flow. As discussed previously, sediment rating curves have been commonly used to compute an average sediment discharge for periods of time during which records of sediment discharge do not exist but records of stream discharge are available (Dainea, 1949; Miller, 1951).

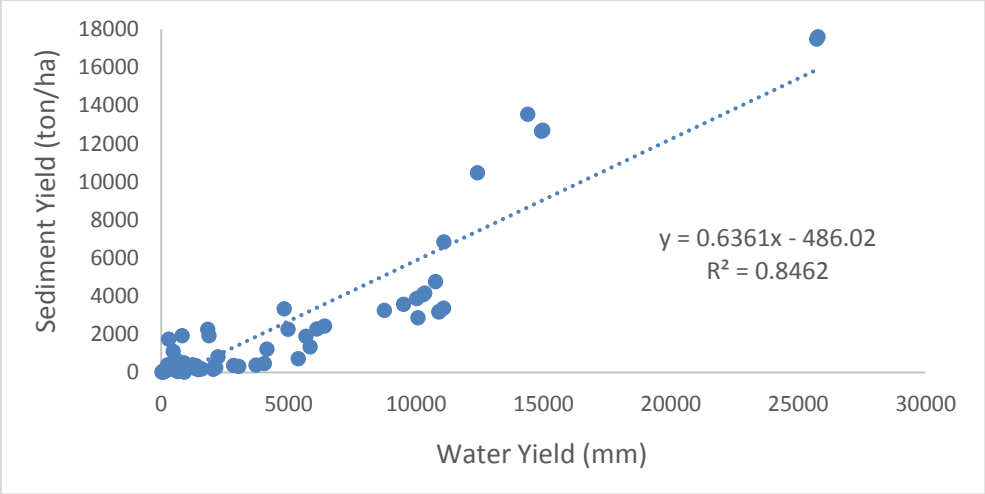

Figure 42: Sediment yield versus water yield

The mean annual runoff during 1970 – 1999 was approximately 500 mm. Figure 42 shows a scatter plot of stream flow and sediment load, which demonstrates a strong relationship with R^2 of 0.84 between stream flow and sediment load (Figure 42).

6.6.1.4. Channel Geometry

Channel geometry including stream width and depth is a useful interrelated variable in order to address the volume of bed load carried in a stream channel. Besides channel form, channel slope, grain size, and water discharge can be considered particularly significant factors when assessing the sediment transport capacity of a stream channel. In fact, coarser sediment materials usually limit the mobility of finer size materials in the stream system (Parker, 1990). Stream width, depth and slope were tested using multiple regression analysis. Only mean channel width for each subbasin correlates significantly with suspended sediment yield with the value of R^2 of 0.66 (Figure 43).

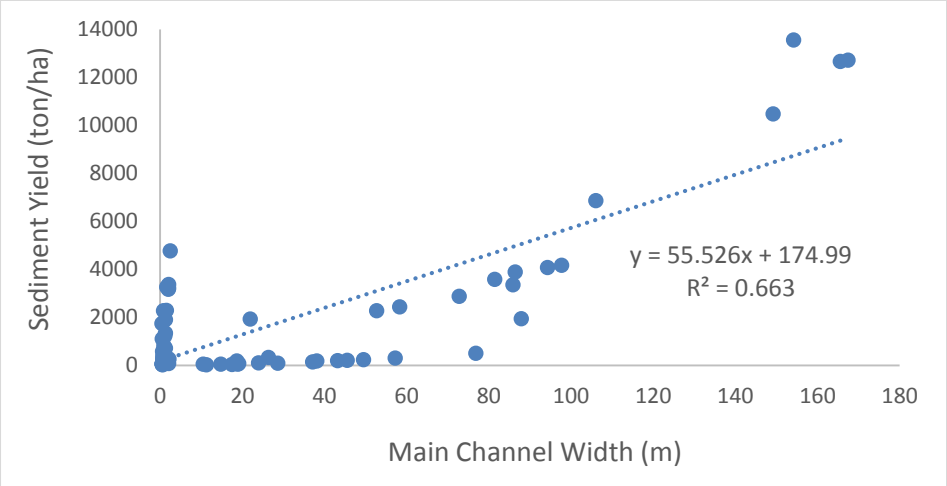

Figure 43: Sediment yield versus mean channel width

Wider channels correspond to more stream discharge, which creates more stream power for sediment transport. It can be also inferred that sediment yield increases with higher stream flow and channel width because higher discharges equate to more potential energy to transport more suspended sediment. Furthermore, increase in runoff from urban areas without sediment sources tends to increase channel bank erosion. In this research, multiple regression models suggest that the current channel width of the Ankara River is likely to correlate with suspended sediment yield at a catchment scale. I also infer that sediment load and stream channel width systematically increase downstream in the watershed.

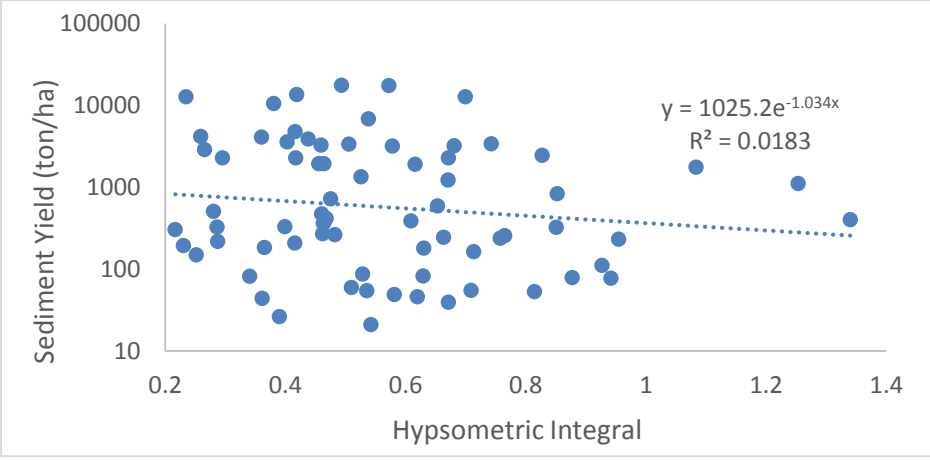

Figure 44: Sediment yield versus hypsometric integral

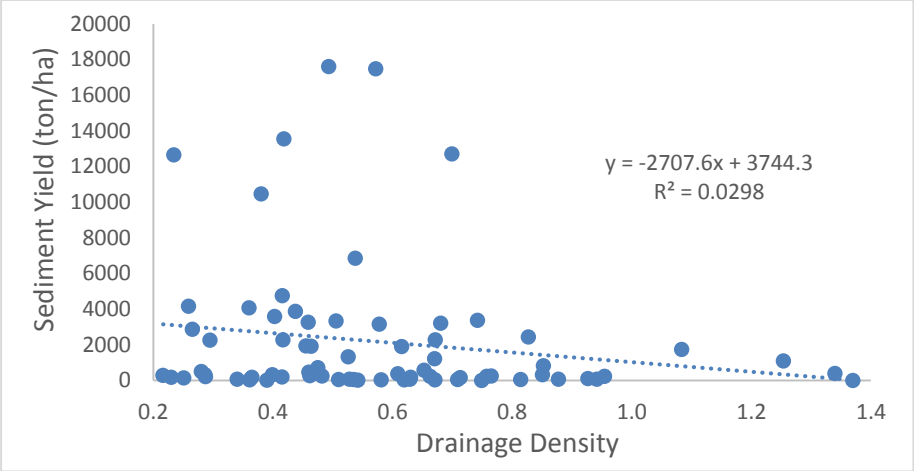

Figure 45: Sediment yield versus drainage density

According to Strahler (1952), there is a strong correlation between hypsometric integral and suspended sediment yield in hilly and gully areas of the Loess Plateau ($R^2 = 0.48$, N = 29, $p < 0.001$), which implies that soil erosion and sediment yield are closely related to landform evolution. In this study, Figure 44 and Figure 45 present the correlation between sediment yield and hypsometric integral and drainage density, respectively. The correlations are quite weak, with the value of $R^2 \approx 0.02$ among these two factors and sediment yield, which means that neither hypsometric integral nor drainage density alone can describe accurately the complex physical processes underlying sediment yield.

6.6.1.5. Topography

Topographic characteristics including elevation, mean slope, and relief ratio are other potential controlling variables at the basin scale. At high altitude, higher difference in daily and seasonal temperature helps to increase the potential effect of mechanical weathering due to variation in temperature and moisture. Slope potentially influences sediment behavior because coarser materials in suspension are temporarily deposited in the floodplain and stream bed until stream power exceeds the threshold for movement. One of the main factors controlling stream power is slope. Increasing main channel slope corresponds to greater overland flow, which

accelerates soil erosion. However, slope has an inverse correlation with sediment yield ($R^2 = 0.11$) (Figure 50).

The data indicate that none of the topographic variables is significantly correlated with sediment yield, although the minimum basin elevation and mean basin elevation demonstrate some degree of association with sediment yield ($R^2 = 0.21$ and $R^2 = 0.17$, respectively). Other types of elevation (maximum elevation, elevation difference) do not explain sediment yield from the basins of the Ankara River catchment.

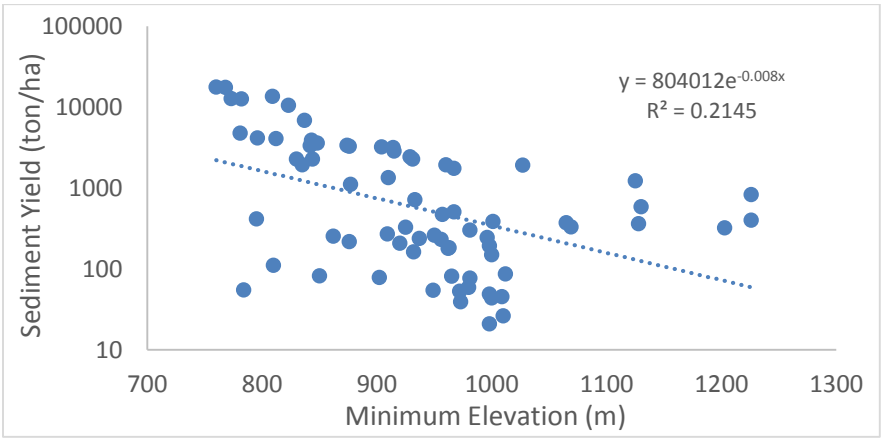

Figure 46: Relationships between sediment yield versus minimum elevation with two outliers excluded

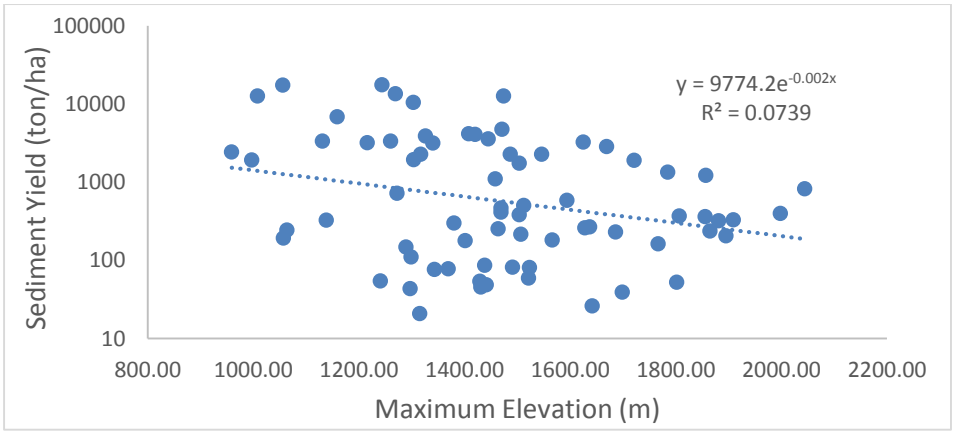

Figure 47: Relationships between sediment yield versus maximum elevation with two outliers excluded

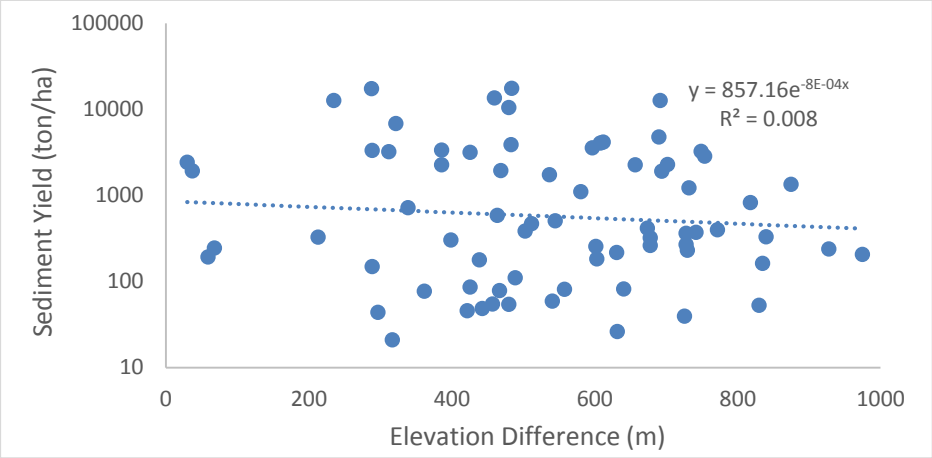

Figure 48: Relationships between sediment yield versus elevation difference with two outliers excluded

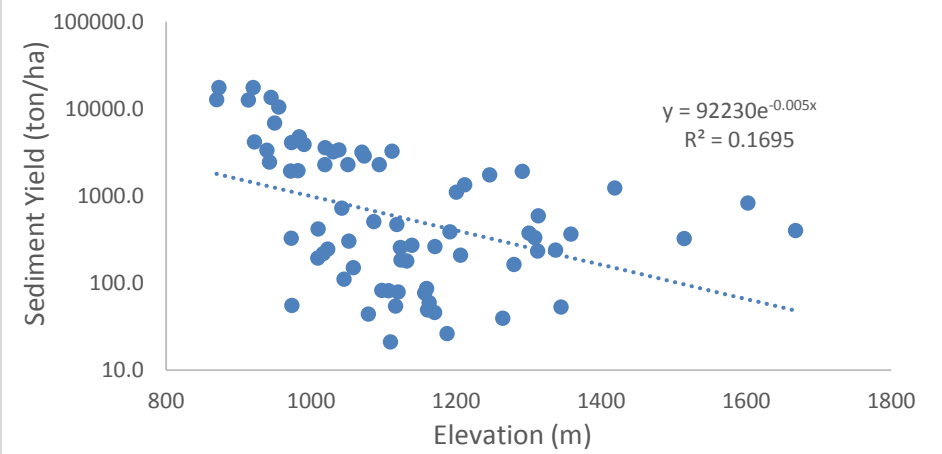

Figure 49: Relationships between sediment yield versus main elevation with two outliers excluded

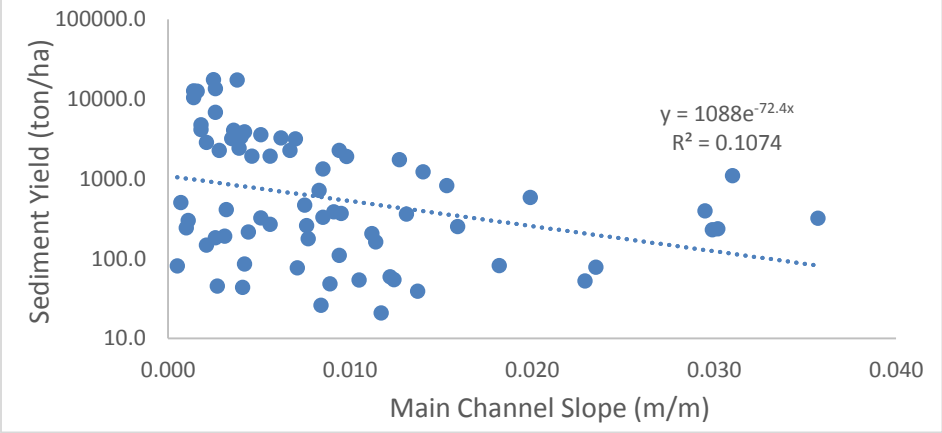

Figure 50: Relationships between sediment yield versus main channel slope with two outliers excluded

The linear regression model also indicates that other topographic variables, such as depth and longest path are not correlated with sediment yield (R^2 = 0.002 and R^2 = 0.004, respectively) in the basin of Ankara River catchment (Figure 51), (Figure 52).

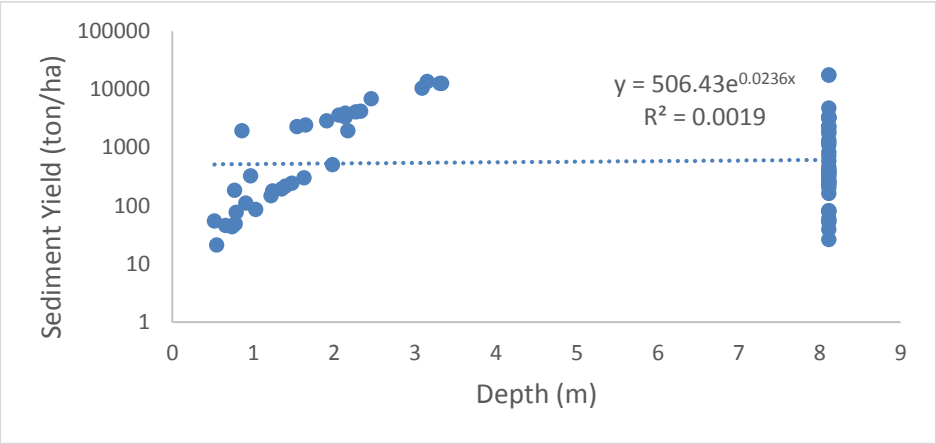

Figure 51: Relationships between sediment yield versus depth

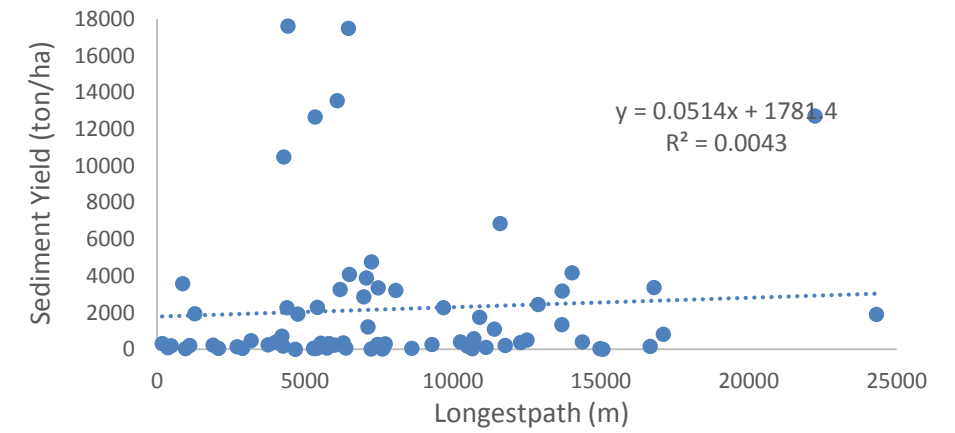

Figure 52: Relationships between sediment yield versus longestpath (distance along the flow path for each subbasin)

6.6.1.6. Human Effect

The main subject of this section is people, who have the ability to alter and change the natural world based on their needs. The southern and western portions of the Ankara River basin have a higher population density and are mainly characterized by alluvial plains, plateaus, and low hills. In the regions with higher population density, people generally spread over the most

productive alluvial plains. Therefore, physical controlling variables potentially play a dominant role in the northern region because of lower population density than the southern region.

Anthropogenic disturbance history such as urbanization, deforestation, and tillage can be a significant controlling variable because of their effects on surface conditions (Boardman et al., 2003). Besides these human activities, farming, grazing, road construction, and stream channel management can significantly influence sediment yield in a stream channel (Langbein and Schumm, 1958). In the absence of high spatial or temporal resolution for basic data, such as spatially distributed data on disturbance history, I could not apply a spatially distributed model for sedimentation processes. However, this research examines potential correlations between sediment movement and disturbance histories. For instance, cultivated areas have potentially higher disturbances including grazing, tillage, or deforestation. In general, rangelands (grasslands) can be associated with low population density and higher overgrazing potential. Therefore, I categorized each subbasin based on distribution of dominant land use and land cover types for multiple regression analysis due to lack of spatial data on disturbance history.

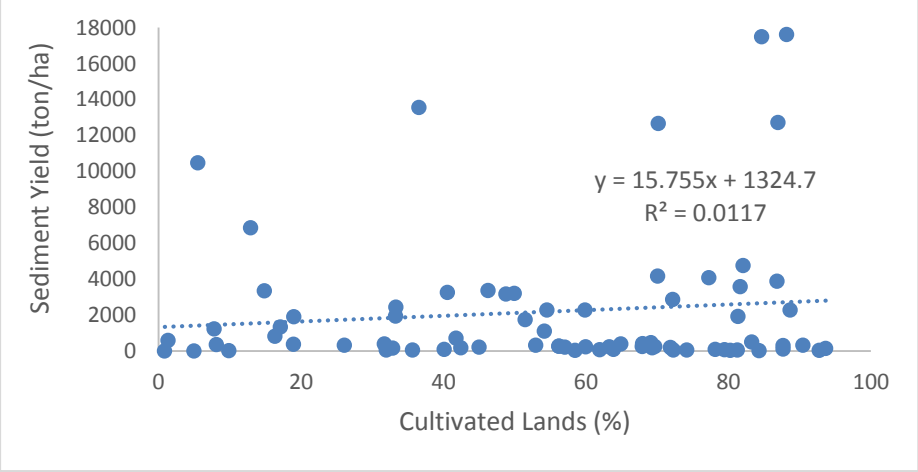

Figure 53: Relationships between sediment yield versus % of cultivated lands

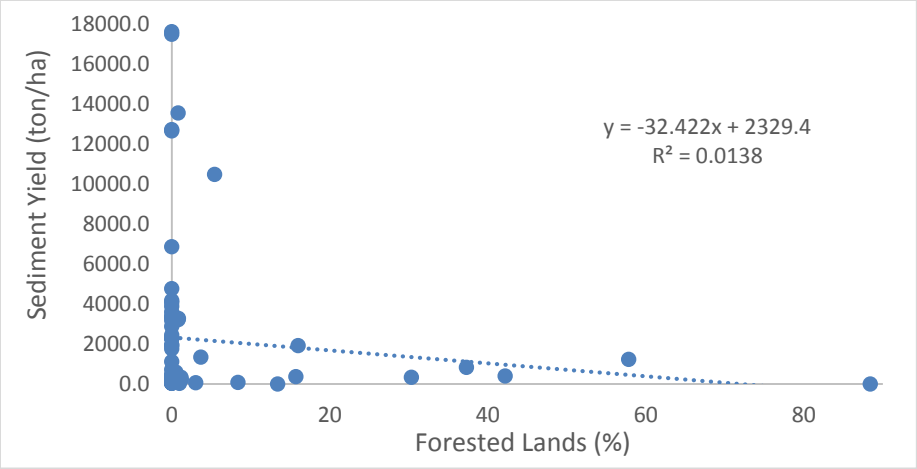

Figure 54: Relationships between sediment yield versus % of forested lands

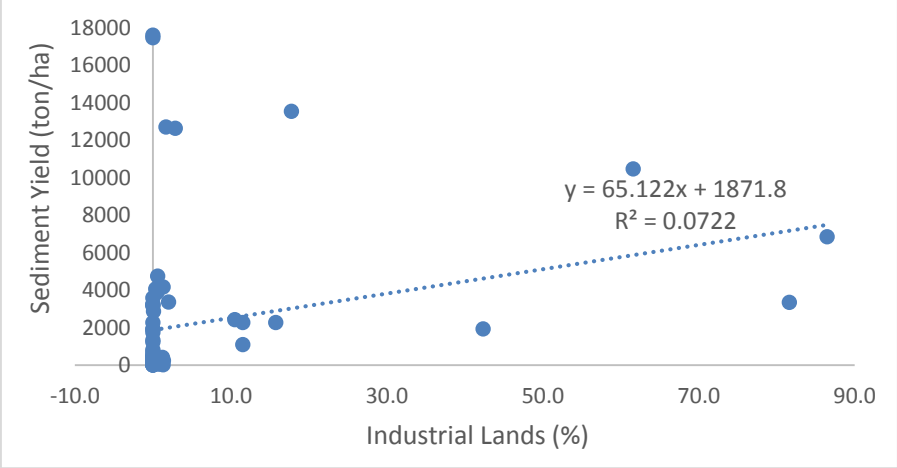

Figure 55: Relationships between sediment yield versus % of Industrial lands

According to the results of the linear regression models, there were no significant correlations among suspended sediment yield and land cover variables such as cultivated, forested lands and industrial lands ($R^2 = 0.001$ and $R^2 = 0.07$, respectively) (Figures 53 - 55).

6.7. Trend in Sediment Load and Land-use

Human effect and natural changes including climate change influence sediment movement and deposition in a river channel as a direct and an indirect effect on hydrology. This research mainly focuses on basin scale sediment yield from the uplands to human-made reservoirs, and reservoir sedimentation in consequence of soil erosion. Sediment yield monitoring at the 1239

sediment station was initiated in 1967 in the upstream portion of the Ova Creek watershed. The data collection indicated that there was a large flood in 1991 in the surrounding area, which covered a total area of 322 km² and had a total daily sediment yield of 13068 ton/day. Sediment yield in the watershed resulting from sheet, rill, and gully erosion is greater in the middle and lower reaches of the catchment. Accelerated erosion results from surface runoff in the catchment caused by deforestation, poor cultivation techniques, and overgrazing (Ongwenyi et. al., 1993).

In conclusion, monthly suspended sediment yield from the result of the SWAT simulation indicates that monthly suspended sediment yield increases progressively from upstream to downstream. However, that might give researchers a methodology to determine upstream and downstream sediment yield variability since downstream areas potentially have more sediment yield gathered from other tributaries.

CHAPTER SEVEN

SPATIAL DISTRIBUTION AND DEPOSITION OF SEDIMENT IN THE CUBUK I AND CUBUK II RESERVOIRS

7.1. Introduction

Understanding the pattern of sediment transport and deposition is an important factor in studying sediment distribution and deposition processes because sediment plays a major role in a reservoir (Mertes et. al., 2007). Sediment trapping by a reservoir can cause stream bed degradation downstream and accelerated rates of bank failure, which can accelerate soil erosion rates and tend to increase sediment inflow to downstream structures. Fine sediment particles carried into a reservoir can be deposited throughout its full length (Sumi and Hirose, 2002).

Sediment transport and deposition in a reservoir depend on reservoir geometry, flood frequency, river regime, sediment consolidation, management practices, and land-use changes over time (Borland and Miller, 1960). There are two common methods for illustrating sediment distribution: (i) sediment distributed by depth and (ii) sediment distributed by longitudinal profile. However, illustrating sediment distribution in a reservoir is a complex phenomenon because of numerous controlling variables affecting sediment load in small retention reservoirs and their translocation under various hydraulic conditions. The main concern in this section was to propose a methodology to assess the effects of reservoir sedimentation by comparing the bathymetric surveys of 1978 and 1983 and determining the spatial and temporal distribution of sediments within the Cubuk I and Cubuk II reservoirs.

7.2. Site Characteristics

Water supply is one of the main concerns in water resource management for the semiarid region of Central Anatolia in Turkey since there is a conflict between potential water supply and demands, especially during the drought periods of 1956, 1977, 1990, 2004, and 2014. Besides meteorological extreme events, anthropologic activities also influence water sources. The reservoirs within a semiarid region are the most important water source for the research area because only 1.3 % of water used comes from ground water and 98.7 % of the capital city of Ankara usage is supplied from Kurtbogazi (57.8 %), Camlidere (29.7 %), Kesikkopru (6.7 %), and Cubuk II (4.5 %) reservoirs (DSI, 2014). Therefore, sustainable sediment management practices are becoming more significant for desired habitats, riverine environments, and clean water sources.

In recent years, the quality and quantity of Ankara's major potable clean water supplies have been influenced by expanding population growth, industry, and other human usage. Cubuk I reservoir especially is adversely affected by sediment loading from development and accelerated soil erosion in the catchment. The total population in the city limits of the capital city, Ankara, was 621,000 in 1940, 2,854,700 in 1980, and 4,771,752 in 2010 (TSI, 2014).

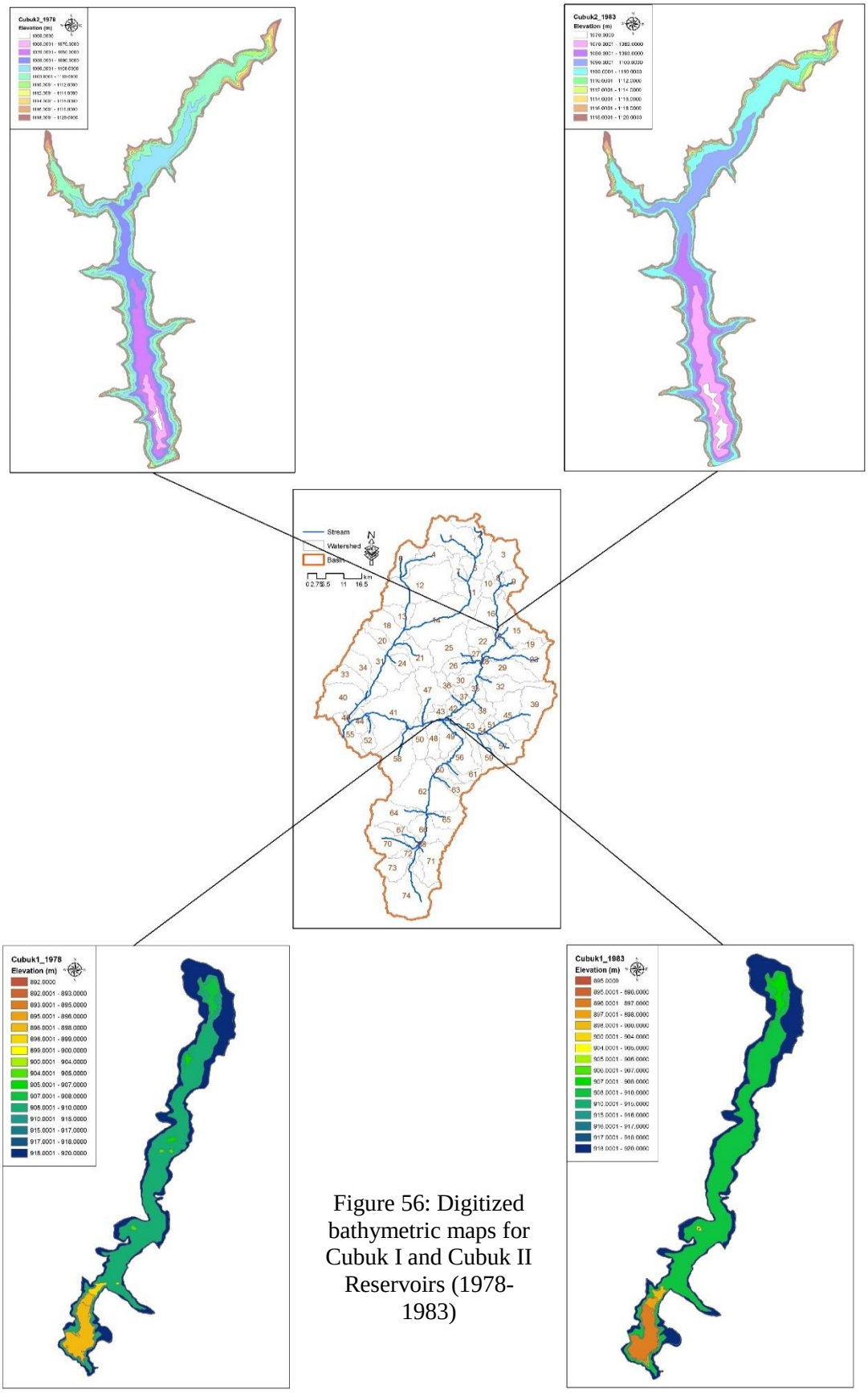

Figure 56: Digitized bathymetric maps for Cubuk I and Cubuk II Reservoirs (1978-1983)

7.3. Materials and Methods

Spatial distribution of sediment within the Cubuk I and Cubuk II reservoirs in the Central Anatolia Peninsula was investigated using bathymetric survey data (Figure 56) as well as areal images. Sediment accumulation in the reservoirs was analyzed by comparing 1978 bathymetric survey data versus 1983 bathymetric surveys from Cubuk I and Cubuk II reservoirs (1/5000 scale). While a previous hard copy of bathymetry was available from DSI, a more detailed and recent digital bathymetry dataset is necessary for reservoir sedimentation practices. In fact, more useful and accurate results requires longer time periods of data with higher resolution.

First, hard copy bathymetric maps obtained from DSI were digitized using ArcGIS 10.2.2 software. However, in the bathymetry of Cubuk I and Cubuk II reservoirs, some contours do not exist after a certain distance, which not only decreases the accuracy of the dataset, but also made the digitizing process more difficult. Second, the contours with elevation and their symbols were integrated into the software and stored in projected UTM coordinates, Zone 36N, using WGS-84 datum. Afterward, changes in the water surface area of the mean depth and changes in the shoreline of the reservoirs between 1978 and 1983 were observed by plotting cross section lines of "X and Y". Comparison of these two digitized bathymetric maps allowed visualization of reservoir bottom topography.

In addition, high resolution infrared images were used to identify whether any depositional features can be seen along the shoreline of the reservoirs. Color infrared image (CIR) images were examined to define what tributaries potentially were capable of depositing larger amounts of sediment into the reservoir. I also observed how deltas expand within the reservoirs by using areal images and Google Earth. The comparison of areal images may facilitate estimating erosion over a longer time period, but generally with less precision than local measurements in the field.

7.3.1. Interpretation of the Bathymetric Surveys (1978-1983) from Cubuk I

The total surface area of the reservoir is 1.20 km² at normal water level. The water surface area of the reservoir increased slightly between 1978 and 1983 (Figure 57). The graph shows the changes in the water surface area versus water depth. Fluctuation at depths of 10 m, 11 m, and 15 m may be caused by sediment accumulation and mobility in the reservoir. Water depths of 26 m, 27 m, and 28 m did not exist in the bathymetric data of 1983, which possibly reflects sediment deposition in the deepest portion of the reservoir. Due to the low resolution of bathymetric data, the results n in this section have some potential errors.

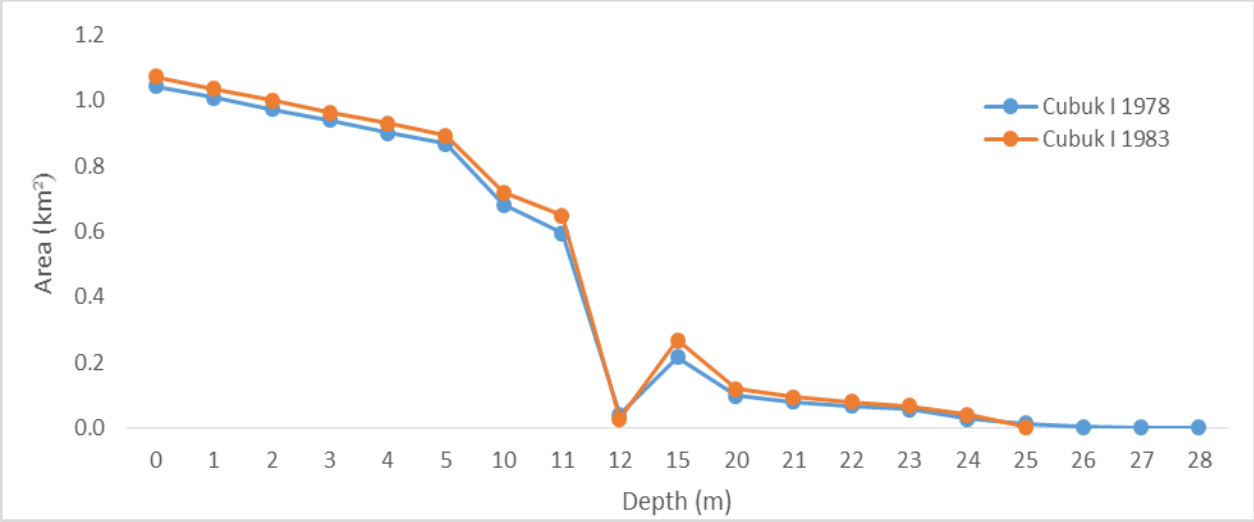

Figure 57: Changes in water surface area of the Cubuk I Reservoir

The bathymetric surveys of Cubuk I Reservoir (1978 – 1983) indicate a variation of the lowest elevation value. The earlier version of the data had the polygon of 892 m as a polygon with the lowest elevation. The latest version of the bathymetry shows 895 m as the lowest polygon, which means a 3 m loss of reservoir capacity at the deepest portion of the reservoir. During this time period, the contours of elevation 905 m (in the bathymetric map of 1978) increased 1 meter, and some of them disappeared in the middle section of the reservoir. Moreover, some contours' geometry, especially at the downstream end of the reservoir, appeared to differ over 6 years. The

northeast portion of the polygon (905 m) appears to be fork shaped in the earlier map, but not in the next version (Figure 58 and Figure 59).

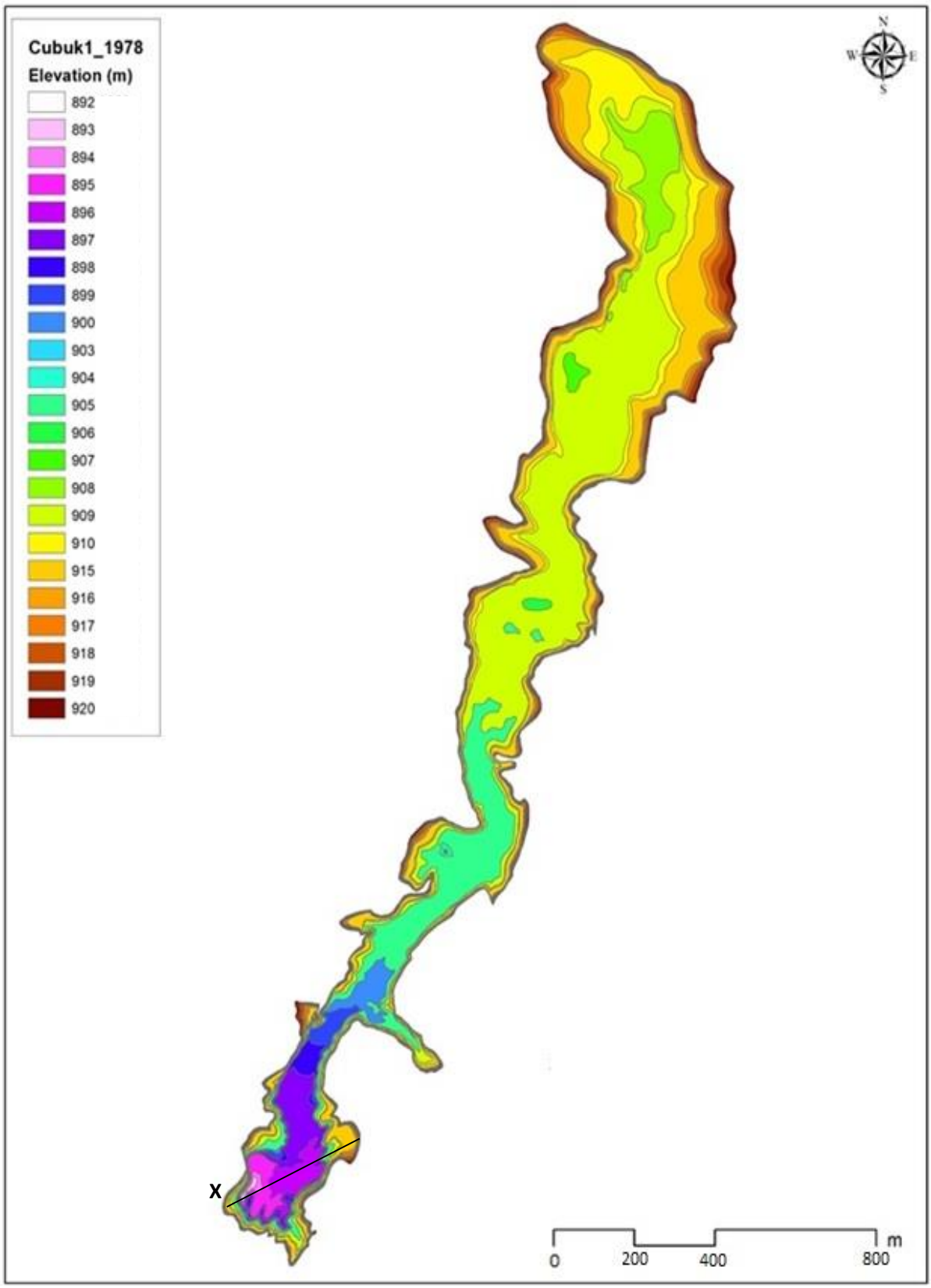

Figure 58: Map of Cubuk I Reservoir bathymetry in 1978 shows cross section line of X

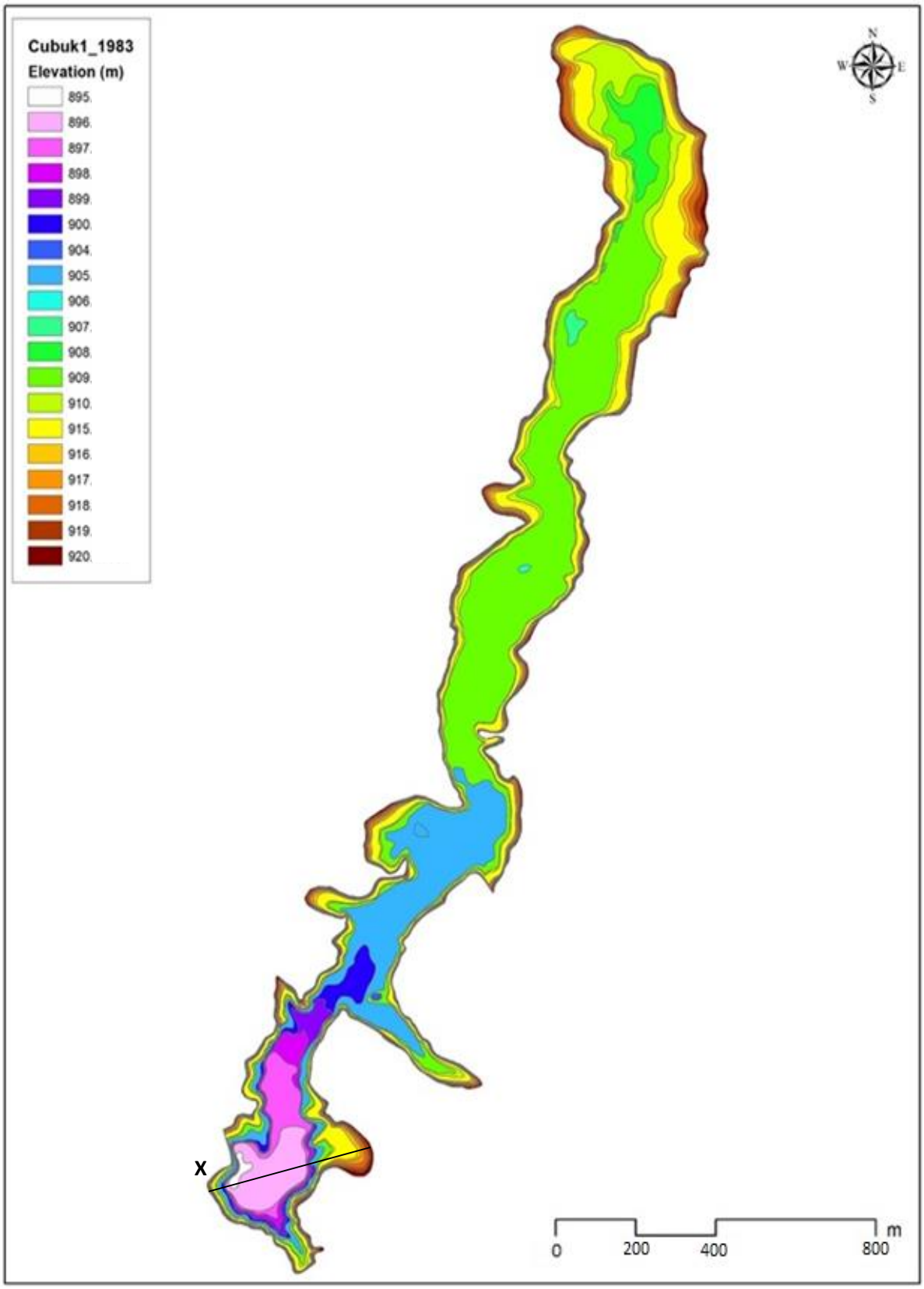

Figure 59: Map of Cubuk I Reservoir bathymetry in 1983 shows cross section line of X

7.3.2. Interpretation of the 1978 and 1983 Bathymetric Surveys from Cubuk II

The total surface area of the Cubuk II Reservoir is also 1.20 km² at normal water level (DSI, 2014). Between 1978 and 1983, the water surface area of the reservoir differs very slightly (Figure 60). Changes in the water surface area versus water depth at 30 m and 50 m can be related to sediment deposition and sediment mobility in the reservoir. Similarly, the depth value of 60 m did not exist in 1983 due to sediment deposition in the deepest portion of the reservoir. The mean depth of the reservoir differs between Cubuk I (~ 25 m) and Cubuk II (~ 60 m).

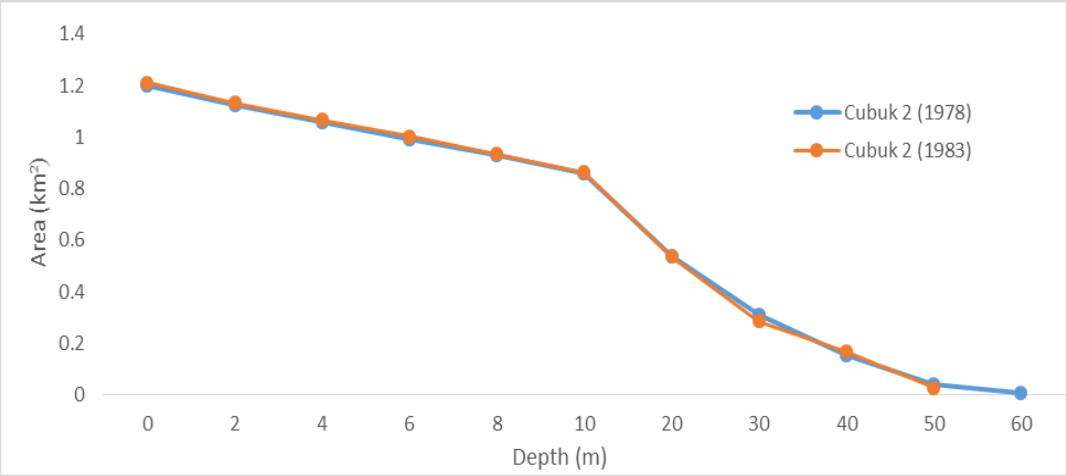

Figure 60: Changes in water surface area of Cubuk II Reservoir

Comparison of bathymetric maps for 1978 and 1983 for Cubuk II reservoir shows a change in the lowest elevation value. The bathymetry map of 1978 had the elevation of 1060 m as the lowest altitude, but the 1983 map had 1070 m as the lowest elevation. The 1070 m contours of 1978 also disappear at the lower portion of the reservoir. Figure 60, showing changes in water surface area, indicates that there was about 10 m of depth lost from deposition in the deepest section of the reservoir. Also, some of the polygons' geometry (e.g., 1080 m and 1090 m polygons) varied during the seven years (Figure 61, Figure 62).

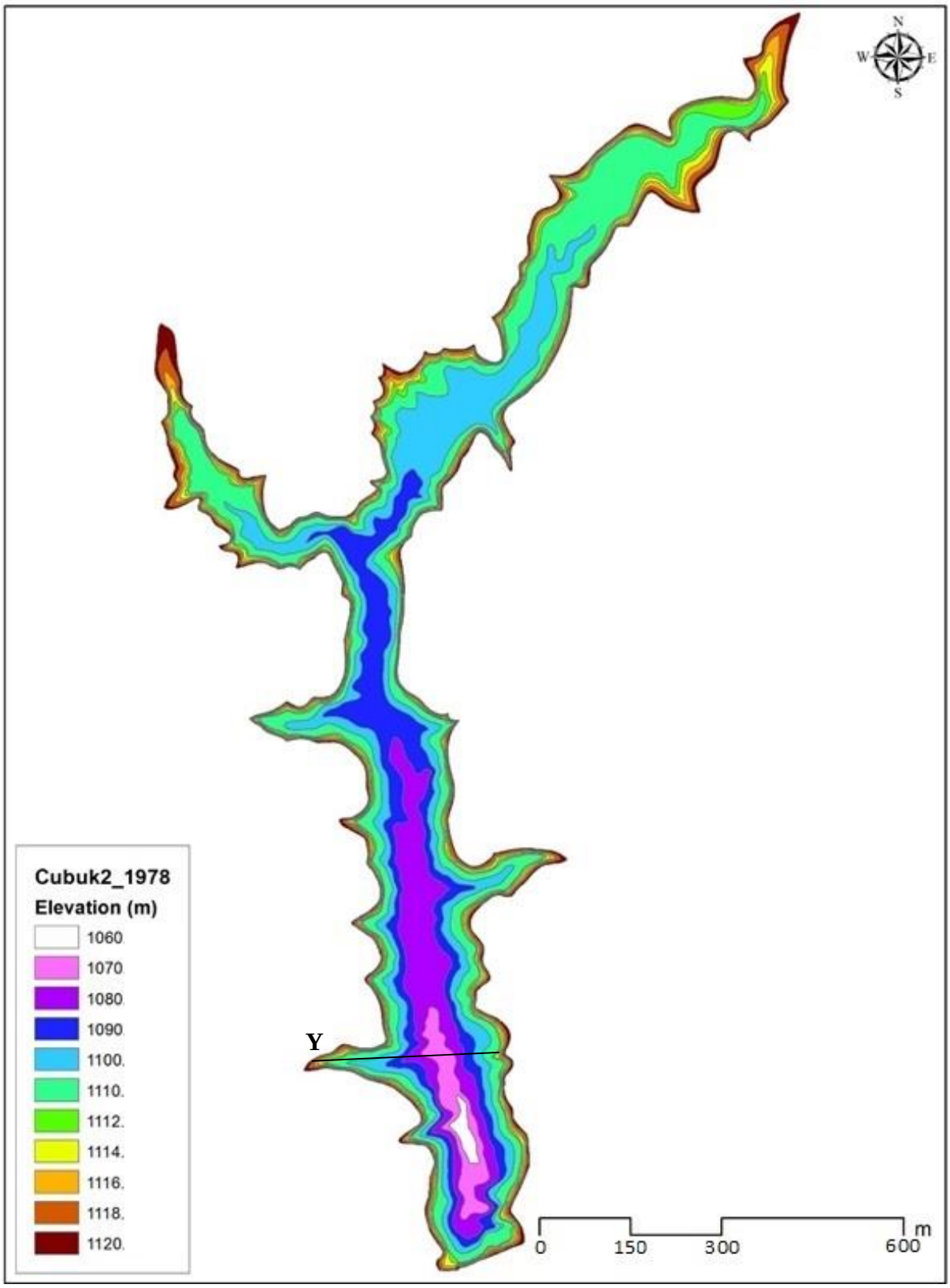

Figure 61: Map of Cubuk II Reservoir bathymetric in 1978

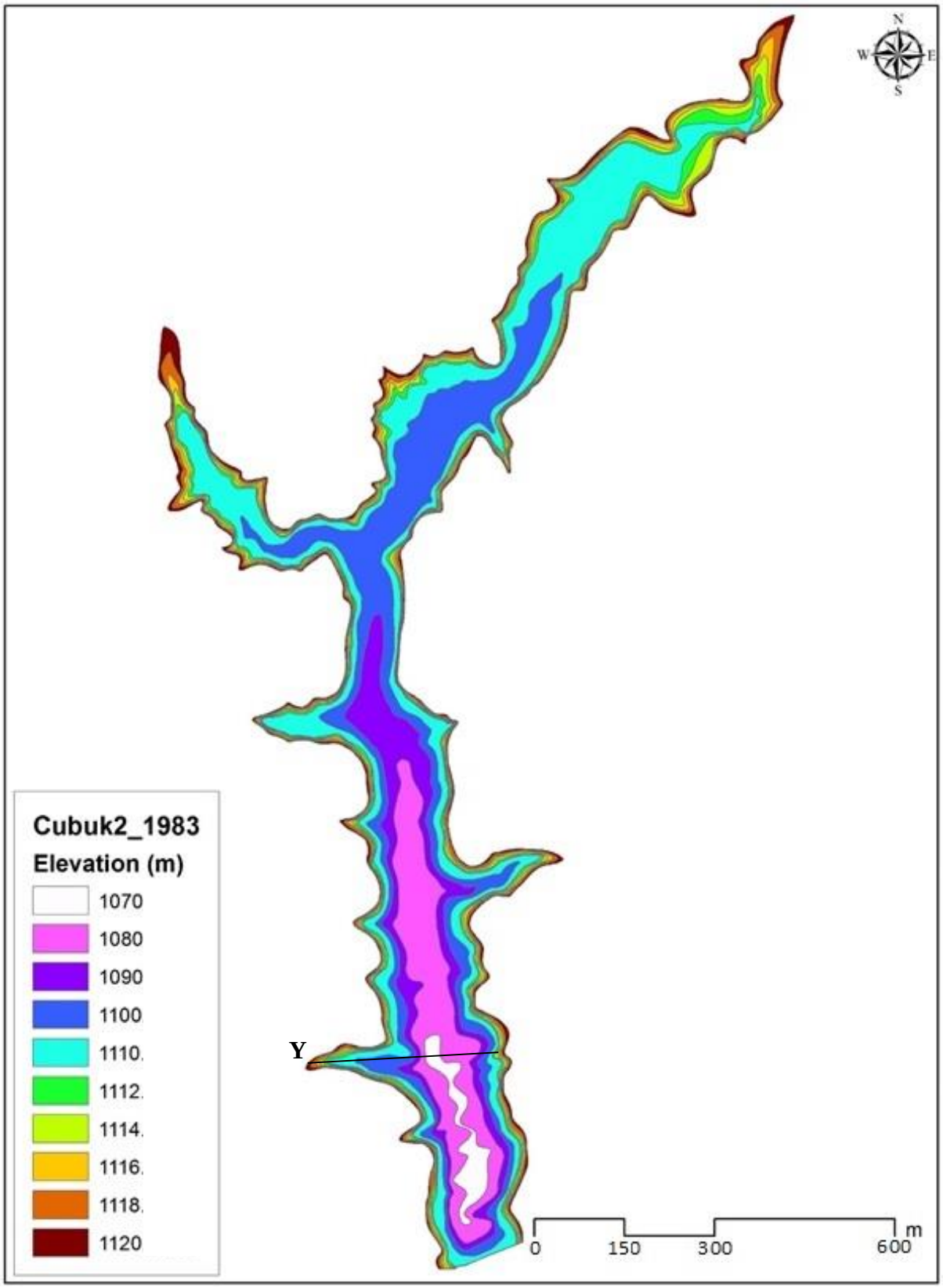

Figure 62: Map of Cubuk II Reservoir bathymetric in 1983

Cross-section profiles were utilized to understand geomorphic and sedimentary units by using digitized bathymetric maps (Figure 63). The cross section profile of X at the western portion of the reservoir shows a steeper side slope with a general semi-circular bottom. The eastern portion of the bottom topography indicates more variation in elevation. In general, the X profile indicates the bottom geometry of the reservoir becoming higher and narrower, the top width of the reservoir remaining almost uniform, and the depth of the reservoir decreasing about 3 meter between 1978 and 1983. The thalweg also accumulated suspended sediment.

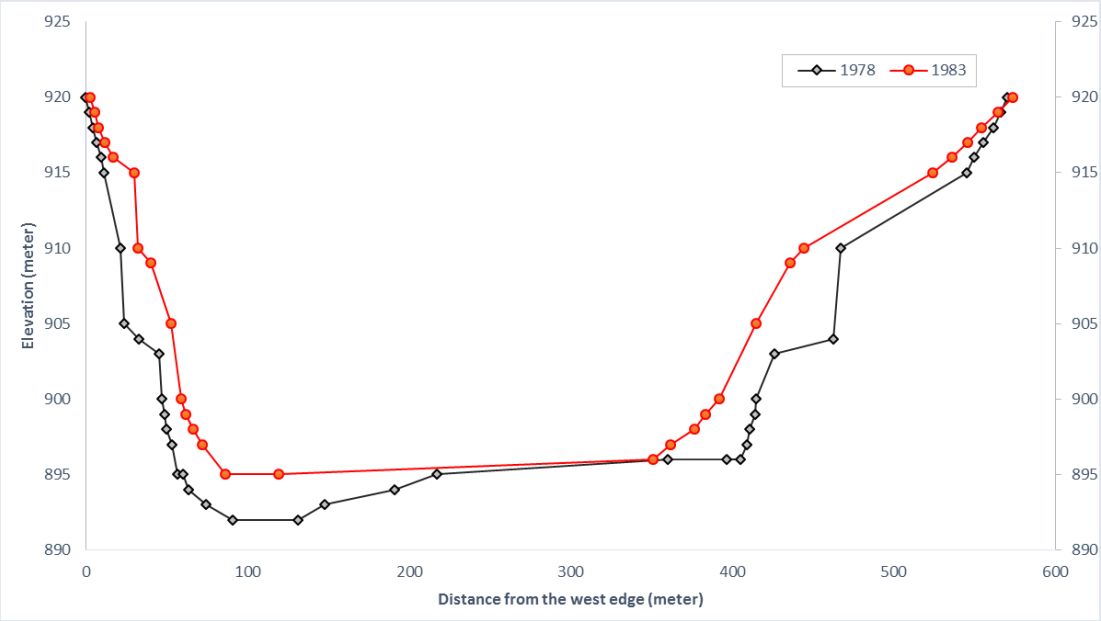

Figure 63: A cross section of X profile from the Cubuk I Reservoir in 1978 and 1983

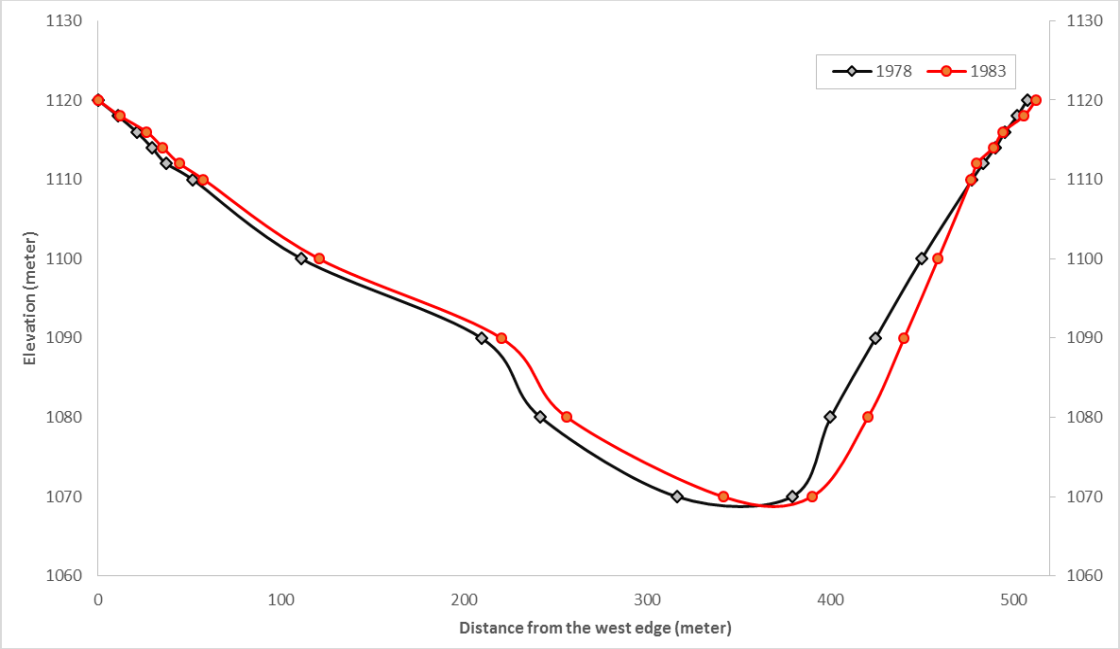

Figure 64: A cross section of Y profile from the Cubuk II Reservoir in 1978 and 1983

A diagrammatic cross-section of Y profile from Cubuk II has an asymmetrical valley cross-section profile. The eastern side of the profile shows a steeper slope compared to the western portion of the reservoir. The elevation at the western portion of the reservoir has been raised. In contrast, the eastern section of the bottom topography shows incision, especially beyond 400 m from the western edge of the reservoir. In terms of the variation in the deepest polygon in the lake, profile Y does not show any variation because the elevation of 1060 m had been narrowed within 7 years and the profile line does not cross the polygon of 1060 m in 1983 (Figure 64). This change was probably due to a higher quantity of sediment deposition which masked the valley bottom topography in the lower portion of the reservoir.

7.4. Results

Sediment transported by stream flow may vary based on the quality and quantity of water entering a reservoir. Besides other variables, a larger amount of stream water caries coarser sediment and a greater quantity of bed load as well as suspended and dissolved load. Based on

long term annual stream flow data obtained from DSI, Cubuk II Reservoir has more variations than Cubuk I Reservoir because Cubuk II (Figure 65) is likely to be more affected by natural events due to being located upstream. On the other hand, the potential water supply for the City of Cubuk and for other purposes such as irrigation decreases inflow to the Cubuk I Reservoir.

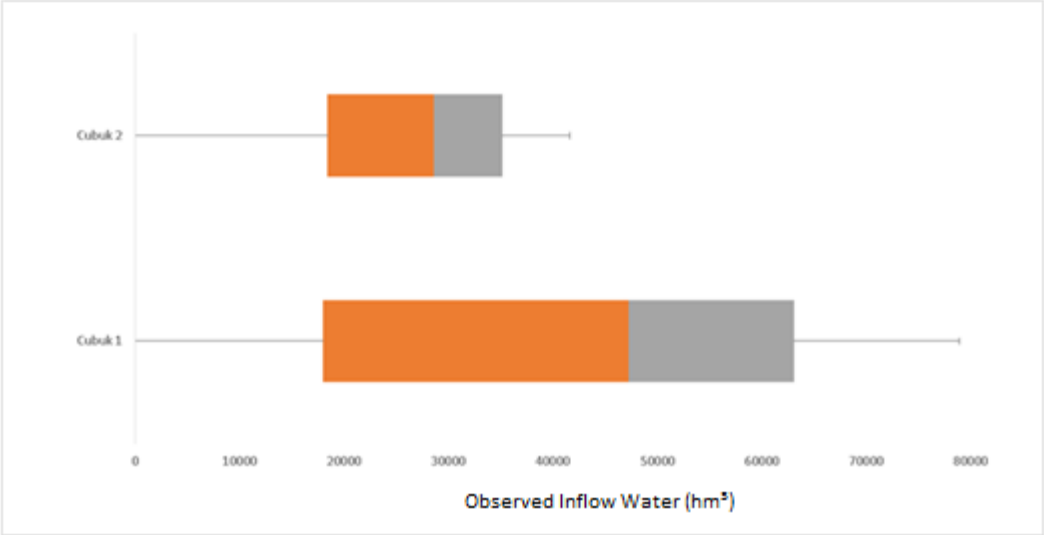

Figure 65: Annual observed runoff into the Cubuk I and Cubuk II Reservoirs (1977-2008)

The amount of sediment deposition in a reservoir also varies based upon the texture and size of sediment in the river system, the shape of the reservoir, detention storage time, and the manner of reservoir operation. Sediment deposited within a reservoir falls into three categories: (i) deltaic deposition at the reservoir headwater areas, (ii) deposition of suspended and dissolved sediment from homogenous flow, and (iii) deposition of suspended and dissolved sediments as a result of stratified flow (turbidity current). In many cases, sediment settles out of the turbidity current and is deposited along the length of the reservoir as a thin layer across the bottom of a reservoir. The turbidity current may be supercritical ($Fr_d > 1$) or subcritical ($Fr_d > 1$) depending on the slope. Although the sediment particles in a turbidity flow are often cohesive, subcritical flow in a gradual slope is capable of carrying large amounts of finer suspended or dissolved materials into the deeper sections of the reservoir. In the following section, sediment distributions in Cubuk

I and Cubuk II Reservoirs were analyzed based on sediment outputs from the SWAT model and areal images studied in order to identify depositional areas in the reservoirs.

7.4.1. Historical Changes in the Storage Capacity

The storage capacity of Cubuk I and Cubuk II Reservoirs decreased between 1936 and 1983. However, there was a slight increase in the storage capacity in 1967 and the storage capacity of Cubuk II Reservoir was increased in 1978 (Table 19). After 1944, the municipality of Cubuk's waste water went into the Cubuk I Reservoir and the reservoir lost its water source functionality within 50 years because of both sedimentation and waste water input caused by population growth.

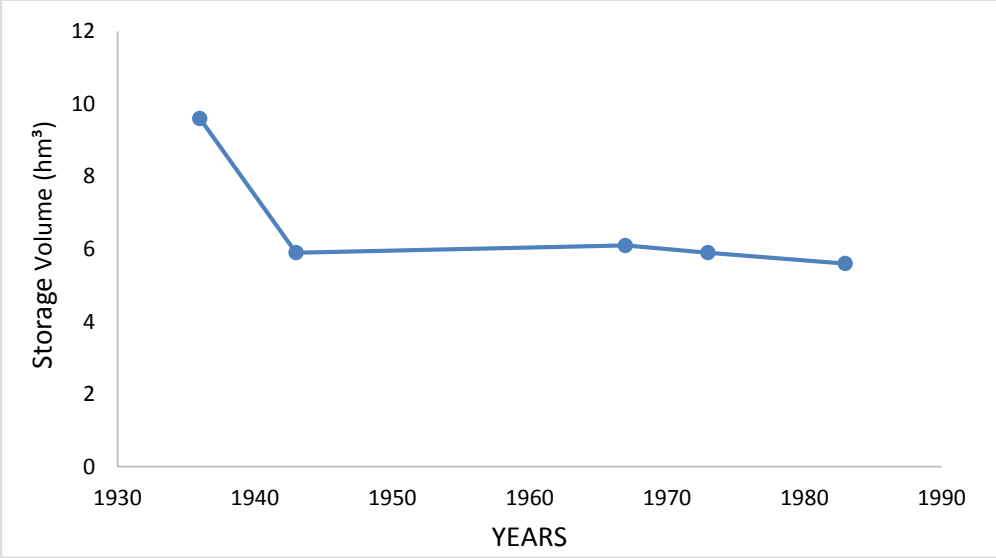

Figure 66: Historical changes of storage capacity in the Cubuk I Reservoir

The main reason for water storage losses of the reservoirs is siltation in the reservoir pool (Figures 66-67). Suspended sediment particles are deposited all over the reservoir as larger amount of sediment load than coarse sediments, which are usually accumulated in the upper reach of the reservoir as a delta. On the other hand, some coarser and finer materials may be deposited in natural and artificial barriers in the channels and their floodplains based on the amount and distribution of

precipitation, steepness and slope of the surface area, soil texture, land cover, and land use (Yilmaz, 2003).

Table 19: The historical changes of storage capacity in the Cubuk I and Cubuk II (DSI)

		1936	1943	1967	1973	1983
Cubuk I	MAX	9.6	5.9	6.1	5.9	5.6
hm^3	MIN	0.4	0	0.1	0	0

		1964	1973	1978	1983
Cubuk II	MAX	25	22.7	23.8	22.4
hm^3	MIN	1.9	0.6	0.6	0.3

The capacity of Cubuk I Reservoir was 12.5 hm^3 at normal water level. The bathymetric data indicate a reduction in volume of ~ 42 %, and the capacity of the reservoir decreased by an average of 5.25 hm^3 between 1936 and 1983. In other words, Cubuk I Reservoir has lost 1 % of its capacity every year, as noted in earlier studies (WCD, 2000). According to previous studies, many reservoirs in the world have been filled by sediment at the rate of ~1 % every years.

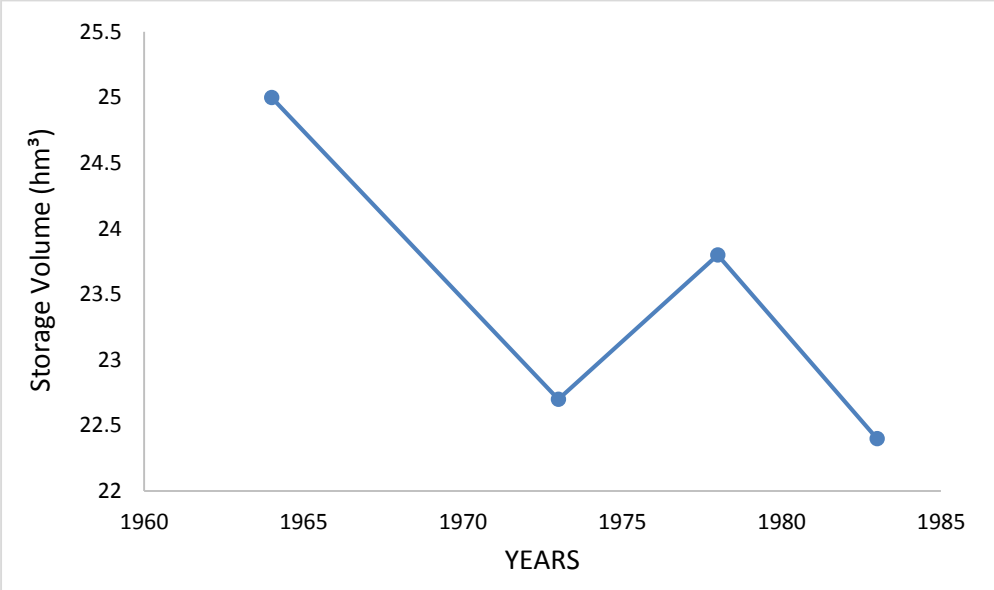

Figure 67: The historical changes of storage capacity in the Cubuk II Reservoir

7.4.2. Sediment Deposition in the Cubuk I Reservoir

Cubuk I Reservoir has basically a one dimensional configuration with the length of the reservoir being much larger than the width. The behavior of the Cubuk I Reservoir respecting sedimentation was expressed by plotting the change in the reservoir capacity between 1936 and 1983 based on the data obtained from DSI. The total sediment yield rate to Cubuk I Reservoir during 1935 – 1964 was computed as 303 m^3 / y/ km^2 (DSI).

The change in the reservoir bottom topography may be occurring at the downstream end due to the finer grain size materials that came from the tributaries. The reservoir was no longer used after 70 years because it filled with sediments. Dominant particle types are silt, clay and sand size materials in the basin (Kilic, 1984). These finer particles are likely transported to the deeper sections of the reservoir and deposited temporarily. An image taken in 2014 when the reservoir is drained shows deposition along the reservoir bed (Figure 68).

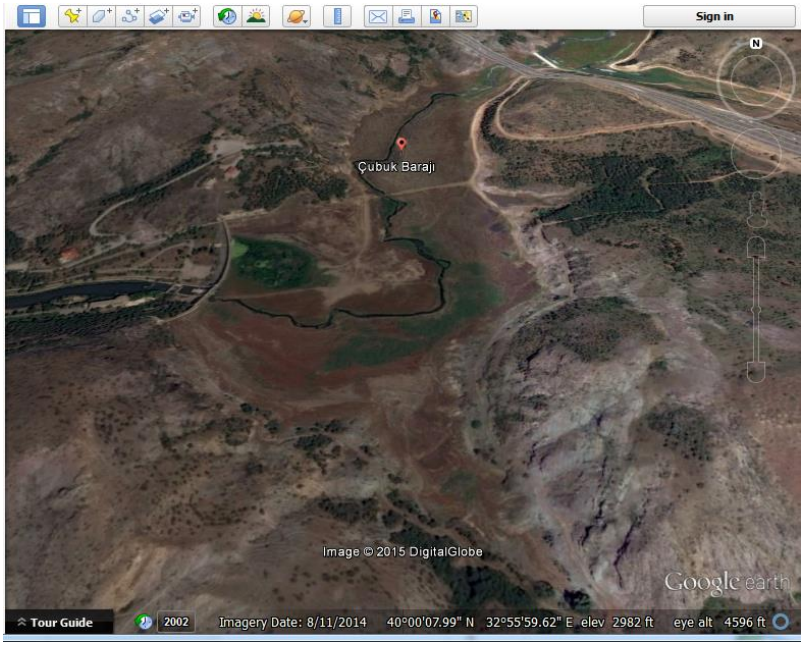

Figure 68: Google Earth Image showing the downstream portion of Cubuk I Reservoir

The SWAT model outputs were also used to plot annual suspended sediment and water inflow to the reservoir during the calibration period of 01/01/1989 – 12/31/1996 (Figure 69).

According to the figure, water and sediment fluxes increased between 1989 and 1996. In April 1992, there was a big rain storm for which the SWAT model simulation predicted huge sediment yields to the reservoir. But, the 1996 flood did not generate a large sediment load to the reservoir because sediment transport depends upon numerous other factors such as hydrology, geology, and land use characteristics.

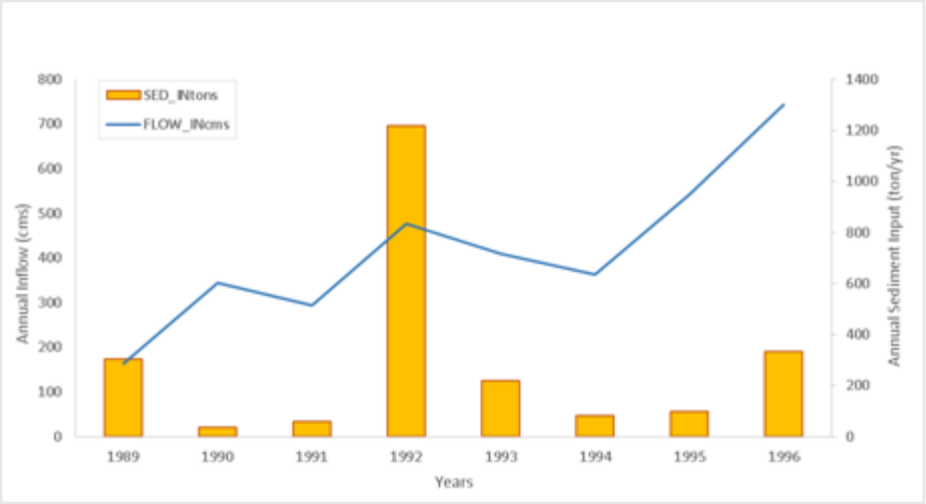

Figure 69: Annual sediment flux to Cubuk I Reservoir (simulated)

7.4.3. Sediment Deposition in the Cubuk II Reservoir

The drainage area of the Cubuk I Reservoir was reduced after the operation of Cubuk II Reservoir (in 1964) because Cubuk II is located upstream of Cubuk I. Cubuk II Reservoir collects most of the sediment coming from upstream, especially during a peak flow. Similarly, the capacity of Cubuk II Reservoir was reduced between 1964 and 1983. The only year of rising storage capacity was the year of 1978.

From the areal images, I identified a delta at the entrance of the main tributary. Delta formation and deposition along the length of the reservoir seem to occur. A recent drought has reduced the water level of Cubuk II and facilitated siltation on the delta (Figure 70).

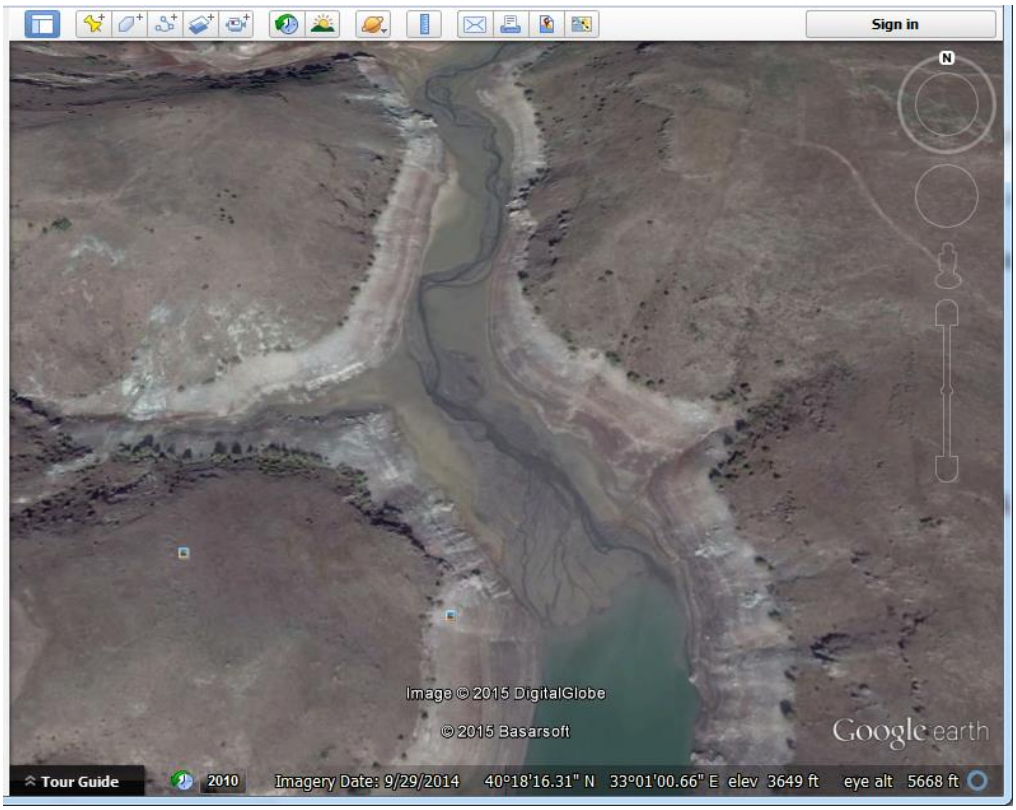

Figure 70: Google Earth image showing the downstream end of Cubuk II Reservoir

The variation in cross sections of the reservoir headwater area indicates that the location of the delta does not influence the channel width at the main stream entrance into the reservoir. However, the river generates a meandering channel in the alluvial deposits (Figure 68 - 70). On the other hand, annual water and sediment inflow to the Cubuk II Reservoir was increased during the calibration period of the SWAT model. Especially during peak flow periods such as in 1992 and in 1996, a huge amount of sediment was brought to the reservoir by peak flow (Figure 71). The chart showing annual sediment and water inflow to Cubuk II Reservoir seems more consistent than the other chart for Cubuk I as higher stream flow generates more sediment flux.

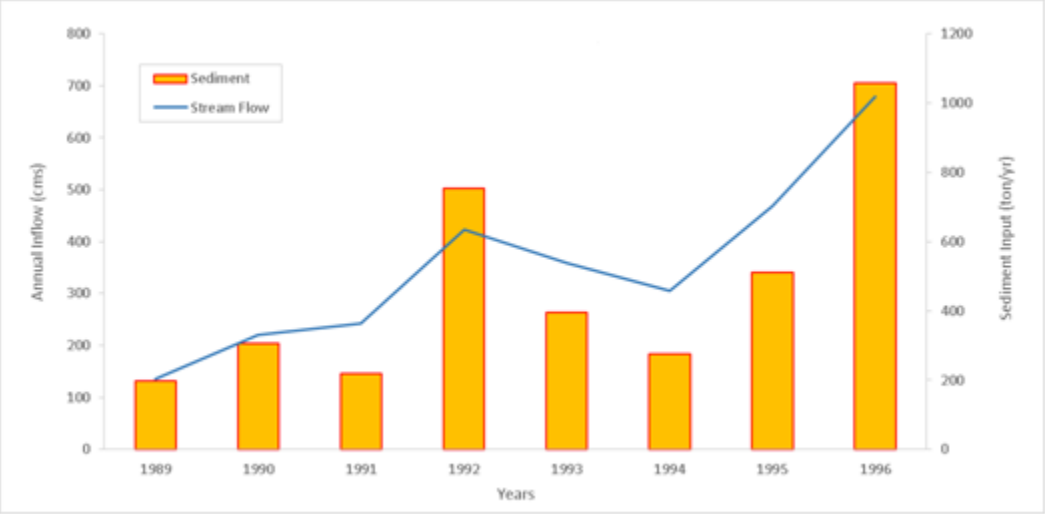

Figure 71: Annual sediment flux to Cubuk II Reservoir (simulated)

7.4.4. Areal Image Interpretation

Color infrared images (CIR) use a portion of the electromagnetic spectrum that ranges from 0.70 µm to 1.0 µm (micrometer). These images are capable of seeing different combinations of main colors (blue, green, red). The CIR imagery is commonly used for identifying land cover since each type of land cover and water surface variously absorb a particular portion of solar radiation, transmitting and reflecting the remaining portions. Infrared images represent clear water as dark blue to black in color because the body of water absorbs most of the near infrared wavelength energy. However, suspended sediment appears in CIR imagery as a lighter color since sediment particles are able to reflect a little more green light than stagnant water.

The main imagery being used was CIR images (2014), obtained from the Turkish General Command of Mapping. With the image, the blue (band 1) and near-infrared (band 4) was engaged using Image Analysis Tool and Normalized Difference Vegetation Index (NDVI) function in Arc GIS 10.2.2 in order to obtain a detailed look through the water for suspended sediment in the lake area.

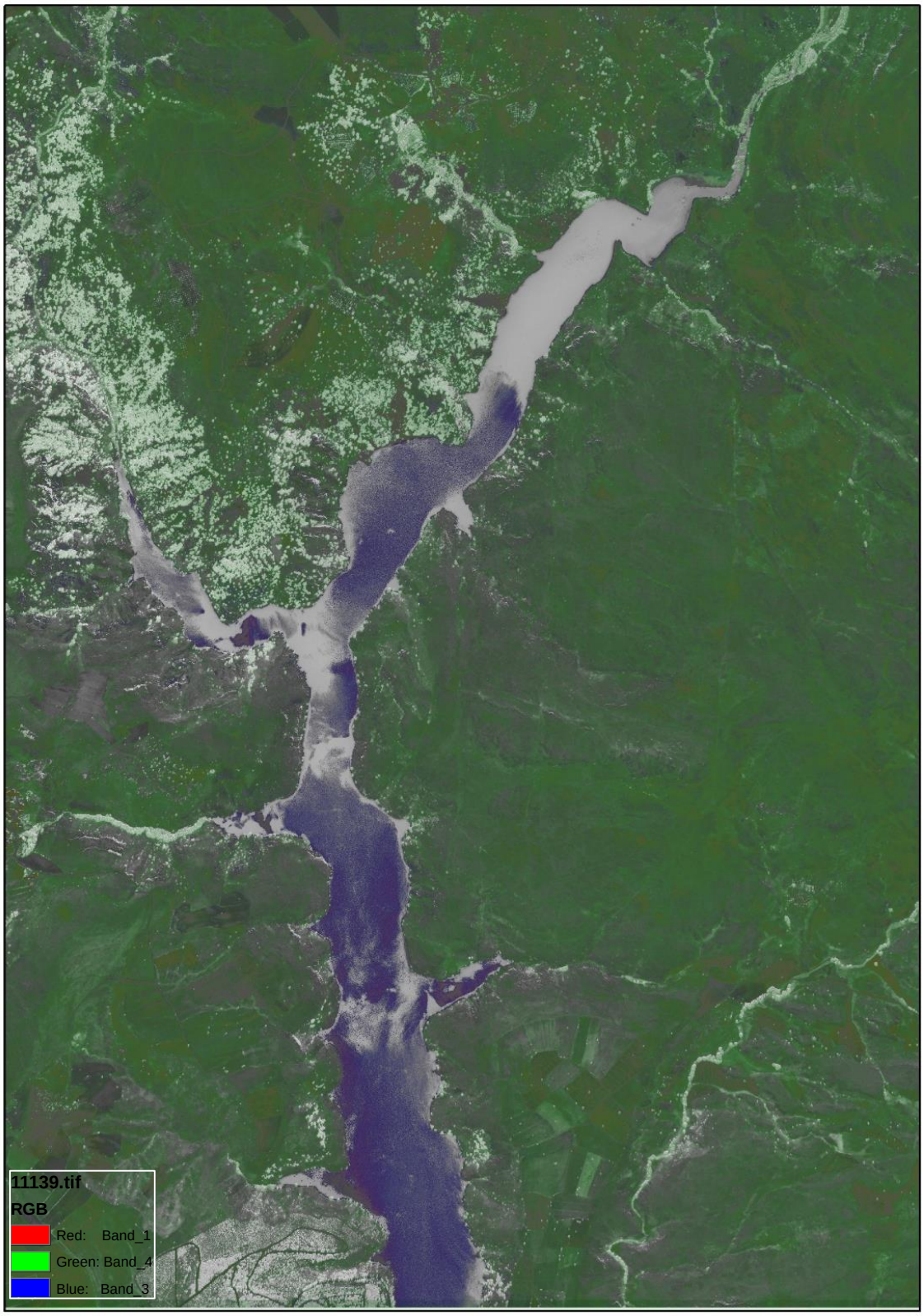

Figure 72: Color infrared images were used to create a false-color image of suspended sediment entering the Cubuk II Reservoir (Infrared data from the Turkish General Command of Mapping)

Finally, various detection options were used to identify changes in the water body. Considering sediment yield instead of vegetation, the red (band 3) and near infrared (band 4) were used for greenness ratio to opposite greenness pixels. Then I used image analysis software (ENVI 5.0) to create a Normalized Difference Suspended Sediment Index that can be shown as a colored image of variation in sediment concentration (Figure 72). According to the image, darker colors represent clearer water and a lighter color represents turbulence and suspended sediment in the water. The figure shows the suspended sediment input from the main tributaries to Cubuk II Reservoir. Lack of CIR imagery for the Cubuk I Reservoir limited the ability to create another suspended sediment index map for Cubuk I. In the following Google Earth imagery of the Cubuk I Reservoir, the water was released and a water treatment plant was built upstream (Figure 73).

Figure 73: Google Earth showing the shoreline of the Cubuk I Reservoir

In the Google Earth imagery of the Cubuk II Reservoir, the water level of the dam had dropped as a result of drought that began in 2012 around the study area. This drought was also combined with a very limited amount of snow melting during the spring and a dry summer. Figure 74 illustrates the comparison of mean annual precipitation between 2013 and 2014, and the long term average from the Esenboga meteorological station over which the Google Earth image was taken. The image clearly shows deltaic formation at the upstream end where the main tributary enters, as well as finer size materials (probably clay size) entering the main tributary (marked with arrow in orange color). A meandering river is barely visible at the bottom of the water accumulated in the dam.

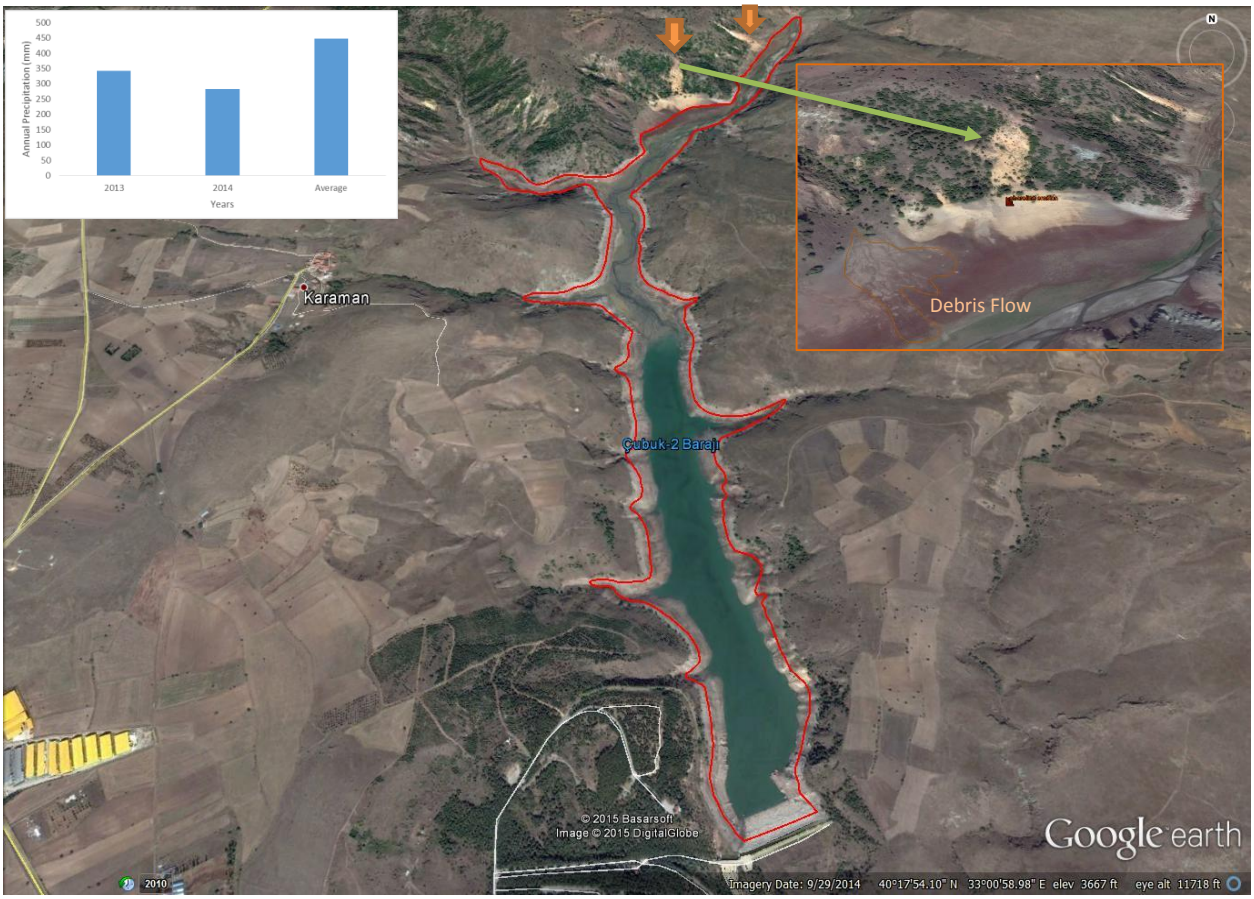

Figure 74: The image showing the shoreline of the Cubuk II reservoir and potential source of sediment input

7.4.5. Watershed Management

Watershed management involves reducing reservoir siltation coming from upstream areas by using methods including change in land use, afforestation or planting other suitable vegetation cover, or placing sediment trapping fences in order to conserve soil and water in the watershed. If the appropriate watershed management practices are not performed, the most productive top soil of the agricultural lands will be transported to natural or human made barriers and cause loss of storage capacity as a consequence of siltation. In order to prevent siltation, several techniques should be combined for a specific site because each region has different characteristics.

One of the main contributing factors to the storage losses of the reservoirs is low forest cover (4% of the total watershed area; Figure 20). For controlling the amount of sediment entering reservoirs, the most significant practice is increasing vegetative cover intensity in the catchment because higher intensity of vegetation cover assists in stabilizing top soil and accordingly protects reservoirs from siltation. Another important practice is teaching and financially supporting farmers to apply sustainable agriculture consisting of stubble burning, tillage, and fallow techniques. The research area commonly experiences intense rain storms in spring and early summer, generally at a time when the soil has been exposed by post-harvest burning. Stubble helps to conserve top soil from water erosion, so stubble burning protects reservoirs from larger amounts of incoming sediment, especially during a rain storm. Tillage is performed upslope and downslope in opposing directions over alternating years in the region due to financial and time concerns, but these results in a net downslope movement of top soil. Plowing land preparatory to letting it lie fallow and over-grazing are other common methods used by farmers, but they also increase soil erosion in the region.

Shorelines contribute huge amounts of sediment to reservoirs in semi-arid regions, but it is not feasible to protect the whole shoreline against erosion due to its long length (Morris and Fan, 1997). Besides reservoir shoreline management practices along the steeper slopes, debris dams (upstream check points) could be used along the main tributaries that bring large amount of sediment into reservoirs. Reservoir sediment management practices should be performed for each upstream debris dam in order to extend the life of the dam. According to Mahmood (1987), these upstream check dams are capable of trapping coarser particles, which prevents major problems for downstream structures. Using bypass systems is another costly practice, but it has been effective for the Gmund Reservoir in Austria and the Palagnedra Reservoir in Switzerland (Howard, 2000), even though it is of limited applicability for arid regions because of the higher amount of water demand in arid regions (Tigrek and Aras, 2012).

Climate change is expected to have significant effects on water resources availability in semi-arid regions of Turkey. According to Sarlan (2007), the region of Turkey most impacted by climate change will be Central Turkey. Sarlan (2007) concluded that climate conditions in the region will be enormously changed in the next 100 years. The study predicts 20% reduction in precipitation and 4-5 ^{o}C increase in temperature by the year 2100. The warmer temperatures are expected to reduce the amount of precipitation, which leads to earlier spring melting of snowpack, affecting surface water flow, ground water level, and soil moisture. Recent climate trends illustrate an increase in temperature and decrease in precipitation during the past couple of decades. River morphology is adapted to the current conditions including water discharge, sediment discharge, grain size, river slope, and vegetative cover. Expected variation in river stream flow or sediment load as a result of different climate scenarios is likely to alter land use and vegetation cover as well

as other potential controlling variables (Garde, and Raga Raju, 2000). The river system may then shift toward new equilibrium condition based on different water and sediment inputs.

CHAPTER EIGHT

CONCLUSION AND RECOMMENDATIONS

Sediment yields caused by soil erosion are becoming a serious issue for arid and semiarid regions, particularly Central Anatolia in Turkey. Despite the complexity of processes influencing sediment yield in this watershed, this research demonstrates that physically based models, specifically the SWAT model, can reasonably estimate suspended sediment yields at a basin scale. However, detailed sensitivity analysis, calibration, and validation should be used to improve the accuracy of the model results.

SWAT reasonably simulates water discharge and suspended sediment yields in the Ankara River catchment because the results obtained from the model satisfactorily predict stream flow and sediment yields in that region, with monthly discharge NSE of 0.79, RE of -0.58, and R^2 of 0.89, and monthly suspended sediment yield NSE of 0.81, RE of 1.55, and R^2 of 0.93 for the calibration period of 01/01/1989 through 12/31/1996. The most sensitive input parameters in the watershed are ground water delay time and base flow regression for water discharge, and soil depth and Manning's coefficient of channel roughness for sediment yields. Using finer scale digital elevation maps (DEMs) and data on soil type, and measuring sediment yields over various sites in the watershed, will potentially improve the model performance.

The multiple regression analysis applied to the second objective of this research indicates that there are statistically significant linear relationships among sediment yields and the following explanatory variables: stream flow, drainage area, and channel width. These controlling variables are statistically significant based on the coefficient interval of 90%. Hypothesis II, that sediment yield correlates most strongly with topography and to a lesser extent with stream discharge,

channel geometry, land cover, and drainage characteristics, was rejected because sediment yields in the watershed are dominantly influenced by stream flow, drainage area, and channel width.

The storage capacity of the Cubuk I and Cubuk II Reservoirs decreased between 1936 and 1983 because of siltation. Generally, stream flow carries substantial sediment after a big storm such as the one in April 1992. The output from the SWAT model indicates the model successfully simulates the storm and generates a higher suspended sediment input to the reservoirs. Delta formation is clearly observed at the headwater area of Cubuk II Reservoir and other ephemeral tributaries also contribute lower amounts of suspended sediments, especially during spring. Collection of more accurate spatially and temporally distributed data on climate and disturbance history can help to reduce model uncertainty. Future studies in the Cubuk catchment should focus on improving the database by obtaining higher resolution input data for the simulation and regression analyses.

Prediction of sediment yield for non-point sources and planning watershed management of a reservoir (reducing sediment inflow to a reservoir and removing siltation from a reservoir) require multidisciplinary approaches. This study established a basis for future multidisciplinary studies on modelling sediment yields and for better understanding of correlations between potential control variables and the resulting sediment yield to reservoirs, which can also facilitate estimation of the probable lifespan of a reservoir and appropriate mitigation measures to limit reservoir sedimentation.

REFERENCES

Abbaspour K. C., M. Vejdani, and S. Haghighat, 2007, SWAT-CUP calibration and uncertainty programs for SWAT. In Proc. Intl. Congress on Modelling and Simulation (MODSIM'07), 1603 1609. L. Oxley and D. Kulasiri, eds. Melbourne, Australia: Modelling and Simulation Society of Australia and New Zealand.

Abbott, M.B., J.C. Bathurst, J.A. Cunge, P.E. O'Connell, and J. Rasmussen, 1986, An introduction to the European Hydrological System – "SHE". J.Hydrol. 87:45-77.

Abernethy, C., 1990, The use of river and reservoir sediment data for the study of regional soil erosion rates and trends. Paper presented at the International Symposium on Water Erosion, Sedimentation and Resource Conservation (Dehradun, India, October, 1990)

Ahmadi, M., J.C. Ascough II, K.C. Dejonge, and M. Arabi, 2014, Multisite-multivariable sensitivity analysis of distributed watershed models: enhancing the perceptions from computationally frugal methods. Ecological Modeling. 279:54–67.

Ahnert, F., 1970, Functional relationships between denudation, relief, and uplift in large mid-latitude drainage basins. American Journal of Science 268:243-263.

Allan, J. D., 1995, Stream ecology: Structure and function of running waters. London: Chapman and Hall. Leopold, L., M.G. Wolman, and J.P. Miller, (1964), Fluvial processes in geomorphology. New York: Dover.

Arnold, J. G., R. Srinivasan, R.S. Muttiah, and J. R. Williams, 1998, Large-area hydrologic modeling and assessment: Part I.Model development. J. American Water Resources Assoc. 34(1): 73-89.

ASCE, 1993, Criteria for evaluation of watershed models. J. Irrig. Drainage Eng. 119(3): 429-442.

Bagnold, R.A., 1966, An Approach to the Sediment Transport Problem from General Physics, USGS Professional Paper 422-I.

Basson, G.R., and G. Di Silvio, 2008, Erosion and sediment dynamics from catchment to coast. UNESCO. International Hydrological Program, Technical Documents in Hydrology, No 82.

Basson, G.R., A. Rooseboom, J. Le Roux, L. Gibson, and V.P. Msadala, 2009, Sedimentation and sediment yield maps for South Africa. Water Research Commission Project K5/1765. Progress Report.

Beasley, D.B. and L.F. Huggins, 1981, ANSWERS User's Manual. EPA-905/9-82-001: USEPA. Chicago, IL.

Boardman, J., J. Poesen, and R. Evans, 2003, Socio-economic factors in soil erosion and conservation. Environ. Sci. Policy, 6:1-6.

Borland W., and C.R. Miller, 1958, Distribution of sediments in large reservoirs. Journal of the Hydraulics Division ASCE. 84: 1–18.

Borland W., and C.R. Miller, 1960, Distribution of sediments in large reservoirs. Transactions, American Society of Civil Engineers, 125:166-180.

Bosch, D. D., J. M. Sheridan, H. L. Batten, and J. G. Arnold, 2004, Evaluation of the SWAT model on a coastal plain agricultural watershed. Trans. ASAE 47(5): 1493-1506.

Boyle, D. P., H. V. Gupta, and S. Sorooshian, 2000, Toward improved calibration of hydrologic models: Combining the strengths of manual and automatic methods. Water Resources Research 36(12): 3663-3674.

Brune, G. M., 1953, Trap efficiency of reservoirs. Transactions, American Geophysical Union 34(3): 407-418.

Buringh, P. and R. Dudal, 1987, Agricultural land use in space and time. In: Land Transformation in Agriculture (ed. by M. G. Wolman & F. G. A. Fournier), SCOPE Report no. 32, 9-43. Wiley, Chichester, UK.

Church, M. and H.O. Slaymaker, 1989, Disequilibrium of Holocene sediment yield in glaciated British Columbia. Nature 337: 452-454.

Cristofano, E.A., 1953, Area-increment method for distributing sediment in a reservoir. Albuquerque. New Mexico. US Bureau of Reclamation.

Daines, N. H., 1949, Study of suspended sediment in the Colorado River, U. S. Bur. of Reclamation report, 11 p.

Dedkov, A. P. and V.I. Moszherin, 1992, Erosion and sediment yield in mountain regions of the world. In: Erosion, Debris Flows and Environment in Mountain Regions (ed. by D. E. Walling , T. R. Davies & B. Hasholt) (Proc. Chengdu Symp., July 1992), 29-36. IAHS Publ. no. 209.

Dendy, F.E. ,1982, Distribution of sediment deposits in small reservoirs. Transactions of the ASAE 25: 100– 104

Dendy, F.E., and G.C. Bolton, 1976, Sediment yield-runoff drainage area relationships in the United States. Journal of Soil and Water Conservation 31: 264-266.

Descheemaeker K., J. Nyssen, J. Poesen, D. Raes, M. Haile, B. Muys, and S. Deckers, 2006, Runoff on slopes with restoring vegetation: a case study from the Tigray highlands, Ethiopia. Journal of Hydrology 331: 219–241.

Dietrich, C.F., 1991, Uncertainty, Calibration and Probability: The Statistics of Scientific and Industrial Measurement 2nd Edition, A.Higler (p. 331).

Douglas, I., 1967, Vegetation and the sediment yield of rivers. Nature, London. 215: 925-928.

DSI Report, 2005, Obtained in 2012 by personal communication.

Dunne, T., 1975, Sediment yield of Kenyan rivers. Report to Ministry of Water Development, Government of Kenya.

Dunne, T., 1979, Sediment yield and land use in tropical catchments. Journal of Hydrology, 42: 281–300.

Eizel-Din, M.A., M.D. Bui, P. Rutschmann E. Failer, C. Grass, K. Kramer, A.S. Hussein, and A. Saghayroon-Elzein, 2010, Trap efficiency of reservoirs on the Nile River. Bundesanstalt fur Wasserbau, ISBN 978-3-939230-00-7.

Evans, J.E., N.S. Levine, S.J. Roberts, J.F. Gottgens, and D.M. Newman, 2002, Assessment using GIS and sediment routing of the proposed removal of Ballville Dam, Sandusky River, Ohio. Journal of the American Water Resources Association, 38: 1549-1565.

Gan, T. Y., E. M. Dlamini, and G.F. Biftu, 1997, Effects of model complexity and structure, data quality, and objective functions on hydrologic modeling. J. Hydrology. 192(1): 81-103.

Garde R. J., and K.G. Raga Raju, 2000, Mechanics of sediment transportation and alluvial streams problem. New Age International (P) Limited, Publishers, New Delhi, India.

Gilbert, G.K., 1877, Report on the geology of the Henry Mountains (Utah): Washington, D.C. Government Printing Office, p.160.

Gitau, M.W. and I. Chaubey, 2010, Regionalization of SWAT model parameters for use in un-gaged watershed. Water 2:849-871.

Griffiths, P.G., R. Hereford, and R.H. Webb, 2006, Sediment yield and runoff frequency of small drainage basins in the Mojave Desert. U.S.A. Geomorphology, 74:232-244.

Halcrow Water, 2001, Sedimentation in storage reservoirs. Final Report. DETR. London.

Hampson, L., 1997, Sediment transport analysis, Carmel River near Carmel, Water years 1992-1995: Monterey Peninsula Water Management District Tech. Memorandum No. 97 03.

Hecht, B., 2000, Drought, fire, and geology key watershed influences in the Northern Santa Lucia Mountains, California: Peninsula Geological Society Spring Field Trip 2000 Guidebook, Salinia/Nacimiento Amalgamated Terrane, Big Sur Coast, Central Calif., p.7.

Holeyer, R.J., 1978, Suspended sediment algorithms. Remote Sensing Env. 10(4): 323-338.

Hotchkiss, R. H., 1995, Reservoir sedimentation, causes and consequences. In W. H. Espey, Jr. and P. G. Combs, eds., Proceedings of the First International Conference of Water Resources Engineering, San Antonio, TX. New York, NY: American Society of Civil Engineers, 1188–1192.

Howard, C.D.D., 2000, Operations monitoring and decommissioning of dams. Thematic Review IV.5 prepared for the World Commission of Dams, Cape Town, March 2000.

Hwang, C., 1980, Suspended sediments of Taiwan Rivers and their geomorphological significance. Bull. National Taiwan Normal Univ. 28: 649-679.

Isik, S., E. Dogan, L.M. Kalinsasal, and N. Agiralioglu, 2008, Effects of anthropogenic activities on the Lower Sakarya River. Catena, 75: 172–181.

Jansson, M., 1988, A global survey of sediment yield. Geogr. Annual. Series A, 70: 81-98.

Julien, P.Y., 1998, Erosion and sedimentation. Cambridge University Press.

Khoram, S., 1981, Use of ocean color scanner data in water quality mapping. Photogram. Eng. Remote Sensing, 47(5): 667-676.

Khorasani G. and L. Zeyun, 2014, Implementation of technology acceptance model (TAM) in business research on web based learning system: International Journal of Innovative Technology and Exploring Engineering (IJITEE), ISSN: 2278-3075, 3(11): 112-116.

Kilic, R., 1984, Cubuk 1 Baraji'nda siltasyonun incelenmesi. Doktora Tezi. Insaat Muhendisligi Bolumu, Gazi Universitesi, Ankara.

Kilic, R., 1986, Cubuk 1 Baraj golune depolanan sedimentlerin sedimentolojisi ve minerolojisi. Gazi Universitesi, 1(1):97-112.

Kling, G. F., 1974. A computer model of diffuse sources of sediment and phosphorus moving into a lake. PhD thesis, Cornell University, Ithaca, N.Y.

Lane, L.J., and M.A. Nearings (eds.), 1989, USDA – Water erosion prediction project: hillslope profile model documentation. NSERL Report No. 2. USDA-ARS National Soil Erosion Research Laboratory, West Layfayette. In.

Langbein, W. B., and S.A. Schumm, 1958, Yield of sediment in relation to mean annual precipitation. Trans. Amer. Geo. Union, 39(6): 1076-1084.

Lavigne, F. and H. Suwa, 2004, Contrasts between debris flows, hyper concentrated flows and stream flows at a channel of Mount Semeru, East Java, Indonesia. Geomorph., 6:41-58.

Leopold, L. B., M. G. Wolman, and J.P. Miller, 1964, Fluvial processes in geomorphology. W. H. Freeman and Company, San Francisco, California.

Lvovich, M. I., G.Y. Karasik, N.L. Bratseva, G.P. Medvedeva, and A.V. Maleshko, 1991, Contemporary Intensity of the World Land Intracontinental Erosion. USSR Academy of Sciences, Moscow.

Ma, L., J.C. Ascough II, L.R. Ahuja, M.J. Shaffer, J.D. Hanson, and K.W. Rojas, 2000, Root zone water quality model sensitivity analysis using Monte Carlo simulation. Trans. ASAE 43(4): 883-895.

Mahmood, K., 1987, Reservoir sedimentation impact extend and mitigation. World Bank Technical Paper. Washington D.C. no 71.

McConvill, C., 2014, The wiki spaces: https://riverrestoration.wikispaces.com/Desert+rivers Retrieved January 29, 2014.

McCully, P., 1996, The ecology and politics of large dams, Silenced Rivers, London.

Meade, R.H., 1969, Errors in using modern stream-load data to estimate natural rates of denudation. Geol. Soc.Am. Bull. 80:1265-1274.

Michalec, B., 2008, An assessment of siltation of small water reservoirs in the Upper Vistula River catchment. Scientific Papers, University of Agriculture in Krabers, Polland. 328. ISSN 1899-3486 p. 193.

Miller, C.R., 1951, Analysis of flow-duration, sediment-rating curve method of computing sediment yield, US. Bur, of Reclamation report, 16 p.

Milliman, J.D., and R.H. Meade, 1983, World-wide delivery of river sediment to the oceans: Jour. Geology: 91:1-21.

Milliman, J.D., Y.S. Qin, M.E. Ren, and Y. Saito, 1987, Man's influence on the erosion and transport of sediment by Asian rivers: the Yellow River (Huanghe) example. Geol. 95: 751-762.

Milliman, J.D. and J.P.M. Syvitski, 1992, Geomorphic tectonic control of sediment discharge to the ocean: the importance of small mountainous rivers. J. Geol. 100:525-544.

Mirsal, I.A., 2008, Soil degradation. Soil Pollution: Origin, Monitoring & Remediation. Springer, p. 100. ISBN 978-3-540-70775-2.

Montgomery, D.R. and M.T. Brandon, 2002, Topographic controls on erosion rates in tectonically active mountain ranges. Earth Planet. Sci. Lett. 201:481–489.

Moriasi, D. N., J. G. Arnold, M. W. Van Liew, R. L. Bingner, R. D. Harmel, and T. L. Veith, 2007, Model evaluation guidelines for systematic quantification of accuracy in watershed simulations. Trans. ASABE 50(3): 885-900.

Morris, M.D., 1991, Fractional sampling plants for preliminary computational experiments. Tecnometrics 33(2):161-174.

Morris, G.L. and J. Fan, 1997, Reservoir sedimentation handbook. McGraw-Hill, New York.

Motovilov, Y. G., L. Gottschalk, K. Engeland, and A. Rodhe, 1999, Validation of distributed hydrological model against spatial observations. Agricultural and Forest Meteorology 98-99: 257-277.

Mutchler, C. K., C.E. Murphree, and K. C. McGregor, 1988, Laboratory and field plots for soil erosion studies. In Soil erosion research methods, ed. R. Lal, 9-36. Soil and Water Conservation Society, Ia.

Neil, D,T., R.K. Mazarari, 1993, Sediment yield mapping using small dam sedimentation surveys. Southern Tablelands, New South Wales, Cetena 20:13-25.

Neitsch, J.G., J.R. Arnold, J.R. Kiniry, and J.D. Williams, 2001, Soil and water assessment tool. Theoretical Documentation – Version 2000. Blackland Research Center – Texas.

Neitsch SL, J.G. Arnold, J.R. Kiniry, R. Srinivasan, and J.R. Williams, 2005, Soil and Water Assessment Tool, Theoretical Documentation: Version 2005. USDA Agricultural Research Service and Texas A&M Blackland Research Center: Temple.

Novotny, V. and H. Olem, 1994, Water Quality: Prevention, identification, and management of diffuse pollution. Van Nostrand Reinhold, New York.

Nyssen, J., J. Poesen, J. Moeyerson, J. Deckers, M. Haile, A. Lang, 2004, Human impact on the environment in the Ethiopian and Eritrean highlands – a state of the art. Earth-Science Reviews, 64: 274-320.

Ongwenyi, G.S., S.M. Kithiia, and F.O. Denga, 1993, An overview of soil erosion and sedimentation problems in Kenya. Sediment Problems: Strategies for Monitoring Prediction and Control (ed. by R. F. Hadley & T. Mizuyama) (Proc. Yokohama Symp., July 1993), 217-224. IAHS Publ. no. 217.

Parker, G., 1990, Surface-based bed-load transport relation for gravel rivers, Journal of Hydraulic Research, 28:417-436.

Pazzaglia F.J., and M.T. Brandon, 1996, Macro-geomorphic evolution of the post-Triassic Appalachian Mountains determined by deconvolution of the offshore basin sedimentary record, Basin Res. 8:255–278.

Peterson, J.R., and J.M. Hamlett, 1998, Hydrological calibration of SWAT model in a watershed containing fragipan soils. J. Amer. Water Resource Ass. 34:531-544.

Phippen, S., E. Wohl, 2003, An assessment of land use and other factors affecting sediment loads in the Rio Puerco watershed, New Mexico. Geomorphology. 52:269-287.

Pinet, P. and M. Souriau, 1988, Continental erosion and large-scale relief. Tectonics. 7:563-582.

Powell, J.W., 1876, Report on the geology of the eastern Uinta Mountain and a region of country adjacent thereto: U.S. Geological and Geographical Survey of the Territories. 7:1-218.

Refsgaard, J. C., 1997, Parameterization, calibration, and validation of distributed hydrological models. J. Hydrology. 198(1): 69-97.

Renard, K.G., J.M. Laflen, G.R. Foster, and D.K. McCool, 1994, The Revised Universal Soil Loss Equation. Soil Erosion Research Metlzods, Rattan La1 (ed.), St. Lucie Press, Delray Beach, Florida.

Saleh, A. and B. Du, 2004, Evaluation of SWAT and HSPF within BASINS program for the Upper North Bosque River watershed in central Texas: Transaction of the American Society of Agricultural Engineering (ASAE), 47(4):1039–1049.

Santhi, C., J.G. Arnold, J.R. Williams, W.A. Dugas, R. Srinivasan, and L.M. Hauck, 2001, Validation of the SWAT model on a large river basin with point and nonpoint sources. Journal of the American Water Resources Association 37(5):1169-1188.

Saylan, L., 2007, Estimation of ecosystem CO_2 exchange, Congress of First Turkish Climate Change, TİKDEK 2007, İstanbul Technical University, İstanbul, 11-13 Nisan 2007.

Schmidt, J., S. Elliot, and l. McKergow, 2008, Land use impacts on catchment erosion for the Waitetuna catchment. New Zealand. Sediment dynamics in changing environments. IAHS Publication 325:453-457.

Schumm, S.A., 1954, The relation of drainage basin relief to sediment loss. International Association of Hydrological Sciences Publ. 36:3216–3219.

Schumm, S.A., 1963, The disparity between present-day denudation and orogeny. US Geol. Surv. Prof. Pap. Washington DC, no: 454-H, p.13.

Sensoy, S., Demircan, M., Ulupinar, Y., Balta, I., 2008, Climate of Turkey. Retrieved from http://dmi.gov.tr/files/en-US/climateofturkey.pdf. May 15, 2015.

Shen, H.W., and R.M. Li, 1976, Watershed sediment yield. Stochastic approaches to water resources, 11: 21-1 – 21-68.

Siakeu, J., T. Oguchi, T. Aoki, Y. Esaki, and P.H. Jarvie, 2004, Change in riverine suspended sediment concentration in central Japan in response to late 20th century human activities. Catena 55: 231–254.

Simons D. B., and F. Senturk, 1992, Sediment Transport Technology Water and Sediment Dynamics. Book Crafters Ins., Chelsea, Michigan, U.S.A.

Smith, Kate and Edwards, Rob (March 8, 2008), 2008: The year of global food crisis. The Herald (Scotland).

Smith, S.E., K.H. Mancy, and A.F.A. Latif, 1980, Application of remote sensing technique towards the management of Aswan high dam reservoir. Proceeding of the International symposium on Remote Sensing of Environment, p. 1297-1307.

Solomonson, V.V., 1973, Remote sensing applications in water resources. Proceeding of International Sym. on Earth Resources Technology, Washington D.C., USA during 10-14 December, 1973.

Strahler, A.N., 1952, Hypsometric (Area-Altitude) analysis of erosional topography. Bulletin of the Geological Society of America 63:1117-1142.

Strand, R.I., and E.L. Pemberton, 1982, Reservoir sedimentation technical guidelines for Bureau of Reclamation, U.S. Bureau of Reclamation, Denver, Colorado, p. 48.

Summerfield M. A. and N.J. Hulton, 1994, Natural controls of fluvial denudation rates in major world drainage basins. J. Geophys. Res. 99:563-582.

Sumi, T. and T. Hirose, 2002, Accumulation of sediments in reservoirs, EOLSS - Encyclopedia of Life Support Systems.

The Guardian, 2007, Global food crisis looms as climate change and population growth strip fertile land. The Guardian, August 30.

Tigrek S. and T. Aras, 2012, Reservoir sediment management. CRC Press. London, UK.

Thornes, JB., 2001, Vegetation and Erosion. Processes and Environments, British Geomorphological Research Group Symposia Series. Wiley: Chichester.

TUIK, 2015, Turkiye Istatistik Yilligi 2014 (Turkey Statistics Yearbook 2014).

Van Griensven, A., and W. Bauwens, 2005, Application and evaluation of ESWAT on the Dender basin and Wister Lake basin. Hydrol. Proc. 19(3): 827-838.

Van Liew, M. W., J. G. Arnold, and D. D. Bosch, 2005, Problems and potential of auto calibrating a hydrologic model. Trans. ASAE 48(3): 1025-1040.

Van Liew, M.W., J.G. Arnold, and J.D. Garbrecht, 2003, Hydrologic simulation on agricultural watersheds choosing between two models: Transaction of the American Society of Agricultural Engineering (ASAE), 46(6):1539–1551

Van Rijn, L. C., 1993, Principles of sediment transport in rivers, estuaries, and coastal seas, Section 3: Fluvial and sediment properties. Aqua Publications.

Veith T., J. Brauns, W. Weisheit, M. Mittag, and C. Buchel, 2009, Identification of a specific fucoxanthin chlorophyll protein, Fcp4, in the light harvesting complex of photosystem I in the diatom Cyclotella meneghiniana Biochimica et Biophysica Acta 1787:905–912.

Verstraeten, G., J. Poesen, J. de Vente, and X. Koninckx, 2003, Sediment yield variability in Spain: a quantitative and semi-quantitative analysis using reservoir sedimentation rates. Geomorphology, 50: 327-348.

Walling D.E., 1994, Measuring sediment yield from river basins in Lal, R. ed., Soil Erosion Research Methods. Soil and Water Conservation Society, Ankeny, IA.

Walling D.E., 1995, Suspended sediment yields in a changing environment. In changing river channels, Gurnel A., Petts G., (eds). Wiley, Chichester: 149-176.

Walling, D. E. and B.W. Webb, 1983, Patterns of sediment yield. Background to Palaeohydrology (ed. by K. J. Gregory), 69-100. Wiley, Chichester, UK.

Walling, D.E. and B.W. Webb, 1996, Erosion and sediment yield: a global overview. Erosion and Sediment Yield: Global and Regional Perspectives, IAHS Publ. no. 236.

WCD, 2000, Dams and Development: A New Framework for Decision-making, Earth-scan, London and Sterling, VA.

Webb, B. W., and D. E. Walling, 1984, Magnitude and frequency characteristics of suspended sediment transport in Devon Rivers. In Catchment experiments in fluvial geomorphology. Edited by T. P. Burt and D. E. Walling. Geo Books, Nonvich, UK, p. 399-415.

White, W. R., 2000, Contributing paper: Flushing of sediments from reservoirs, prepared for Thematic Review IV. 5: Operation, Monitoring and Decommissioning of Dams. HR Wallingford, UK.

Williams, J.R., 1975, Sediment-yield predictions with universal equation using runoff energy factor. In Present and Prospective Technology for Predicting Sediment Yield and Sources. U.S. Dept. Agr., ARS-S-40. Washington, D.C. p. 244-252.

Williams, J.R., and H.D. Berndt, 1977, Sediment yield prediction based on watershed hydrology. Trans. Of the ASAE. p. 1100-1104.

Williams, J., and W.V.G. Matthews, 1986, The 1983 erosion event on Tularcitos Creek, Monterey County, and its aftermath: Proceedings of the California Watershed Management

Conference, Nov. 18-20, 1986, West Sacramento, California. University of California Wild lands Resources Center Report No. 11, p. 155.

Yilmaz, S., 2003, Prediction of reservoir siltation: Theory and Practice. 34th International Post-Graduate Course on Hydrology, Hungary.

Young, R.A., C.A. Onstad, D.D. Bosch and W.P. Anderson, 1986, Agricultural nonpoint source pollution model: A watershed analysis tool. USDA-ARS, Morris, MN.

Zuazo, V.H.D. and C.R.R. Pleguezuelo, 2009, Soil-erosion and runoff prevention by plant covers: a review. In Lichtfouse, Eric et al. Sustainable agriculture. Springer. p. 785. ISBN 978-90-481-2665-1

APPENDIX A

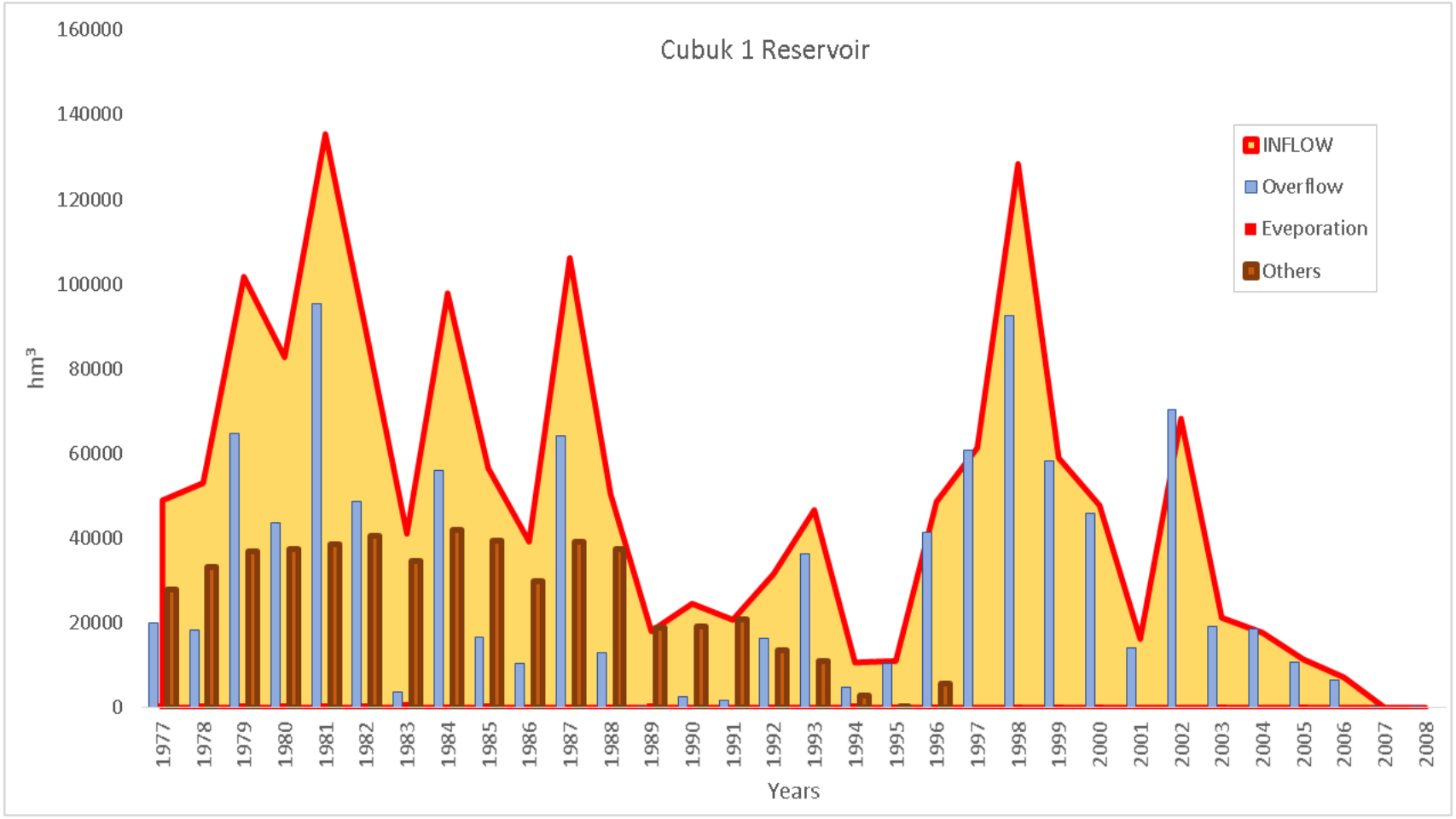

Figure 75: Observed Annual Water Input to the Cubuk I Reservoir

APPENDIX B

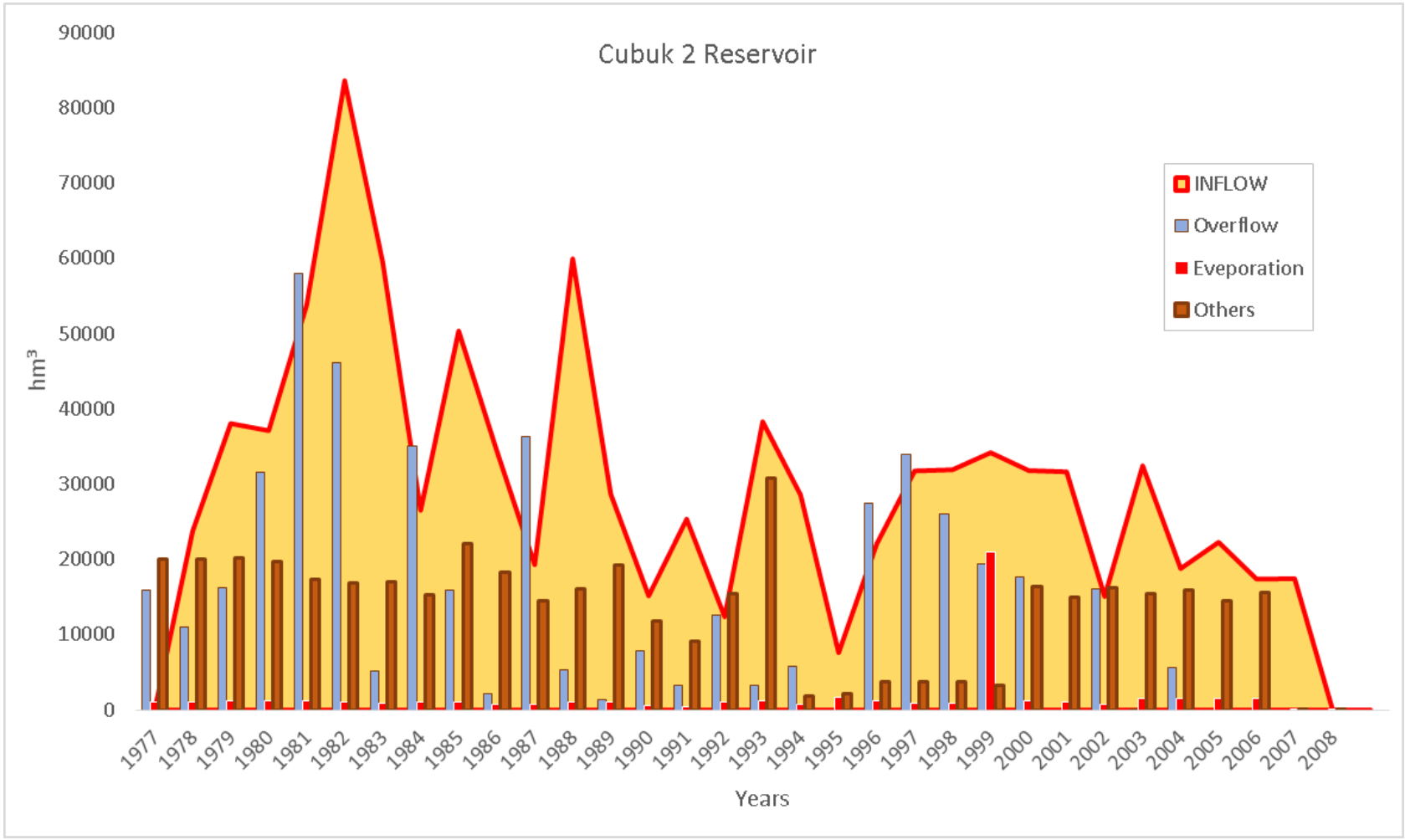

Figure 76: Observed Annual Water Input to the Cubuk II Reservoir

APPENDIX C

Table 20: Observed Monthly Precipitation for the Cubuk I Reservoir

STATION NAME			ÇUBUK RESERVOIR II					OPERATOR		DSİ			
STATION NUMBER			12-013					ALTITUDE		1005 m			
REGION			5					OPENIND DATE		9/1/1964			
CITY NAME			ANKARA-ÇUBUK					COORDINATES		40° 16' K - 33° 03' D			
OBSERVATION TYPE			MONTHLY PRECIPITATION (mm)										
YEAR	JAN	FEB	MARCH	APR	MAY	JUNE	JULY	AUGT	SEP	OCT	NOV	DEC	ANNUAL
1960	43.0	48.5	47.4	65.0	25.5	28.8	21.0	2.0	7.5	35.5	25.0	45.5	394.7
1961	16.9	86.0	49.5	10.0	36.9	82.0	5.0	.	30.8	31.6	4.5	57.5	410.7
1962	26.9	71.0	61.4	20.0	13.3	7.1	1.6	12.4	49.8	17.4	8.1	112.1	401.1
1963	89.3	81.2	34.3	53.7	127.7	17.1	23.3	.	57.9	28.4	5.8	60.3	579.0
1964	2.8	52.3	36.4	16.1	41.8	53.1	16.4	2.3	8.9	0.0	50.6	75.8	356.5
1965	24.1	62.3	31.2	42.9	61.2	20.5	0.3	2.2	.	11.0	47.0	51.1	353.8
1966	51.8	9.9	63.4	49.0	75.3	17.3	32.0	26.5	6.2	11.0	24.7	-	-
1967	41.4	26.5	56.5	99.0	59.2	11.0	15.4	16.4	.	9.0	32.3	47.1	413.8
1968	91.2	30.6	58.6	52.6	54.7	51.4	8.5	10.3	47.7	35.1	62.4	93.2	596.3
1969	76.7	77.6	68.2	85.9	60.6	29.3	3.3	.	21.0	5.0	34.8	79.7	542.1
1970	55.7	73.2	46.9	19.6	42.1	27.3	25.5	.	24.4	52.5	31.4	48.3	446.9
1971	36.9	16.0	54.6	59.8	66.6	31.3	1.9	10.2	22.5	15.2	55.9	56.5	427.4
1972	17.9	27.1	16.3	35.7	25.8	56.0	41.5	21.8	25.7	62.7	17.8	15.9	364.2
1973	12.4	28.0	41.4	70.8	46.4	41.8	8.3	4.6	6.8	3.6	15.9	48.6	328.6
1974	7.3	27.5	27.4	29.6	93.5	27.6	16.1	30.5	14.1	18.0	11.9	65.7	369.2
1975	66.7	39.9	46.9	85.7	91.1	36.1	0.9	14.6	.	19.3	61.6	51.1	513.9
1976	64.0	12.3	10.2	49.3	60.3	19.4	2.5	2.5	5.7	59.5	14.5	57.9	358.1
1977	36.6	10.9	36.6	55.2	34.3	6.5	.	6.2	48.8	10.2	15.1	28.6	289.0
1978	45.0	49.8	32.6	75.4	9.5	0.6	.	.	34.3	50.8	3.4	70.9	372.3
1979	94.0	28.2	12.3	6.8	67.4	18.3	3.9	1.7	.	30.4	38.5	44.6	346.1
1980	87.6	19.2	35.4	34.4	88.7	31.2	5.9	1.7	.	1.7	82.0	33.7	421.5
1981	70.7	39.8	70.5	21.4	54.6	16.3	5.9	6.1	9.3	12.8	56.9	73.7	438.0
1982	34.3	9.5	24.5	82.6	19.8	50.5	23.1	49.5	1.2	16.0	2.0	31.8	344.8
1983	48.5	42.9	17.5	30.7	80.7	49.9	19.5	.	8.0	23.0	93.9	29.0	443.6
1984	30.4	24.3	53.8	101.5	44.8	17.3	40.3	28.5	.	0.0	46.7	10.9	398.5
1985	67.2	63.0	18.5	75.0	52.7	6.0	11.5	.	.	56.7	63.8	32.7	447.1
1986	92.4	64.6	26.0	16.2	55.6	49.7	3.0	.	18.5	8.0	29.2	75.5	438.7
1987	137.2	32.1	54.5	41.8	41.9	39.8	27.6	15.8	.	15.7	22.0	80.8	509.2
1988	14.5	42.0	79.5	60.5	66.8	70.6	10.5	.	6.5	72.4	73.5	32.2	529.0
1989	-	12.2	15.0	-	30.7	21.2	9.7	2.0	3.0	57.4	82.0	20.2	-
1990	.	15.0	9.5	83.4	53.2	25.0	17.7	17.7	55.0	42.4	19.3	57.4	395.6
1991	11.9	38.0	19.7	66.6	82.4	28.9	3.2	8.1	.	42.2	10.3	17.4	328.7
1992	1.0	4.4	54.6	33.9	-	69.1	28.0	6.0	3.5	28.8	34.6	15.0	-
1993	10.4	0.0	6.0	52.0	77.1	11.0	15.0	-	-	-	-	-	-

CLOSED

APPENDIX D

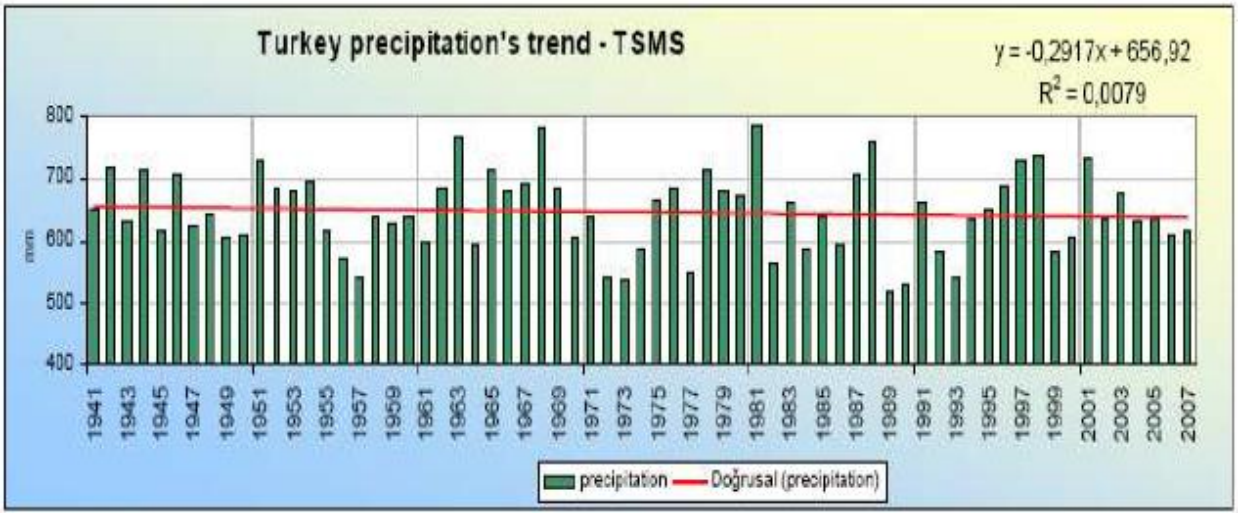

Figure 77: Turkey annual precipitation and its trend (Sensoy et. al., 2008, Figure 3)

APPENDIX E

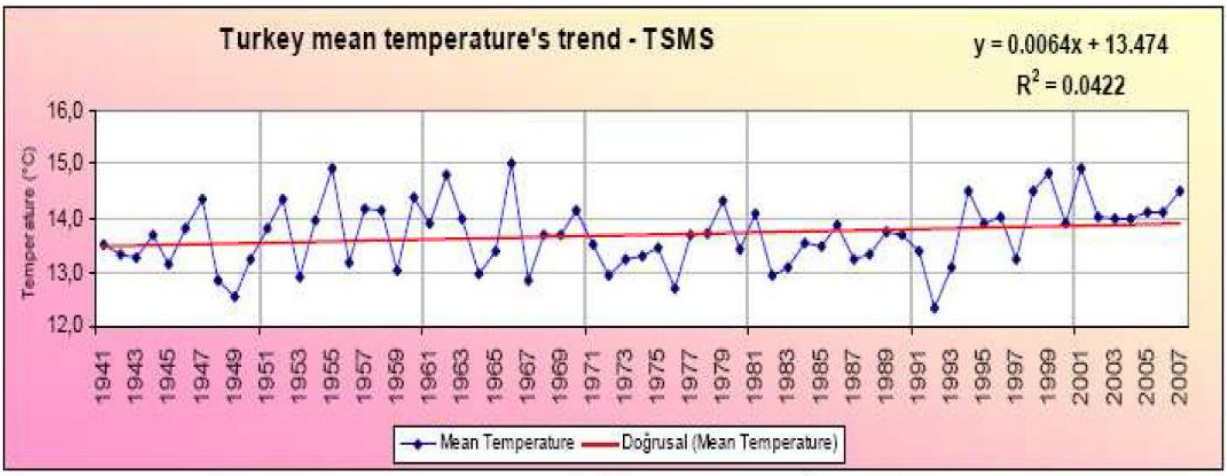

Figure 78: Turkey mean temperature and its trend (Sensoy et. al., 2008, Figure 7)

APPENDIX F

Table 21: Observed Monthly Precipitation for the Cubuk II Reservoir

STATION NAME	ÇUBUK RESERVOIR II							OPERATOR	DSİ			
STATION NUMBER	12-013							ALTITUDE	1005 m			
REGION	5							OPENIND DATE	9/1/1964			
CITY NAME	ANKARA-ÇUBUK							COORDINATES	40° 16' K - 33° 03' D			
OBSERVATION TYPE	MONTHLY PRECIPITATION (mm)											
YEAR	JAN	FEB	MARCH	APR	MAY	JUNE	JULY	AUGT	SEP	OCT	NOV	DEC	ANNUAL
1964	-	-	-	-	-	-	-	-	13.3	0.0	22.2	77.7	-
1965	18.0	76.1	53.6	50.8	48.6	13.2	9.2	4.1	.	8.6	46.4	66.2	394.8
1966	113.7	6.9	67.1	49.9	61.9	47.6	7.0	9.8	6.4	8.4	35.0	71.3	485.0
1967	28.0	19.5	16.8	81.7	70.7	5.6	.	7.4	.	19.4	19.7	59.4	328.2
1968	67.9	32.9	94.7	46.5	86.9	31.8	5.4	18.9	37.0	42.5	59.2	90.0	613.7
1969	54.6	60.0	80.2	50.4	84.8	25.0	.	9.1	7.6	8.1	20.9	182.5	583.2
1970	43.3	138.8	54.2	22.1	54.9	31.7	5.3	.	28.9	56.7	36.3	39.5	511.7
1971	43.2	42.9	68.3	40.7	81.5	37.3	18.0	65.0	17.4	9.5	81.5	75.9	581.2
1972	-	27.8	25.2	60.3	76.7	108.8	56.8	17.0	80.6	71.0	17.4	8.6	-
1973	15.1	48.2	30.2	56.1	11.0	24.1	7.9	6.0	19.1	10.0	16.1	39.4	283.2
1974	7.2	51.3	49.5	47.6	99.4	37.0	18.8	22.1	34.2	17.7	13.7	50.7	449.2
1975	96.0	28.6	43.2	87.9	180.7	11.3	6.9	12.0	11.1	29.5	58.4	50.0	615.6
1976	-	9.6	32.8	64.4	60.8	29.5	12.2	5.0	18.5	61.4	24.9	100.7	-
1977	17.8	5.6	26.6	57.5	76.1	15.4	6.2	6.8	42.1	8.6	30.0	36.4	329.1
1978	63.0	98.6	42.8	76.0	52.0	0.9	3.4	7.2	57.2	63.3	5.0	115.7	585.1
1982	-	-	-	-	-	27.7	11.0	32.6	.	28.8	3.7	27.4	-
1983	37.4	27.1	7.6	75.1	54.6	72.6	66.1	32.8	6.4	31.2	111.2	65.9	588.0
1984	38.9	21.7	54.6	81.7	58.0	52.8	27.6	14.1	.	0.0	66.9	2.2	418.5
1985	81.0	79.7	25.0	65.2	55.0	27.8	22.2	.	-	-	-	-	-
1986	-	36.2	17.4	15.3	17.7	46.5	.	.	28.0	7.4	22.9	78.2	-
1987	126.5	25.8	37.7	38.0	38.8	55.6	14.7	.	0.2	9.8	16.6	75.0	438.7
1988	5.6	27.1	80.3	46.9	43.6	77.2	11.0	1.2	5.4	67.9	52.2	33.1	451.5
1989	-	11.7	18.3	6.0	47.5	44.8	13.3	38.3	0.3	-	-	-	-

CLOSED

APPENDIX G

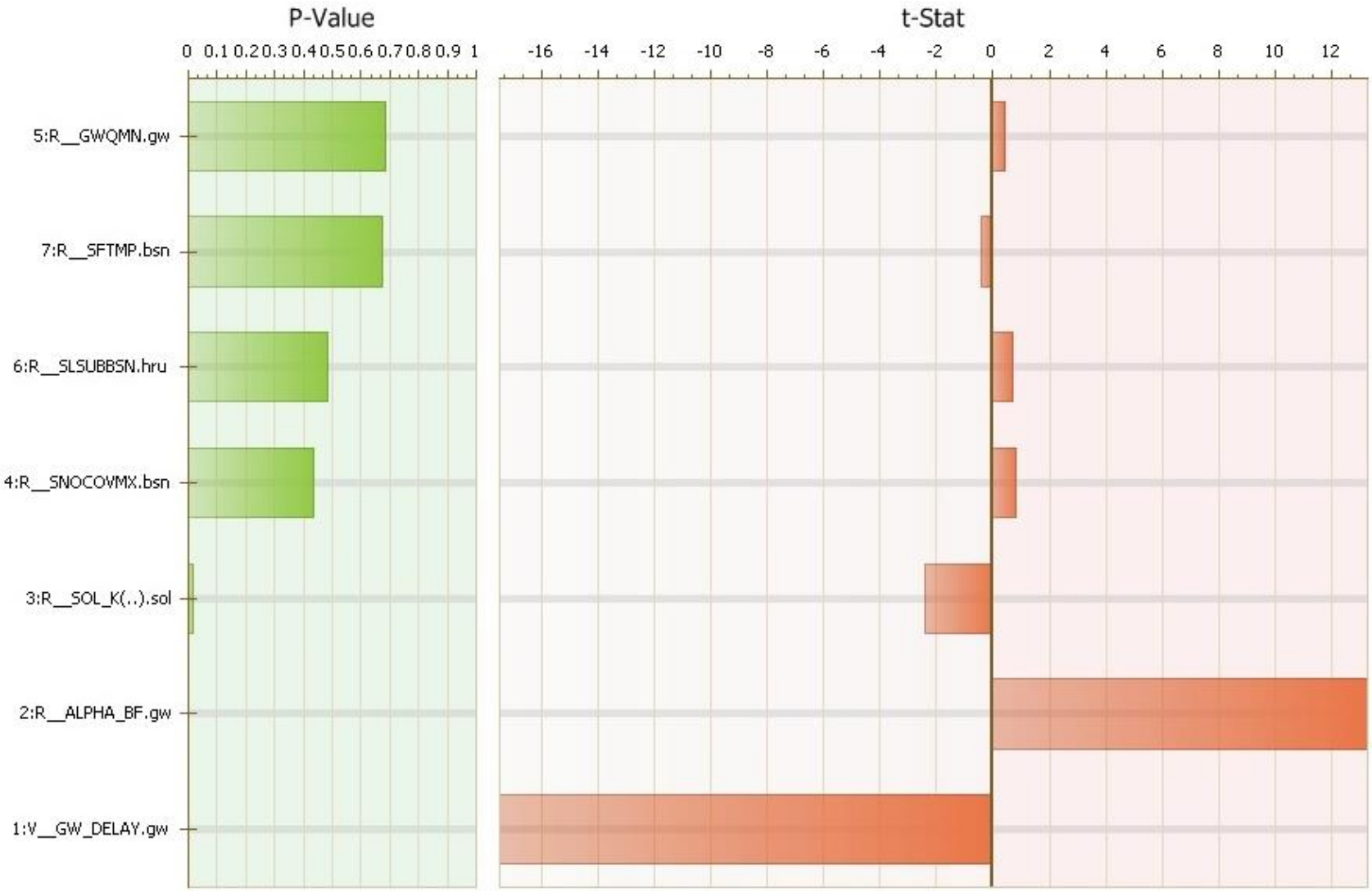

Figure 79: Global Sensitivity Analysis for Stream Flow

APPENDIX H

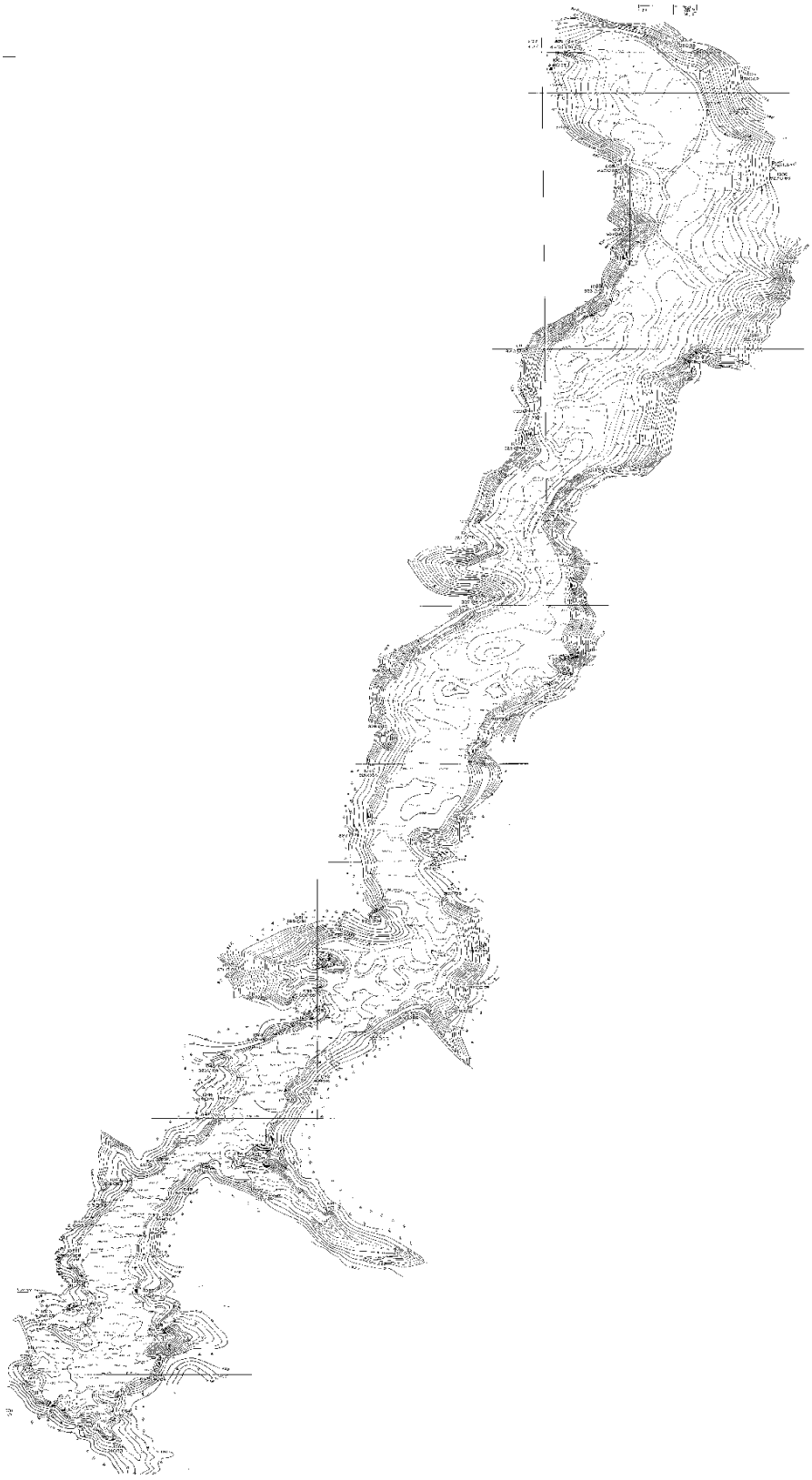

Figure 80: Bathymetric Map of Cubuk I Reservoir (1978)

APPENDIX I

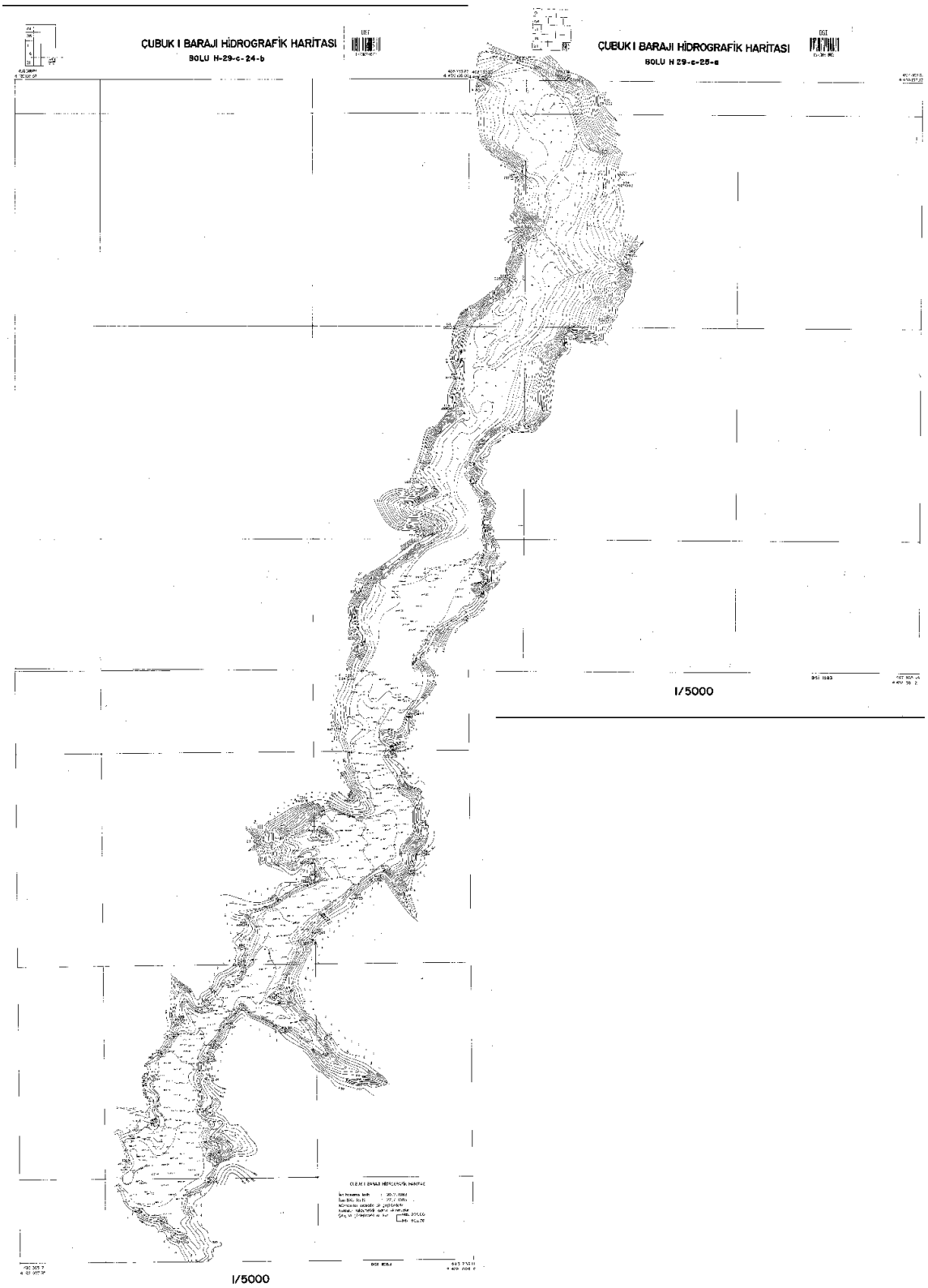

Figure 81: Bathymetric Map of Cubuk I Reservoir (1983)

APPENDIX K

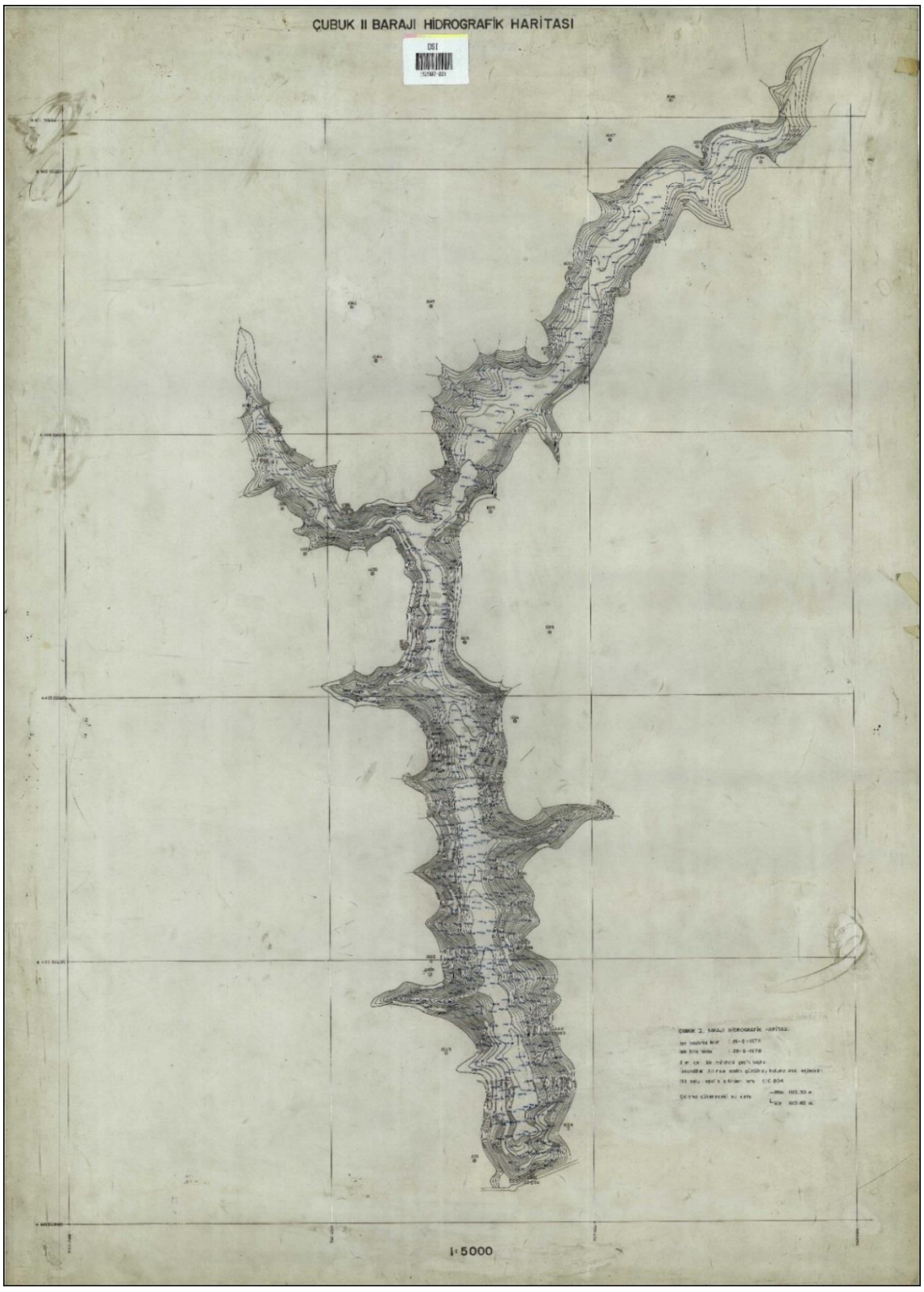

Figure 82: Bathymetric Map of Cubuk II Reservoir (1978)

APPENDIX L

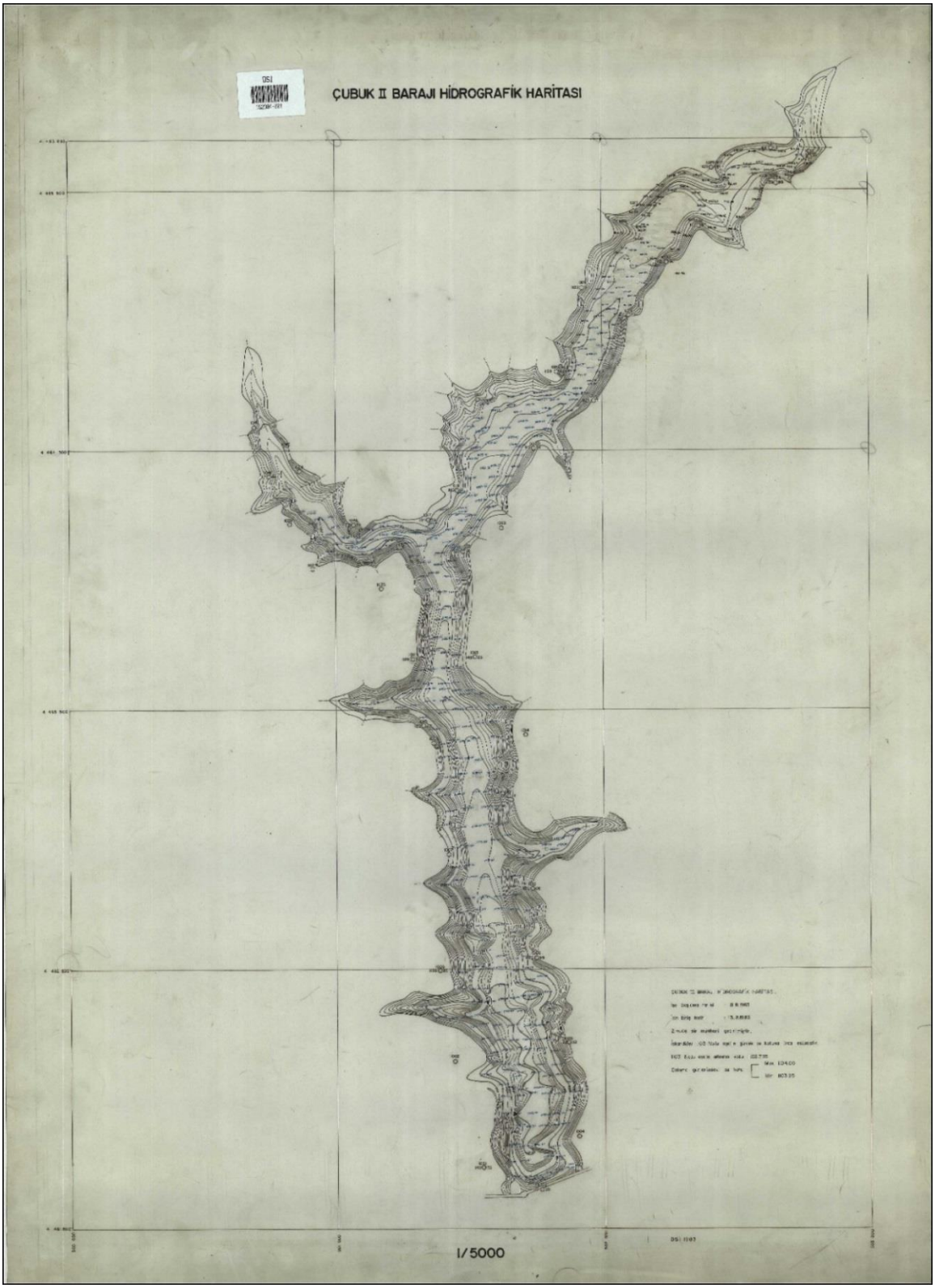

Figure 83: Bathymetric Map of Cubuk II Reservoir (1983)